A Study of Modifications to Quantum Mechanics

Zachary E. Lewis

Dissertation submitted to the Faculty of the
Virginia Polytechnic Institute and State University
in partial fulfillment of the requirements for the degree of

Doctor of Philosophy
in
Physics

Tatsu Takeuchi, Chair
Ezra Brown
Mark Pitt
Eric Sharpe

February 21, 2013
Blacksburg, Virginia

Keywords: Physics, Quantum Mechanics, Foundations of Quantum Mechanics

A Study of Modifications to Quantum Mechanics

Zachary E. Lewis

(ABSTRACT)

In this work, the consequences of several modifications to quantum mechanics are examined. These modifications, motivated by string theory, fall into two categories: ones in which the canonical commutation relations between position and momentum are deformed and ones in which the space of states used are vector spaces over Galois fields instead of complex Hilbert spaces. The particular deformation of the canonical commutation relations used leads to a minimum value of the uncertainty in position which is interpreted as a minimum length scale. Both harmonic and anharmonic oscillators are studied in this framework with normalizable, positive energy eigenstates found in both cases. The quantum uncertainty relations and classical counterparts to these states are discussed. Creating modified quantum theories by replacing the Hilbert spaces of canonical quantum mechanics with vector spaces defined over several finite, Galois fields is accomplished. Correlation functions are calculated in these theories and the maximum values are shown to not behave as would be expected by the standard, Bell-like, bounding inequality theorems. The interpretations and implications of these theories are discussed.

This work was partially supported by the U.S. Department of Energy, grant DE-FG05-92ER40609, Task A and grant DE-FG05-92ER40677, Task A.

Dedication

To my parents,
brother, and extended family,
for all of their love and support.

Acknowledgments

This work wouldn't have been possible without the guidance and friendship of Prof. Tatsu Takeuchi. His mentoring has made me a better scientist and a better teacher. For these things, I am forever grateful.

Further thanks are due to fellow students, past and present, who have patiently played the role of sounding board and offered encouragement and criticism, in appropriate measure: Andrew, Yee, and Ben.

Lastly, I would like to thank my committee for their patience and cooperation throughout the defense process.

Contents

1 History and Motivation **1**

1.1 The Theory Group and its Inspirations 1

1.2 Minimal Length 2

1.2.1 Minimal Length Uncertainty Relation 3

1.2.2 Phase Space and the Density of States 6

1.2.3 The Cosmological Constant 9

1.2.4 UV/IR connection and 'Jamming' 12

1.2.5 Towards a Model of 'Jamming' 14

1.3 Supercorrelations 15

1.3.1 Correlations in Classical and Quantum Mechanics 16

1.3.2 Guidance from String Theory 20

1.3.3 Galois Fields 23

2 Minimal Length through Modified Commutation Relations **25**

2.1 Background 25

2.2 Canonical Harmonic Oscillators 27

2.3 Energy Eigenstates of The Deformed Harmonic Oscillator 31

2.4 Limiting Cases: $\lambda \to \infty$ 40

2.5 Limiting Cases: $\lambda \to 1$ 42

2.6 Limiting Cases: $\lambda \to \frac{1}{2}$ 43
2.7 The Classical Equations of Motion 44
2.7.1 $\boldsymbol{m > 0}$ case 46
2.7.2 $\boldsymbol{m < 0}$ Case 49
2.8 Compactification 58
2.9 Classical Probablities 60
2.10 Further Discussion 64

3 Galois Fields as State Spaces **66**
3.1 Background 66
3.2 The Probability Path 73
3.2.1 Preliminaries 73
3.2.2 $\mathbb{Z}_2$ Quantum Mechanics 75
3.2.3 Two Particle States 80
3.2.4 Geometric Characterization 82
3.2.5 Local Rotations 83
3.2.6 Two Particle Observables 83
3.2.7 Entanglement and the Impossibility of Hidden Variables . . . 85
3.2.8 The CHSH Bound 87
3.2.9 $\mathbb{Z}_3$ case 88
3.2.10 $\mathbb{Z}_4$ case 91
3.2.11 $\mathbb{Z}_5$ case 96
3.2.12 Comments 99
3.3 Expectation Value Path 100
3.3.1 Biorthogonal Systems over Galois Fields 100
3.3.2 Observables 102

3.3.3 Physical States 103
3.3.4 Expectation Values 103
3.3.5 2D Vector Space over $\boldsymbol{GF(3)}$ 105
3.3.6 2D Vector Space over $\boldsymbol{GF(9)}$ 109
3.3.7 Spin Correlations 113
3.3.8 Expectation Values without Definite Probabilities 120
3.3.9 Comments 123

A A Useful Integral Formula for Gegenbauer Polynomials **131**

List of Figures

1.1 The δp-dependence of the lower bound of δx under the minimal length uncertainty relation Eq. (1.6) (red curve). The bound for the usual Heisenberg relation $\delta x \geq \hbar/(2\delta p)$ is shown in blue, and the linear bound $\delta x \geq (\hbar\beta/2)\delta p$ is shown in green. 4

2.1 Plots of λ_+ (blue) and λ_- (red), Eq. (2.44), as functions of $\kappa^2 = \beta\hbar\sqrt{k|m|}$. 34

2.2 λ-dependence of the wave-functions of the first few energy eigenstates. The $\lambda > 1$ values correspond to $m > 0$, while the $\frac{1}{2} \leq \lambda < 1$ values correspond to $m < 0$. The $\lambda = 1$ case corresponds to the limit $|m| \to \infty$. 36

2.3 Δp versus Δx for the lowest six energy eigenstates of the harmonic oscillator. Δx is in units of $\Delta x_{\min} = \hbar\sqrt{\beta}$, while Δp is in units of $1/\sqrt{\beta} = \hbar/\Delta x_{\min}$. The location of the state along the curves shown is determined by the value of λ defined in Eq. (2.44). The $\lambda = 1$ points correspond to the case $1/m = 0$. As $1/m$ is increased to the positive side, the value of λ will increase away from one and the state will move toward the left along the $\Delta x \sim 1/\Delta p$ branch. If $1/m$ is decreased into the negative, the value of λ will decrease toward $1/2$, and the state will move toward the right along the $\Delta x \sim \Delta p$ branch. The $n = 0$ curve (shown in red) corresponds to the minimal length uncertainty bound, Eq. (2.6). 39

2.4 The dependence of the classical behavior of a positive mass particle in a harmonic oscillator potential on the parameter $C = 2mE\beta = \beta m^2\omega^2 A^2$, where E is the particle's energy, and A is the amplitude of the oscillation in x. The undeformed $\beta = 0$ case is shown in red. The other four cases are $C = 1$ (orange), $C = 2$ (green), $C = 4$ (blue), and $C = 8$ (purple). 48

2.5 The classical behavior of a positive mass particle in a harmonic oscillator potential with modified Poisson brackets, Eq. (2.87), in the limit $m \to \infty$ with $C = 2mE\beta$ where E and β are kept fixed. $\rho(t)$ and $x(t)$ take on the behavior of the position and momentum of a particle in an infinite square well. 50

2.6 The dependence of the classical behavior of a negative mass particle in a harmonic oscillator potential on the parameter $C = -2\mu E\beta = -\beta|m|kB^2$, where E is the particle's energy, and B is the distance of closest approach to the origin in x-space. Note that due to the negative mass, $p(t)$ is negative when $\dot{x}(t)$ is positive, and vice versa. The undeformed $\beta = 0$ case is shown in red. The other three cases are $C = -\frac{1}{16}$ (orange), $C = -\frac{1}{4}$ (green), $C = -1$ (blue), and $C = -4$ (purple). 53

2.7 ωT as a function of $-C = 2|m|E\beta$, where $\omega = \sqrt{k/|m|}$, and E is the particle's energy. $T/2$ is the time it takes for the particle to traverse the entire trajectory. 54

2.8 The classical behavior of a zero-energy particle with negative mass in a harmonic oscillator potential. The particle starts out at $x = -\infty$ at time $t = 0$ and asymptotically approaches the origin. 57

2.9 The periodic behavior of the negative-mass particle in a harmonic oscillator potential in compactified x-space. The example shown is for $C = -1$. 59

2.10 Classical probabilities in ρ-, p-, and x-spaces of a negative mass particle in a harmonic oscillator potential for the case $C = -2|m|E\beta = -1$. The time dependence of this solution was shown in Fig. 2.9. Though the trajectory of the particle is not confined to a finite region of phase space, the classical probabilities of finding the particle near the phase-space-origin is still finite due to the finiteness of the time it takes for the particle to traverse the entire trajectory. 61

2.11 Comparison of quantum and classical probabilities in ρ-, p-, and x-spaces for a negative mass particle in a harmonic oscillator potential for the case $\lambda = \frac{3}{4}$ and $n = 30$, which corresponds to the classical $C = -2|m|E\beta = -5044$. The quantum distribution in x-space is discrete due to the existence of the minimal length. There is also some seepage of the probability into classically forbidden regions in x-space as is expected of quantum probabilities. 63

3.1 The 6 spin-like directions of $DQM(2,2)$. Allowed $SO(3)$ rotations are those that rotate the equilateral triangle *abc* onto itself. 78

3.2 The implication chart for the state $\big|S\big\rangle$. Arrows point from the condition toward the implication. By tracing the arrows, it is easy to see that no classical configurations, and thus no hidden variable theory, can satisfy all of these requirements. If we ignore the observable X and look at only Y and Z, then the assignments within the dashed boxes are possible classical configurations. However, neither allow for the pairs $(Y_1 Z_2)$ and $(Z_1 Y_2)$ to be anti-correlated, which occurs with probability 1/3 in our toy quantum model. 87

3.3 To map 'rotations' in $PGL(2,3) \cong S_4$ to rotations in $SO(3)$: (a) label the faces of an octahedron with four symbols as shown. Then, every permutation of the four labels *abcd* will correspond a rotation of the octahedral group. (b) The 'spin' observable A_{ab} in $DQM(2,3)$ can be mapped onto a direction in 3D space as shown. (c) The urchin diagram showing all 12 'spin' directions $DQM(2,3)$. 90

3.4 To map 'rotations' in $PGL(2,4) \cong A_5$ to rotations in $SO(3)$: (a) label the faces of an icosahedron with five symbols as shown above left. Then, to every even permutation of the five labels *abcde* will correspond a rotation belonging to the icosahedral group. (b) The 'spin' observable A_{ab} in $DQM(2,4)$ can be mapped onto a direction in 3D space as shown. (c) The urchin diagram showing all 20 'spin' directions of $DQM(2,4)$. 94

3.5 Not all 'rotations' in $PGL(2,5) \cong S_5$ can be mapped to rotations in $SO(3)$. The even permutations, isomorphic to A_5, can be mapped as follows: (a) label the faces of a dodecahedron with six symbols as shown above left. Then, to every even permutation of the six labels $abcdef$ will correspond a rotation belonging to the icosahedral group. (b) The 'spin' observable A_{ab} in $DQM(2,5)$ can be mapped onto the direction in 3D space as shown. (c) The urchin diagram showing all 30 'spin' directions of $DQM(2,5)$. 98

3.6 The correspondence between the dihedral group D_4 and the projective orthogonal group $PO(2,3)$. Every D_4 rotation of the quadrangle corresponds to a permutation of the four vertex labels $abcd$ belonging to $PO(2,3)$. 109

3.7 The correspondence between the octahedral group O and the projective unitary group $PU(2,9)$. Every O rotation of the octahedron corresponds to a permutation of the six vertex labels $abcdef$ belonging to $PU(2,9)$. 112

List of Tables

3.1 The probabilities of the two outcomes + and − for all combinations of observables and states in $DQM(2,2)$. 80

3.2 Correlations of observables for the six entangled states. 86

3.3 $PGL(2,5)$ is a subgroup of S_6, which is isomorphic to S_5. This table shows how many elements in each conjugate class of S_6 are in $PGL(2,5)$, and the conjugate class in S_5 that they correspond to. The signs adjacent to the Young tableaux indicate the signature of the permutations in each class. Only the even permutations in $PGL(2,5)$, which form an invariant subgroup of order 60 isomorphic to A_5, can be mapped to elements in $SO(3)$. 95

3.4 Expectation values and uncertainties of spin-like observables in biorthogonal quantum mechanics on $V(2,3)$. 108

3.5 Expectation values and uncertainties of spin-like observables in biorthogonal quantum mechanics on $V(2,9)$. 110

3.6 The number of CHSH correlators with the respective absolute values for the three states $|S\rangle$, $|T\rangle$, and $|U\rangle$. 119

3.7 The probabilities of the four possible outcomes ++, +−, −+, and −− in canonical quantum mechanic when $\tilde{\sigma}_3 \otimes \tilde{\sigma}_3$ is measured on the canonical states $\left|\tilde{S}\right\rangle$, $\left|\tilde{T}\right\rangle$, and $\left|\tilde{U}\right\rangle$. 121

Chapter 1

History and Motivation

1.1 The Theory Group and its Inspirations

The goal in this work is to analyze particular, string theory motivated, extensions of quantum mechanics. The material contained herein is a compilation and exposition of the work carried out by an informal theory group at Virginia Tech, of which I have been a recent participant, but that is more regularly comprised of Prof. Lay Nam Chang, Prof. Djordje Minic, and Prof. Tatsu Takeuchi. Previous participants that aided in the progression of the research that is presented herein were Prof. Chia Tze, Sandor Benczik, Naotoshi Okamura, and Saifuddin Rayyan .

To completely describe the motivations that drive such a diverse group would be a study in itself, though, the common threads are strong and clearly distinguishable. There is an ambition to address the major outstanding puzzles in theoretical physics, such as the cosmological constant problem, the incompatibility of the gravitational interaction with the Standard Model, and the limits of quantum mechanics. Also, although we are theorists with lofty aspirations, there is always a pressing desire to find ways to connect our theories to experiment; a desire that is not often known to the public as they view us working in our ivory ~~trailer~~ tower. We also find ourselves applying new techniques and conceptual frameworks to old problems, as will be seen shortly through the influence of string theory in guiding our efforts.

It is my aim in this chapter to give an overview of some of the ideas and reasoning that have led to the results that will be discussed in chapters 2 and 3. Chapter 2 will discuss our success in the study of the addition of a minimal length scale to

quantum mechanics and chapter 3 will detail our attempts at replacing the usual Hilbert spaces in quantum theory with the more exotic Galois fields. Parts of this overview have appeared in the follow review letters: Refs. ([1, 2]).

1.2 Minimal Length

Just as c defines the velocity scale at which special relativity becomes important and $\hbar$ defines the phase space volume scale at which quantum mechanical effects become prominent, the length scale defined by $\ell_{\rm P} = \sqrt{\hbar G_{\rm N}/c^3}$ (called the Planck length) is expected to be of similar importance to any quantum theory of gravity. This length scale has been suggested by Wheeler [3] and others (Refs. [4][5][6][7], to list a few) to be a minimal length scale, below which spacetime intervals may not be resolvable, as expressed by

$$\delta s \gtrsim \ell_{\rm P} \ . \tag{1.1}$$

Since G_N does not appear in the formalism of ordinary quantum mechanics, such a length scale would have to be introduced through an appropriate modification of said formalism.

Although we will be considering a modification that is motivated by the length scale in string theory that specifies the spacetime extent of a string, $\ell_s = \sqrt{\alpha'}$ where $\hbar c/\alpha'$ is the string tension (as can be found in introductory textbooks on the subject [8]), there is a relatively long history of attempts to include a minimal length scale, of various sorts, in quantum mechanics.

Heisenberg, first in a letter to Bohr [9], used a minimal length and difference equations to address the self energy problem of the electron in the newly formulated theory of quantum electrodynamics [10]. Born also considered a minimum length, in the form of a finite electron radius, when he proposed a quantizible Lagrangian for the electromagnetic field [11].

Snyder noticed that there were discrete, Lorentz-invariant spacetime coordinates, and showed that they had nonstandard commutation relations [12]. Yang then extended that work by generalizing the invariance to include translations, albeit in a de Sitter space [13]. Mead used perturbation theory to explore the consequences that an assumed minimal uncertainty in position may have on the uncertainty in energy for several systems [14].

Various ways to more drastically deform or extend quantum theory have also been

suggested, such as Weinberg's non-linear generalization [15] or the non-Hermitian, PT symmetric theory of Bender, Brody, and Jones [16]. The focus of the group's analysis has been on the consequences of the introduction of a minimal length scale into quantum mechanics through the modification of its algebraic structure, as done by Maggiore [17] and Kempf [18].

1.2.1 Minimal Length Uncertainty Relation

Before discussing the algebraic structure, let's identify the way in which a minimal length scale is manifested; via the minimal length uncertainty relation (MLUR),

$$\delta x \ \sim \ \left(\frac{\hbar}{\delta p} + \alpha' \frac{\delta p}{\hbar} \right) \ . \tag{1.2}$$

This form can be motivated from the study of string-string collisions as done by Amati, Ciafaloni, and Veneziano in Ref. [19] and Gross and Mende in Ref. [20]. The viewpoint of these papers is qualitatively similar to that of Heisenberg's microscope thought experiment, in which he reasoned that one could view the uncertainty in a particle's position as being cause by the uncertainty in the recoil direction of an electron after interacting with a photon that is used to probe said electron's position [21]. The referenced papers use fundamental strings as probe and target instead of photons probing the position of electrons.

The first term on the right-hand side is the usual Heisenberg term, that can be seen as coming from the lessening of the probe's wavelength as its momentum is increased, while the second term can be viewed as being due to the increasing of the length of the probe string as it becomes more energetic:

$$\delta p \ = \ \frac{\delta E}{c} \ \sim \ \frac{\hbar}{\alpha'} \delta x \ . \tag{1.3}$$

Eq. (1.2) implies that the uncertainty in position, δx, is bounded from below by the string length scale,

$$\delta x \ \gtrsim \ \sqrt{\alpha'} \ = \ \ell_s \ . \tag{1.4}$$

The associated minimum in δp occurs at

$$\delta p \ \sim \ \frac{\hbar}{\sqrt{\alpha'}} \ = \ \frac{\hbar}{\ell_s} \ \equiv \ \mu_s \ . \tag{1.5}$$

From this, ℓ_s can be interpreted as a length scale below which distances cannot be resolved with any certainty, as is consistent with Eq. (1.1).

Of key interest here is that for large momenta, $\delta p \gg \mu_s$, the MLUR is dominated by the linear behavior of Eq. (1.3). The direct implication is that large δp, or ultraviolet (UV), behavior corresponds to large δx, or infrared(IR), behavior and that one could expect there to be some coupling between the physics at these scales. Relationships between the UV and IR scales have been found in various string dualities [8], and in the context of AdS/CFT correspondence [22].

Since these relations often connect small scale structure with large scale structure, it is hoped that their study may lead to resolution of the cosmological constant problem, as will be discussed shortly. With this target in mind, we will see first how to manifest the MLUR in quantum mechanics and then see what the direct implications are for the cosmological constant.

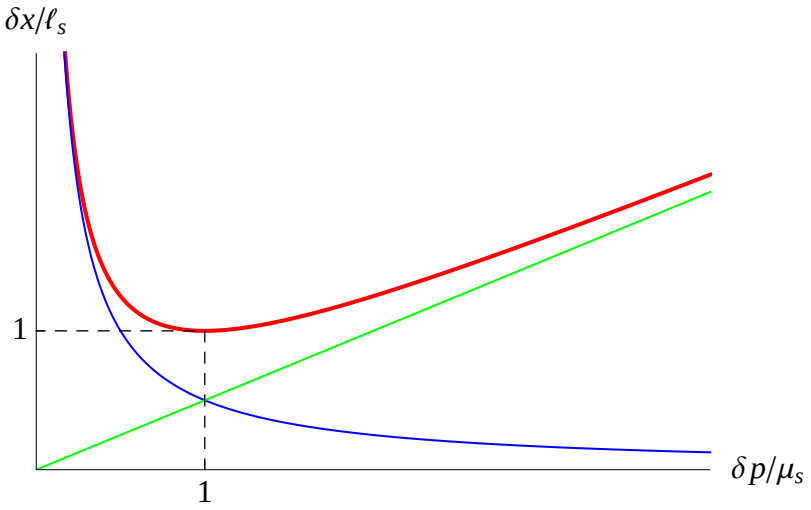

Figure 1.1: The δp-dependence of the lower bound of δx under the minimal length uncertainty relation Eq. (1.6) (red curve). The bound for the usual Heisenberg relation $\delta x \geq \hbar/(2\delta p)$ is shown in blue, and the linear bound $\delta x \geq (\hbar\beta/2)\delta p$ is shown in green.

To further the study of the MLUR, Eq. (2.6), we start by rewriting it in the usual form as

$$\delta x\, \delta p \;\geq\; \frac{\hbar}{2}\left(1 + \beta\, \delta p^2\right) \;, \tag{1.6}$$

where the parameter $\beta = \alpha'/\hbar^2$ is chosen for later convenience. The minimum value of δx as a function of δp is plotted in Fig. 1.1.

This uncertainty relation can be reproduced by modifying the canonical commutation relation between $\hat{x}$ and $\hat{p}$ via

$$\frac{1}{i\hbar}\,[\,\hat{x},\,\hat{p}\,] \;=\; 1 \qquad \longrightarrow \qquad \frac{1}{i\hbar}\,[\,\hat{x},\,\hat{p}\,] \;=\; A(\hat{p}^2)\;. \tag{1.7}$$

Setting $A(p^2) = 1 + \beta p^2$, we find

$$\delta x\,\delta p \;\geq\; \frac{1}{2}\Big|\big\langle[\,\hat{x},\,\hat{p}\,]\big\rangle\Big| \;=\; \frac{\hbar}{2}\left(1+\beta\langle\hat{p}^2\rangle\right) \;\geq\; \frac{\hbar}{2}\left(1+\beta\,\delta p^2\right)\;, \tag{1.8}$$

since $\delta p^2 = \langle\hat{p}^2\rangle - \langle\hat{p}\rangle^2$; the second inequality becoming equality in the case of bound states, for which $\langle\hat{p}\rangle = 0$. As seen in Ref. [23], the function $A(p^2)$ can be more generic, so, βp^2 could be viewed as the linear term in an expansion of $A(p^2)$ in powers of p^2.

In the case of multiple spatial dimensions, the modification in Eq. (1.7) generalizes to

$$\frac{1}{i\hbar}[\,\hat{x}_i,\,\hat{p}_j\,] \;=\; A(\hat{\mathbf{p}}^2)\,\delta_{ij} + B(\hat{\mathbf{p}}^2)\,\hat{p}_i\hat{p}_j\;, \tag{1.9}$$

where $\hat{\mathbf{p}}^2 = \sum_i \hat{p}_i^2$, as usual. This is the most general form that a) depends only on the momentum and b) respects rotational symmetry, which it does by only depending on the magnitude of the momentum vector. Assuming that the components of the momentum commute among themselves,

$$[\,\hat{p}_i,\,\hat{p}_j\,] \;=\; 0\;, \tag{1.10}$$

the Jacobi identity demands that [24]

$$\frac{1}{i\hbar}[\,\hat{x}_i,\,\hat{x}_j\,] \;=\; -\Big\{\,2(\hat{A}+\hat{B}\hat{\mathbf{p}}^2)\hat{A}' - \hat{A}\hat{B}\,\Big\}\,\hat{L}_{ij}\;, \tag{1.11}$$

where we have used the shorthand $\hat{A} = A(\hat{\mathbf{p}}^2)$, $\hat{A}' = \dfrac{dA}{d\mathbf{p}^2}(\hat{\mathbf{p}}^2)$, $\hat{B} = B(\hat{\mathbf{p}}^2)$, and $\hat{L}_{ij} = (\hat{x}_i\hat{p}_j - \hat{x}_j\hat{p}_i)\,/\hat{A}$. That $\hat{L}_{ij}$ generates rotations can be seen from the following:

$$\begin{aligned}
\frac{1}{i\hbar}[\,\hat{L}_{ij}\,,\hat{x}_k\,] &= \delta_{ik}\hat{x}_j - \delta_{jk}\hat{x}_i\;,\\
\frac{1}{i\hbar}[\,\hat{L}_{ij}\,,\hat{p}_k\,] &= \delta_{ik}\hat{p}_j - \delta_{jk}\hat{p}_i\;,\\
\frac{1}{i\hbar}[\,\hat{L}_{ij}\,,\hat{L}_{k\ell}\,] &= \delta_{ik}\hat{L}_{j\ell} - \delta_{i\ell}\hat{L}_{jk} + \delta_{j\ell}\hat{L}_{ik} - \delta_{jk}\hat{L}_{i\ell}\;.
\end{aligned} \tag{1.12}$$

Various choices for the functions $A(\mathbf{p}^2)$ and $B(\mathbf{p}^2)$ have been considered in the literature. Maggiore [17] proposed

$$A(\mathbf{p}^2) \;=\; \sqrt{1+2\beta\mathbf{p}^2}\,, \qquad B(\mathbf{p}^2) \;=\; 0\,, \qquad \frac{1}{i\hbar}[\,\hat{x}_i,\,\hat{x}_j\,] \;=\; -2\beta\hat{L}_{ij}\,, \tag{1.13}$$

while Kempf [18] assumed

$$A(\mathbf{p}^2) \;=\; 1+\beta\mathbf{p}^2\,, \qquad B(\mathbf{p}^2) \;=\; \beta' \;=\; \text{constant}\,, \tag{1.14}$$

in which case

$$\frac{1}{i\hbar}[\,\hat{x}_i,\,\hat{x}_j\,] \;=\; -\left\{\,(2\beta-\beta')+\beta(2\beta+\beta')\hat{\mathbf{p}}^2\right\}\hat{L}_{ij}\,. \tag{1.15}$$

Kempf's choice encompasses the algebra of Snyder [12]

$$A(\mathbf{p}^2) \;=\; 1\,, \qquad B(\mathbf{p}^2) \;=\; \beta'\,, \qquad \frac{1}{i\hbar}[\,\hat{x}_i,\,\hat{x}_j\,] \;=\; \beta'\hat{L}_{ij}\,, \tag{1.16}$$

and that of Brau [25, 26]

$$A(\mathbf{p}^2) \;=\; 1+\beta\mathbf{p}^2\,, \qquad B(\mathbf{p}^2) \;=\; 2\beta\,, \qquad \frac{1}{i\hbar}[\,\hat{x}_i,\,\hat{x}_j\,] \;=\; O(\beta^2)\,, \tag{1.17}$$

for which the components of the position approximately commute. In the following analysis, we follow Kempf and use Eq. (1.14).

1.2.2 Phase Space and the Density of States

Rewriting the 1-D deformed commutator as

$$[\,\hat{x},\,\hat{p}\,] \;=\; i\hbar A(\hat{p}^2) \tag{1.18}$$

Since $\hbar$ determines the phase space volume for which quantum effects dominate, it is instructive to see how a momentum dependent phase space volume is effected by time evolution. In classical mechanics, Liouville's theorem states that phase space volumes are preserved under canonical transformations. To see how this result changes, we'll modify the Poisson bracket of classical mechanics via the Dirac correspondence principle, as done in Ref. [24],

$$\frac{1}{i\hbar}[\,\hat{x},\,\hat{p}\,] \;=\; A(\hat{p}^2) \qquad \longrightarrow \qquad \{\,x,\,p\,\} \;=\; A(p^2)\,, \tag{1.19}$$

The Poisson brackets among the x_i's and p_i's for the multidimensional case are

$$\begin{aligned} \{\, x_i,\, p_j \,\} &= A\,\delta_{ij} + B\,p_i p_j \ , \\ \{\, p_i,\, p_j \,\} &= 0 \ , \\ \{\, x_i,\, x_j \,\} &= -\left[\frac{2(A + B\,\mathbf{p}^2)}{A}\,\frac{dA}{d\mathbf{p}^2} - B\right](x_i p_j - x_j p_i) \ . \end{aligned} \tag{1.20}$$

The generic Poisson bracket of arbitrary functions of the coordinates and momenta can then be defined as

$$\{F, G\} = \left(\frac{\partial F}{\partial x_i}\frac{\partial G}{\partial p_j} - \frac{\partial F}{\partial p_i}\frac{\partial G}{\partial x_j}\right)\{x_i, p_j\} + \frac{\partial F}{\partial x_i}\frac{\partial G}{\partial x_j}\{x_i, x_j\} \ . \tag{1.21}$$

Here, we use the Einstein convention that repeated indices are summed. Assuming that the equations of motion of x_i and p_i are given formally by:

$$\begin{aligned} \dot{x}_i &= \{\, x_i,\, H \,\} = \quad \{\, x_i,\, p_j \,\}\frac{\partial H}{\partial p_j} + \{\, x_i,\, x_j \,\}\frac{\partial H}{\partial x_j} \ , \\ \dot{p}_i &= \{\, p_i,\, H \,\} = -\{\, x_j,\, p_i \,\}\frac{\partial H}{\partial x_j} \ , \end{aligned} \tag{1.22}$$

the evolution of x_i and p_i during an infinitesimal time interval δt is found to be:

$$\begin{aligned} x_i' &= x_i + \dot{x}_i\,\delta t = x_i + \left[\{\, x_i,\, p_j \,\}\frac{\partial H}{\partial p_j} + \{\, x_i,\, x_j \,\}\frac{\partial H}{\partial x_j}\right]\delta t \ , \\ p_i' &= p_i + \dot{p}_i\,\delta t = p_i - \{\, x_j,\, p_i \,\}\frac{\partial H}{\partial x_j}\delta t \ . \end{aligned} \tag{1.23}$$

To find the change in phase space volume associated with this evolution, we calculate the Jacobian of the transformation from $(x_1, x_2, \cdots, x_D; p_1, p_2, \cdots, p_D)$ to $(x_1', x_2', \cdots, x_D'; p_1', p_2', \cdots, p_D')$:

$$d^D\mathbf{x}'\, d^D\mathbf{p}' = \left|\frac{\partial(x_1', x_2', \cdots, x_D'; p_1', p_2', \cdots, p_D')}{\partial(x_1, x_2, \cdots, x_D; p_1, p_2, \cdots, p_D)}\right| d^D\mathbf{x}\, d^D\mathbf{p} \ . \tag{1.24}$$

Since

$$\begin{aligned} \frac{\partial x_i'}{\partial x_j} &= \delta_{ij} + \frac{\partial \dot{x}_i}{\partial x_j}\,\delta t \ , & \frac{\partial x_i'}{\partial p_j} &= \frac{\partial \dot{x}_i}{\partial p_j}\,\delta t \ , \\ \frac{\partial p_i'}{\partial x_j} &= \frac{\partial \dot{p}_i}{\partial x_j}\,\delta t \ , & \frac{\partial p_i'}{\partial p_j} &= \delta_{ij} + \frac{\partial \dot{p}_i}{\partial p_j}\,\delta t \ , \end{aligned} \tag{1.25}$$

we find:

$$\left|\frac{\partial(x_1', x_2', \cdots, x_D'; p_1', p_2', \cdots, p_D')}{\partial(x_1, x_2, \cdots, x_D; p_1, p_2, \cdots, p_D)}\right| = 1 + \left(\frac{\partial \dot{x}_i}{\partial x_i} + \frac{\partial \dot{p}_i}{\partial p_i}\right)\delta t + O(\delta t^2) \ , \tag{1.26}$$

where

$$\begin{aligned}
\frac{\partial \dot{x}_i}{\partial x_i} + \frac{\partial \dot{p}_i}{\partial p_i} &= \frac{\partial}{\partial x_i}\left[\{\, x_i,\, p_j \,\}\frac{\partial H}{\partial p_j} + \{\, x_i,\, x_j \,\}\frac{\partial H}{\partial x_j}\right] + \frac{\partial}{\partial p_i}\left[-\{\, x_j,\, p_i \,\}\frac{\partial H}{\partial x_j}\right] \\
&= \frac{\partial}{\partial x_i}\Big[\{\, x_i,\, x_j \,\}\Big]\frac{\partial H}{\partial x_j} - \frac{\partial}{\partial p_i}\Big[\{\, x_j,\, p_i \,\}\Big]\frac{\partial H}{\partial x_j} \\
&= -(D-1)\left[\frac{2(A+B\,\mathbf{p}^2)}{A}\,\frac{dA}{d\mathbf{p}^2} - B\right] p_j \frac{\partial H}{\partial x_j} \\
&\qquad - \left[2\,\frac{dA}{d\mathbf{p}^2} + 2\,\frac{dB}{d\mathbf{p}^2}\mathbf{p}^2 + (D+1)B\right] p_j \frac{\partial H}{\partial x_j} \\
&= -\left[(D-1)\left(\frac{2(A+B\,\mathbf{p}^2)}{A}\frac{dA}{d\mathbf{p}^2}\right)\right. \\
&\qquad \left. +2\left(\frac{dA}{d\mathbf{p}^2} + \frac{dB}{d\mathbf{p}^2}\mathbf{p}^2 + B\right)\right] p_j \frac{\partial H}{\partial x_j}\,. \qquad (1.27)
\end{aligned}$$

On the other hand, using

$$\delta\mathbf{p}^2 \;=\; 2p_i\delta p_i \;=\; 2p_i\,\dot{p}_i\,\delta t \;=\; -2\,(A+B\mathbf{p}^2)\,p_j\frac{\partial H}{\partial x_j}\,\delta t\,, \qquad (1.28)$$

we have

$$\begin{aligned}
A' &= A + \frac{dA}{d\mathbf{p}^2}\delta\mathbf{p}^2 \\
&= A\left[1 - \left(\frac{2(A+B\mathbf{p}^2)}{A}\,\frac{dA}{d\mathbf{p}^2}\right) p_j\frac{\partial H}{\partial x_j}\,\delta t\right]\,, \\
A' + B'\mathbf{p}'^2 &= (A+B\mathbf{p}^2) + \left(\frac{dA}{d\mathbf{p}^2} + \frac{dB}{d\mathbf{p}^2}\,\mathbf{p}^2 + B\right)\delta\mathbf{p}^2 \\
&= (A+B\mathbf{p}^2)\left[1 - 2\left(\frac{dA}{d\mathbf{p}^2} + \frac{dB}{d\mathbf{p}^2}\,\mathbf{p}^2 + B\right) p_j\frac{\partial H}{\partial x_j}\,\delta t\right]\,, \qquad (1.29)
\end{aligned}$$

where we have used a the shorthand $A' = A(\mathbf{p}'^2)$ and $B' = B(\mathbf{p}'^2)$. Thus

$$\begin{aligned}
\frac{(A')^{D-1}(A'+B'\mathbf{p}'^2)}{A^{D-1}(A+B\mathbf{p}^2)} &= \left[\,1 - \left\{(D-1)\left(\frac{2(A+B\,\mathbf{p}^2)}{A}\frac{dA}{d\mathbf{p}^2}\right)\right.\right. \\
&\qquad \left.\left. +2\left(\frac{dA}{d\mathbf{p}^2} + \frac{dB}{d\mathbf{p}^2}\mathbf{p}^2 + B\right)\right\} p_j\frac{\partial H}{\partial x_j}\delta t\,\right]\,. \qquad (1.30)
\end{aligned}$$

Comparing Eqs. (1.27) and (1.30), it is clear that the ratio

$$\frac{d^D\mathbf{x}\,d^D\mathbf{p}}{A^{D-1}(A+B\mathbf{p}^2)} \qquad (1.31)$$

is invariant under time evolution.

This behavior of the phase space volume can be demonstrated using simple Hamiltonians. In Ref. [24], the harmonic oscillator and coulomb potential problems for the case $A = 1 + \beta \mathbf{p}^2$ and $B = \beta'$ are analyzed There, in addition to the behavior of the phase space volumes, it is found that the orbits of particles in these potentials no longer close on themselves.

For the case $B = 0$, Eq. (1.31) reduces to $d^D\mathbf{x}\, d^D\mathbf{p}/A^D$, and the interpretation of $\hbar A(p^2)$ as the momentum dependent scale of phase space volumes becomes apparent. Integrating Eq. (1.31) over space,

$$\frac{1}{V}\int \frac{d^D\mathbf{x}\, d^D\mathbf{p}}{A^{D-1}(A + B\mathbf{p}^2)} \;=\; \frac{d^D\mathbf{p}}{A^{D-1}(A + B\mathbf{p}^2)}\;, \tag{1.32}$$

we can identify

$$\rho(\mathbf{p}^2) \;=\; \frac{1}{A^{D-1}(A + B\mathbf{p}^2)} \tag{1.33}$$

as the density of states in momentum space. At high momentum where A and $B\mathbf{p}^2$ become large, $\rho(\mathbf{p}^2)$ will be suppressed. Next, we look at the direct impact that this has on the cosmological constant. In Chapter 2, it will be noticed that this momentum dependent density of states can be used to interpret an unexpected result in what would normally be an unphysical system.

1.2.3 The Cosmological Constant

The origin of the cosmological constant remains a mystery, and its understanding presents a major challenge to theoretical physics, as Refs. [27] explain in detail. It is a contentious issue for string theory, as string theory is putatively the leading candidate for a theory of quantum gravity,though various hints exist that may point towards its resolution [28, 29]. Furthermore, the problem has recently assumed added urgency due to observations that the cosmological constant is small, positive, and clearly non-zero [30].

Let us briefly identify the scope of the cosmological constant problem. At its heart, it is a disagreement between the observed energy density of the vacuum of space and the calculated value from quantum field theory. The observed value of the vacuum

energy density is

$$\begin{aligned}\frac{c^2\Lambda}{8\pi G_{\rm N}} &= c^2\rho_{\rm crit}\,\Omega_\Lambda \;=\; \left(\frac{3H_0^2c^2}{8\pi G_{\rm N}}\right)\Omega_\Lambda \\ &= (8.096\times10^{-47}\,{\rm GeV}^4/\hbar^3c^3)(\Omega_\Lambda h^2) \;\sim\; 10^{-47}\,{\rm GeV}^4/\hbar^3c^3\,. \end{aligned} \quad (1.34)$$

where H_0 is the Hubble parameter and Ω_Λ is the ratio of the cosmological constant's contribution to the total energy density of the universe and the critical density of the Friedmann equations that model cosmological expansion. The order of magnitude of this result is set by the dimensionful prefactor in the parentheses which can be expressed in terms of the Planck length $\ell_{\rm P} = \hbar/\mu_{\rm P} = \sqrt{\hbar G_{\rm N}/c^3} \sim 10^{-35}\,{\rm m}$, and the scale of the visible universe $\ell_0 = \hbar/\mu_0 \equiv c/H_0 \sim 10^{26}\,{\rm m}$ as

$$\frac{H_0^2c^2}{G_{\rm N}} \;=\; \frac{c}{\hbar^3}\,\mu_{\rm P}^2\mu_0^2 \;=\; \frac{\hbar c}{\ell_{\rm P}^2\,\ell_0^2}\,. \quad (1.35)$$

In quantum field theory (QFT), the cosmological constant is calculated as the sum of the vacuum fluctuation energies of all momentum states. This is clearly infinite, so the integral is usually cut off at the Planck scale $\mu_{\rm P} = \hbar/\ell_{\rm P}$ beyond which spacetime itself is expected to become foamy [3], and the calculation untrustworthy. For a massless particle,

$$\frac{1}{(2\pi\hbar)^3}\int^{\mu_{\rm P}} d^3\mathbf{p}\left[\frac{1}{2}\hbar\omega_p\right] = \frac{c}{4\pi^2\hbar^3}\int_0^{\mu_{\rm P}} dp\; p^3 = \frac{c}{16\pi^2\hbar^3}\,\mu_{\rm P}^4 = \frac{\hbar c}{16\pi^2}\,\frac{1}{\ell_{\rm P}^4} \sim 10^{74}\,\frac{{\rm GeV}^4}{\hbar^3c^3}, \quad (1.36)$$

which is about 120 orders of magnitude above the measured value. Note that this difference is essentially a factor of $(\ell_0/\ell_{\rm P})^2$, the scale of the visible universe in Planck units squared. The change in the density of states in the presence of modified commutation relations would lead to the slightly different calculation:

$$\frac{1}{(2\pi\hbar)^3}\int^{\infty} d^3\mathbf{p}\;\rho(\mathbf{p}^2)\left[\frac{1}{2}\hbar\omega_p\right] \;=\; \frac{c}{4\pi^2\hbar^3}\int_0^{\infty} dp\;\frac{p^3}{A(p^2)^2[A(p^2)+p^2B(p^2)]}\,. \quad (1.37)$$

For the case $A(p^2) = 1+\beta p^2$, $B(p^2) = 0$, we find, as in Ref. [31]:

$$\frac{c}{4\pi^2\hbar^3}\int_0^{\infty} dp\;\frac{p^3}{(1+\beta p^2)^3} = \frac{c}{16\pi^2\hbar^3\beta^2} = \frac{c}{16\pi^2\hbar^3}\,\mu_s^4 = \frac{\hbar c}{16\pi^2}\,\frac{1}{\ell_s^4},\; \ell_s \;=\; \frac{\hbar}{\mu_s} \;=\; \hbar\sqrt{\beta}\,. \quad (1.38)$$

The integral is finite, without a UV cutoff, due to the suppression of the contribution of high momentum states.

However, if we make the identification $\ell_s = \ell_{\rm P}$, then this result is identical to Eq. (1.36) and nothing is gained. Of course, this is not surprising given that ℓ_s is the only scale in the calculation, and effectively plays the role of the UV cutoff.

To obtain the correct value of the cosmological constant from the above expression, we must choose $\ell_s \sim \sqrt{\ell_{\rm P}\ell_0} \sim 10^{-5}\,{\rm m}$, which is too large to be the minimal length, or equivalently, $\mu_s = \hbar/\ell_s \sim \sqrt{\mu_{\rm P}\mu_0} \sim 10^{-3}\,{\rm eV}/c$, which is too small to be the UV cutoff.

We could introduce a second scale into the problem by letting $B(p^2) = \beta' \neq 0$. This leads to

$$\begin{aligned} \frac{c}{4\pi^2\hbar^3}\int_0^\infty dp\,\frac{p^3}{(1+\beta p^2)^2[1+(\beta+\beta')p^2]} &= \frac{c}{8\pi^2\hbar^3}\,\frac{1}{\beta\beta'}\left[1-\frac{\beta}{\beta'}\ln\left(1+\frac{\beta'}{\beta}\right)\right] \\ &\xrightarrow{\beta'\gg\beta} \frac{c}{8\pi^2\hbar^3}\,\frac{1}{\beta\beta'} = \frac{c}{8\pi^2\hbar^3}\,\mu_s^2\mu_s'^2 \\ &= \frac{\hbar c}{8\pi^2}\,\frac{1}{\ell_s^2\ell_s'^2}\,, \end{aligned} \tag{1.39}$$

where $\ell_s' = \hbar/\mu_s' = \hbar\sqrt{\beta'}$. If we identify $\ell_s = \ell_{\rm P}$, then we must have $\ell_s' \sim \ell_0$, which is even more problematic than $\sqrt{\ell_{\rm P}\ell_0}$.

As these considerations show, such simple choices for $A(p^2)$ and $B(p^2)$ succeed in rendering the cosmological constant finite, but do not provide an adequate suppression. Would some other choice of $A(p^2)$ and $B(p^2)$ do better? To this end, let's try to see whether we can reverse engineer these functions so that the correct order of magnitude is obtained. Let us write

$$\epsilon^4 \;=\; \int_0^\infty dp\;\rho(p^2)\,p^3\;. \tag{1.40}$$

To generate the correct value for the cosmological constant, we must have $\epsilon \sim \sqrt{\mu_{\rm P}\mu_0} = 10^{-3}{\rm eV}/c$, as we have seen. At this point, we invoke some numerology and note that if the SUSY breaking scale $\mu_{\rm SUSY}$ is on the order of a few ${\rm TeV}/c$, then the seesaw formula,

$$\epsilon \;\sim\; \frac{\mu_{\rm SUSY}^2}{\mu_{\rm P}} \;\sim\; 10^{-3}\,{\rm eV}/c\,, \tag{1.41}$$

would give the correct size for ϵ as observed by Banks [32]. This expression is reminiscent of the seesaw mechanism used to explain the smallness of neutrino masses [33].

One way to obtain this result is to have the density of states scale as $\rho(p^2) \sim p^4/\mu_{\rm P}^4$, and place the UV cutoff at $\mu_{\rm SUSY}$, beyond which the bosonic and fermionic contributions cancel. This would yield $\epsilon^4 \sim \mu_{\rm SUSY}^8/\mu_{\rm P}^4$. Unfortunately, this density of states is problematic since $p^4/\mu_{\rm P}^4 \ll 1$ for the entire integration region, so we are effectively suppressing everything. Furthermore, to obtain this suppression, we must have $A(p^2) \sim (\mu_{\rm P}/p)^{4/3} \gg 1$, making the effective value of $\hbar$, and thus the phase space volume scale for quantum effects, huge at low energies, in clear contradiction to reality.

In retrospect, this result is not surprising since raising the UV cutoff from $\sqrt{\mu_{\rm P}\mu_0} \sim 10^{-3}\,{\rm eV}/c$ to much higher values naturally requires the drastic suppression of contributions from below the cutoff. Thus, it is clear that the modification to the density of states, as suggested by the MLUR, by itself cannot solve the cosmological constant problem.

1.2.4 UV/IR connection and 'Jamming'

In the above discussion of summing over momentum states, the unstated assumption was that states at different momentum scales were independent, and that their total effect on the vacuum energy was the simple sum of their individual contributions. Of course, this assumption is the basis of the decoupling between small (IR) and large (UV) momentum scales, which underlies the use of effective field theories. However, there are hints that this assumption is what needs to be reevaluated in order to solve the cosmological constant problem.

First and foremost, the expression for the vacuum energy density itself, $H_0^2c^2/G_{\rm N} = \hbar c/\ell_{\rm P}^2\ell_0^2$, is dependent upon an IR scale ℓ_0 and a UV scale $\ell_{\rm P}$, suggesting that whatever theory that explains its value must be aware of both scales, and have some type of dynamical connection between them. Note that effective QFT's are not of this type, but string theory is, given the UV/IR mixing relations discovered in several contexts as mentioned previously.

Second, the contributions of the sub-Planckian modes ($p < \mu_{\rm P}$) independently by themselves are clearly too large, and there is a limit to the tweaking that can be done to the density of states in the IR since those modes undeniably exist. A way out of this dilemma would be to cancel the contribution of the sub-Planckian modes against those of something else, like the contribution from the trans-Planckian modes ($p > \mu_{\rm P}$), by introducing a dynamical connection between the two regimes, as suggested by Banks [32].

That the sub-Planckian and trans-Planckian modes should cancel against each other is also suggested by the following argument: Consider how the MLUR, Eq. (1.6), would be realized in field theory. The usual Heisenberg relation $\delta x\,\delta p = \hbar/2$ is a simple consequence of the fact that coordinate and momentum spaces are Fourier transforms of each other. The more one wishes to localize a wave-packet in coordinate space (smaller δx), the more momentum states one must superimpose (larger δp). In the usual case, there is no lower bound to δx: one may localize the wave-packet as much as one likes by simply superimposing states with ever larger momentum, and thus ever shorter wavelength, to cancel out the tails of the coordinate space distributions. On the other hand, the MLUR implies that if one continues superimposing states with momenta beyond $\mu_{\rm P} = 1/\sqrt{\beta}$, then δx ceases to decrease and starts increasing instead. (See Fig 1.1.) The natural interpretation of such a phenomenon would be that the trans-Planckian modes ($p > \mu_{\rm P}$) when superimposed with the sub-Planckian ones ($p < \mu_{\rm P}$) would 'jam' the sub-Planckian modes and prevent them from canceling out the tails of the wave-packets effectively.

The mechanism envisioned here is analogous to the 'jamming' behavior seen in non-equilibrium statistical physics, in which systems are found to freeze with increasing temperature [34]. In fact, it has been argued that such "freezing by heating" could be characteristic of a background independent quantum theory of gravity [35].

Note that in the above calculation, the phase space over which the integration was performed was fixed and flat. Quantum gravity will naturally change the situation, leading to a fluctuating dynamical spacetime background. Furthermore, the MLUR implies that energy-momentum space will be a fluctuating dynamical entity as well, as proposed in Ref. [36].

First, the necessity of "jamming" between the sub-Planckian and trans-Planckian modes to implement the MLUR in field theory clearly illustrates that momentum space cannot be the simple Fourier transform of coordinate space, but must rather be an independent entity.

Second, the quantum properties of spacetime geometry may be understood in terms of effective expressions that involve the spacetime uncertainties:

$$g_{ab}(x)\,dx^a dx^b \quad \rightarrow \quad g_{ab}(x)\,\delta x^a \delta x^b\,. \tag{1.42}$$

The UV/IR relation $\delta x \sim \hbar\beta\,\delta p$ in the trans-Planckian region implies that this geometry of spacetime uncertainties can be transferred directly to the space of energy-momentum uncertainties, endowing it with a geometry as well:

$$g_{ab}(x)\,\delta x^a \delta x^b \quad \rightarrow \quad G_{ab}(p)\,\delta p^a \delta p^b\,. \tag{1.43}$$

The usual intuition that local properties in spacetime correspond to non-local features of energy-momentum space (as implied by the canonical uncertainty relations) is obviated by the linear relation between the uncertainties in coordinate space and momentum space.

What would a dynamical energy-momentum space entail? Let us speculate. It has been argued, in Refs. [3] and [37], that a dynamical spacetime, with its foamy UV structure, would manifest itself in the IR via the uncertainties in the measurements of global spacetime distances as:

$$\delta\ell \;\sim\; \sqrt{\ell\,\ell_{\rm P}}\,, \tag{1.44}$$

a relation which is reminiscent of the famous result for Brownian motion derived by Einstein [38], and is also covariant in $3+1$ dimensions. Let us assume that a similar 'Brownian' relation holds in energy-momentum space due to its 'foaminess' [36]:

$$\delta\mu \sim \sqrt{\mu\,\mu_{\rm P}}\,. \tag{1.45}$$

If the energy-momentum space has a finite size, a natural UV cutoff, at $\mu_+ \gg \mu_{\rm P}$, then its fluctuation $\delta\mu_+$ will be given by $\delta\mu_+ = \sqrt{\mu_+\,\mu_{\rm P}} \gg \mu_{\rm P}$. The MLUR implies that the mode at this scale must cancel, or 'jam,' against another which shares the same δx, namely, the mode with an uncertainty given by $\delta\mu_- = \mu_{\rm P}^2/\delta\mu_+ = \mu_{\rm P}\sqrt{\mu_{\rm P}/\mu_+} = \sqrt{\mu_-\mu_{\rm P}} \ll \mu_{\rm P}$, that is:

$$\mu_- \;=\; \frac{\mu_{\rm P}^2}{\mu_+} \;=\; \frac{\delta\mu_-^2}{\mu_{\rm P}} \;\ll\; \mu_{\rm P}\,. \tag{1.46}$$

All modes between μ_- and μ_+ will 'jam.' Therefore, μ_- will be the effective UV cutoff of the momentum integral and not μ_+, which would yield

$$\epsilon^4 \;\sim\; \mu_-^4 \;\sim\; \frac{\delta\mu_-^8}{\mu_{\rm P}^4} \;\sim\; \frac{\mu_{\rm P}^8}{\mu_+^4}\,. \tag{1.47}$$

This reproduces the seesaw formula, Eq. (1.41), and if $\delta\mu_- \sim$ few TeV$/c$, we obtain the correct cosmological constant.

1.2.5 Towards a Model of 'Jamming'

In order to study the possibilities of jamming, it is essential to find a model in which it explicitly exists. Specifically, one would want a model which contains some states

for which $\delta x \sim 1/\delta p$ and other states for which $\delta x \sim \delta p$. The relationships and interactions between such states, for the reasons given in the previous section, are expected to be the place to look for jamming.

In Chapter 2, it will be shown that for the quantum harmonic oscillator with modified commutation relations, there do indeed exist both kinds of states, in which $\delta x \sim 1/\delta p$ and $\delta x \sim \delta p$. Unfortunately, these states exist in different regions of the physical parameter space. The states with $\delta x \sim 1/\delta p$ occur when the mass is taken to be positive whereas the states with $\delta x \sim \delta p$ occur when the mass is negative.

Though this result is not what we ultimately want, it is still encouraging for a couple of reasons. The existence of positive energy, normalizable states for the negative mass case is in opposition to the usual intuition and results from ordinary quantum mechanics. A physical interpretation is provided with the assistance of the results of the analysis of the correspondingly modified classical system. The other encouraging feature is that the $\delta x \sim \delta p$ behavior occurs for physical states of a system that is relatively straightforward to analyze. This provides hope that similar states exist in other familiar systems.

While consideration of other systems, such as ones containing linear potentials, the group began discussing other ways to move beyond quantum mechanics.

1.3 Supercorrelations

Another way of modifying quantum mechanics was motivated by the ability of Bell's inequalities to clearly distinguish between classical and quantum theories. It was hoped that by studying Bell-like inequalities we could gain some insight on how modifications to quantum mechanics could be tested.

As is widely known, the Bell inequalities, based on the assumption of classical local realism, are theoretically and experimentally violated by the correlations of canonical quantum mechanics [39]. This remarkable feature of quantum mechanics is often attributed to the 'non-locality' of quantum mechanics. However, even quantum correlations, with their apparent non-locality, are bounded and satisfy another inequality discovered by Cirel'son [40].

It was wondered whether modifications to quantum mechanics would share the Cirel'son bound, or would have some other, greater bound; implying the existence of states with extremely high degrees of correlations, or supercorrelations. Popescu and

Rohrlich have demonstrated that such supercorrelations can be consistent with relativistic causality (aka the no-signaling principle) [41]. Another question is whether or not the Bell and Cirel'son bounds can even be associated with the boundaries between classical, quantum, and superquantum theories in some other framework than the one in which they were originally derived.

So, we set out to find a toy model of a modified quantum mechanics in which the apparent bound on the strength of correlations surpassed the Cirel'son bound with the goal of answering these questions. We were guided by heuristic arguments, based on non-perturbative string theory, that suggest features to look for in a model of such a superquantum theory. Before discussing these arguments and the, positive, results of the search, let's review the Bell inequalities and the Cirel'son bound.

1.3.1 Correlations in Classical and Quantum Mechanics

Consider two classical variables A and B, which represent the outcomes of measurements performed on some isolated physical system by detectors 1 and 2 placed at two causally disconnected spacetime locations. Assume that the only possible values of both A and B are ± 1. Denote the state of detector 1 by a, and that of detector 2 by b. The local realism condition demands that A depend only on a, and B depend only on b and they can also depend on some hidden, but shared, information, λ.

The correlation between $A(a,\lambda)$ and $B(b,\lambda)$ is then

$$P(a,b) \;=\; \int d\lambda\, \rho(\lambda)\, A(a,\lambda)\, B(b,\lambda)\;, \qquad \int d\lambda\, \rho(\lambda) \;=\; 1\;, \tag{1.48}$$

where $\rho(\lambda)$ is the probability density of the hidden information λ. This classical correlation is bounded by the following form of Bell's inequality [42] as formulated by Clauser, Horne, Shimony and Holt (CHSH) [43]:

$$\Big| P(a,b) + P(a,b') + P(a',b) - P(a',b') \Big| \;\leq\; 2\;. \tag{1.49}$$

The quantum version of these correlations violate this bound, but are themselves bounded by a similar inequality obtained by replacing the 2 on the right-hand side with $2\sqrt{2}$. This is the famous Cirel'son bound [40], the extra factor of $\sqrt{2}$ being determined by the Hilbert space structure of QM. The same Cirel'son bound has been shown to apply for quantum field theoretic (QFT) correlations also [44].

To see how these bounds emerge, and following Refs. [40] and [45], consider 4 classical stochastic variables A, A', B, and B', each of which takes values of $+1$ or -1. Obviously, the quantity

$$C \;\equiv\; AB + AB' + A'B - A'B' \;=\; A(B+B') + A'(B-B')\;, \tag{1.50}$$

can be only $+2$ or -2 and thus the absolute value of its expectation value is bounded by 2:

$$\Big|\big\langle C\big\rangle\Big| \;=\; \Big|\big\langle AB + AB' + A'B - A'B'\big\rangle\Big| \;\leq\; 2\;. \tag{1.51}$$

This is the CHSH version of Bell's inequality. For the quantum case, we replace the classical stochastic variables with Hermitian operators acting on a Hilbert space.

Following Ref. [40], we find that if $\hat{A}^2 = \hat{A}'^2 = \hat{B}^2 = \hat{B}'^2 = 1$ and $\big[\hat{A},\hat{B}\big] = \big[\hat{A},\hat{B}'\big] = \big[\hat{A}',\hat{B}\big] = \big[\hat{A}',\hat{B}'\big] = 0$, then C is replaced by

$$\hat{C} \;=\; \hat{A}\hat{B} + \hat{A}\hat{B}' + \hat{A}'\hat{B} - \hat{A}'\hat{B}'\;, \tag{1.52}$$

from which we find

$$\hat{C}^2 \;=\; 4 - \big[\hat{A},\hat{A}'\big]\cdot\big[\hat{B},\hat{B}'\big]\;. \tag{1.53}$$

If these operators commute, we recover the classical bound of 2. If they do not, we can use the uncertainty relations $\big|\big\langle i\big[\hat{A},\hat{A}'\big]\big\rangle\big| \leq 2\|\hat{A}\|\cdot\|\hat{A}'\|$ and $\big|\big\langle i\big[\hat{B},\hat{B}'\big]\big\rangle\big| \leq 2\|\hat{B}\|\cdot\|\hat{B}'\|$ to obtain

$$\big\langle \hat{C}^2\big\rangle \;\leq\; 4 + 4\,\|\hat{A}\|\cdot\|\hat{A}'\|\cdot\|\hat{B}\|\cdot\|\hat{B}'\| \;=\; 8 \qquad\longrightarrow\qquad \Big|\big\langle\hat{C}\big\rangle\Big| \;\leq\; \sqrt{\big\langle\hat{C}^2\big\rangle} \;\leq\; 2\sqrt{2}\;, \tag{1.54}$$

which is the Cirel'son bound.

Alternatively, following Ref. [45], let $\hat{A}\,|\psi\rangle = |A\rangle$, $\hat{B}\,|\psi\rangle = |B\rangle$, $\hat{A}'\,|\psi\rangle = |A'\rangle$, and $\hat{B}'\,|\psi\rangle = |B'\rangle$. These 4 vectors all have unit norms and

$$\Big|\big\langle\hat{C}\big\rangle\Big| \;=\; \Big|\big\langle\psi\big|\hat{C}\big|\psi\big\rangle\Big| \;=\; \Big|\big\langle A\big|B+B'\big\rangle + \big\langle A'\big|B-B'\big\rangle\Big| \;\leq\; \Big\|\,|B\rangle + |B'\rangle\,\Big\| + \Big\|\,|B\rangle - |B'\rangle\,\Big\|\;, \tag{1.55}$$

which implies:

$$\Big|\big\langle\hat{C}\big\rangle\Big| \;\leq\; \sqrt{2\left(1+\mathrm{Re}\,\big\langle B\big|B'\big\rangle\right)} + \sqrt{2\left(1-\mathrm{Re}\,\big\langle B\big|B'\big\rangle\right)} \;\leq\; 2\sqrt{2}\;. \tag{1.56}$$

This second proof suggests that the Cirel'son bound is actually independent of the requirement of relativistic causality. If relativistic causality is broken, then the $\hat{A}$'s

and $\hat{B}$'s will not commute. Then $\hat{C}$ must be symmetrized as

$$\hat{C} \;=\; \frac{1}{2}\left[\left(\hat{A}\hat{B}+\hat{B}\hat{A}\right)+\left(\hat{A}\hat{B}'+\hat{B}'\hat{A}\right)+\left(\hat{A}'\hat{B}+\hat{B}\hat{A}'\right)-\left(\hat{A}'\hat{B}'+\hat{B}'\hat{A}'\right)\right]\,, \tag{1.57}$$

to make it hermitian, and its expectation value will be

$$\left\langle\hat{C}\right\rangle \;=\; \mathrm{Re}\Big[\left\langle A\middle|B+B'\right\rangle+\left\langle A'\middle|B-B'\right\rangle\Big]\,, \tag{1.58}$$

which is clearly subject to the same bound as before. So it is the Hilbert space structure of quantum mechanics alone which determines this bound.

Indeed, Popescu and Rohrlich have demonstrated that one can abstractly concoct super-quantum correlations which violate the Cirel'son bound, while still maintaining consistency with relativistic causality [41]. Their construction is information theoretical and they do not replicate the quantum formalism, as we would wish to do. Though they are not bounded by the Cirel'son bounds, such super-quantum correlations are also bounded; the value of X in Eq. (1.49) being replaced, not by $X_{\mathrm{QM}}=2\sqrt{2}$ but, by $X=4$:

$$\Big|P(a,b)+P(a,b')+P(a',b)-P(a',b')\Big| \;\leq\; 4\,. \tag{1.59}$$

Note, though, that this is not a physical bound per se, as the value of 4 is the absolute maximum that the left-hand side can possibly be since each of the 4 terms has its absolute value bounded by one. If the four correlations represented by these 4 terms were completely independent, then, in principle, there seems to be no reason why this bound cannot be saturated.

But what type of theory would predict such correlations? It has been speculated that a specific super-quantum theory could essentially be derived from the two requirements of relativistic causality and the saturation of the $X=4$ bound, in effect elevating these requirements to the status of 'axioms' which define the theory [41]. In a similar fashion, quantum mechanics may also be derivable from causality and the Cirel'son bound as 'axioms' [46]. However, to our knowledge, no concrete realization of such a program has thus far emerged.

A related development has been the proof by van Dam that super-quantum correlations which saturate the $X=4$ bound can be used to render all communication complexity problems trivial [47]. Subsequently, Brassard et al. discovered a protocol utilizing correlations with $X > X_{\mathrm{cc}} = 4\sqrt{2/3}$, which solves communication complexity problems trivially in a probabilistic manner [48]. We also do not yet

see experimental evidence of correlations that are stronger than those of quantum mechanics.

Due to these reasons, it has been speculated that nature somehow disfavors super-quantum theories, and that super-quantum correlations, especially those with $X > X_{\rm cc}$, should not exist [49]. However, none of these arguments preclude the existence of superquantum theories or of their realizations in nature.

One proposal for a super-quantum theory discussed in the literature uses a formal mathematical redefinition of the norms of vectors from the usual ℓ^2 norm to the more general ℓ^p norm [50]. In a 2D vector space with basis vectors $\{\mathbf{e}_1, \mathbf{e}_2\}$, the ℓ^p norm is

$$\Big\| \alpha \mathbf{e}_1 + \beta \mathbf{e}_2 \Big\|_p \;=\; \sqrt[p]{\alpha^p + \beta^p}\;. \tag{1.60}$$

If one identifies $|B\rangle = \mathbf{e}_1$ and $|B'\rangle = \mathbf{e}_2$, then

$$\Big\| \, |B\rangle \pm |B'\rangle \, \Big\|_p \;=\; 2^{1/p}\;. \tag{1.61}$$

Eq. (1.59) would then be saturated for the $p = 1$ case.

Unfortunately, it is unclear how one can construct a physical theory based on this proposal in which dynamical variables evolve in time while preserving total probability.

At this point, we make the very simple observation that it is the procedure of 'quantization', which takes us from classical to quantum,that increases the bound from the Bell/CHSH value of 2 to the Cirel'son value of $2\sqrt{2}$. That is, quantization increases the bound by a factor of $\sqrt{2}$. Thus, if one could perform another step of 'quantization' onto QM, would it not lead to the increase of the bound by another factor of $\sqrt{2}$, thereby take us from the Cirel'son value of $2\sqrt{2}$ to the ultimate 4? That would be marvelous, but, of course, is difficult to do explicitly. To gain some guidance on where to look, we'll turn to string theory.

From the point of view of general mathematical deformation theory [51], quantum mechanics is a theory with one deformation parameter $\hbar$, while string theory is a theory with two. The first deformation parameter of string theory is the world-sheet coupling constant α', which measures the essential non-locality of the string, and is responsible for the organization of perturbative string theory [8]. The second deformation parameter of string theory is the string coupling constant g_s, which controls the non-perturbative aspects of string theory, such as D-branes and related membrane-like solitonic excitations, and the general non-perturbative string field

theory [52]. Therefore, string theory can be expected to be more 'quantum' in some sense than canonical quantum mechanics, given the presence of the second deformation parameter.

As previously mentioned, super-quantum correlations point to a non-locality which is more non-local, so to speak, than the non-locality of quantum mechanics and quantum field theory. However, quantum field theories are actually local theories, and true non-locality is expected only in theories of quantum gravity. That quantum gravity must be non-local stems from the requirement of diffeomorphism invariance, as has been known from the pioneering days of that field [53]. So, by looking at string theory, which should contain quantum gravity, it is possible that we can encounter specific consequences of non-locality with which we can use to construct our model.

1.3.2 Guidance from String Theory

Given that a super-quantum theory is may be more 'quantum' than ordinary quantum mechanics, let us now consider the the extreme quantum limit of quantum mechanics, $\hbar \to \infty$. Therefore, the $\hbar \to \infty$ limit of quantum mechanics may also be a sensible theory, but at the same time quite different from quantum mechanics. After all, if the $\hbar \to 0$ limit is to recover classical mechanics, with the Bell bound of $X_{\text{Bell}} = 2$, and apparently quite different from quantum mechanics, it may not be too farfetched to conjecture that the $\hbar \to \infty$ limit would flow to a super-quantum theory, with the super-quantum bound of $X = 4$.

What would the $\hbar \to \infty$ limit mean from the point of view of the path integral? Given that the path-integral measure is $e^{iS/\hbar}$, in the $\hbar \to \infty$ limit this measure will be unity for any S, and all histories in the path integral contribute with equal unit weight. Similarly all phases, measured by $e^{iS/\hbar}$, will be washed out. Because the phases are washed out, we cannot distinguish between $|B\rangle + |B'\rangle$ and $|B\rangle - |B'\rangle$ as $-1 = e^{i\pi}$ and can be absorbed into a phase of $|B'\rangle$). This suggests

$$\left\| \, |B\rangle \pm |B'\rangle \, \right\| \;=\; \Big\| |B\rangle \Big\| + \Big\| \, |B'\rangle \, \Big\| \,, \tag{1.62}$$

which, if applied to the proof of the Cirel'son bound given earlier, leads to the super-quantum bound of 4. This property is similar to what was obtain by replacing the ℓ^2 norm with an ℓ^1 (or ℓ^∞) norm, *cf.* Eq. (1.61), but presumably, unlike the change of norm, this relation is independent of the choice of basis. This argument seems to suggest that the $\hbar \to \infty$ limit is indeed super-quantum.

However, this observation is perhaps a bit naive since the proof of the Cirel'son bound itself may no longer be valid under the washed-out of all phases. Let us invoke here an optical-mechanical analogy: geometric optics is the zero wavelength limit of electromagnetism, which would correspond to the $\hbar \to 0$ limit of quantum mechanics. The $\hbar \to \infty$ limit of quantum mechanics would therefore correspond the extreme near field limit of electromagnetism, and in that case, the superposition of waves is washed out. Note also, that from a geometric point of view, the holomorphic sectional curvature $2/\hbar$ of the projective Hilbert space CP^N of canonical quantum mechanics goes to zero as $\hbar \to \infty$, and CP^N becomes just C^N. For a general discussion of the geometry of quantum theory and its relevance for quantum gravity and string theory, see [35]. From these observations, it is clear that the usual Born rule to obtain probabilities will no longer apply.

But before we ask what rule should replace that of Born, let us confront the obvious problem that in the limit $\hbar \to \infty$, only the ground state of the Hamiltonian will remain in the physical spectrum and the theory will be rendered trivial. This can also be argued via the general Feynman-Schwinger formulation of quantum mechanics [54]:

$$\delta S \, \psi \;=\; i\hbar \, \delta\psi \; . \tag{1.63}$$

By taking the $\hbar \to \infty$ limit, we eliminate the classical part δS, so that we are left only with $\delta\psi = 0$ and thus ψ must be a constant $\psi \equiv |\psi|$, a trivial result.

Could the $\hbar \to \infty$ limit of quantum mechanics be made less-than-trivial? Consider the corresponding $\alpha' \to \infty$ and $g_s \to \infty$ limits in string theory. In the $\alpha' \to \infty$ limit of string theory, as opposed to the usual $\alpha' \to 0$ field theory limit, one seemingly ends up with an infinite number of fields and a non-trivial higher spin theory [55].

The $g_s \to \infty$ limit of string theory appears in the context of M-theory, one of whose avatars arises in the $g_s \to \infty$ limit of type-IIA string theory [52]. Neither the high spin theory, nor the avatars of M-theory are trivial, the presence of the tunable second deformation parameter saving them from triviality. Thus, the introduction of a second tunable parameter into quantum mechanics, perhaps something related to Newton's gravitational constant G_N, may be necessary for the limit $\hbar \to \infty$ to be non-trivial.

Another issue here is that of interpretation: in the classical ($\hbar \to 0$) case we have one trajectory, and one event (position, for example) at one point in time. One could speculate that the super-quantum ($\hbar \to \infty$) limit would correspond to the complement of all other virtual trajectories. A general linear map relating virtual and classical trajectories is presumably non-symmetric (there are in principle more

possibilities than actual events). Very naively, one would then expect that if we impose the condition that all possible events can be 'mapped' to actual events, we could end up with a symmetric linear map corresponding to quantum theory ($\hbar \sim 1$), with a natural 'map' between the actual events and possibilities, presumably realized by the Born probability rule. Note that according to this scenario, the super-quantum theory would correspond essentially to a theory of possibilities and without actual events, so interpretation may be difficult.

Also, one could imagine the existence of a new experimental 'knob' needed to test a doubly quantized approach to super-quantum correlations. In the classic experimental tests of the violation of Bell's inequalities [39], such a 'knob' is represented by the relative angle between polarization vectors of entangled photos. If we have another quantization, there should be, in principle, another angle-like "knob." Thus, the usual one dimensional data plot [39] should be replaced by a two dimensional surface. By cutting this surface at various values of the new, second angle, we should be able to obtain one dimensional cuts for which the value of the CHSH bound varies depending on the cut: exceeding $2\sqrt{2}$ in some cases, and perhaps not exceeding 2 in others. Thus, the second "knob" may very well allow us to interpolate between the classical, quantum, and superquantum cases.

Putting this insight together, we are lead to believe that a toy model of supercorrelations should possibly contain 1) some increased degeneracy in the phases structure, and 2) some extra degree or parameter of quantization, while 3) possibly containing interpretational issues with regards to probabilities.

Before discussing our progress in the search for such a toy model, it should be mentioned that though normally correlations are thought of in the context of quantum communication and information, signatures of supercorrelations could manifest themselves elsewhere, such as in cosmology. The current understanding of the large scale structure of the universe, *i.e.* the distribution of galaxies and galaxy clusters, is that they are seeded by quantum fluctuations in the early universe. In standard calculations, it is assumed that the quantum correlations of these fluctuations are Gaussian,though non-Gaussian correlations have also been considered. If there were to exist correlations in the early universe that were in fact super-quantum, their signature could appear as some type of deviation from the standard predicted large scale structure based on Gaussian correlations.

1.3.3 Galois Fields

A key piece of inspiration came from a paper by Nambu [56], in which he was describing the possibility of defining quantum field theory on a special type of discretized position space. He chose to let position be an element of a Galois field, as opposed to the usual real number field.

Galois fields are group theoretic generalizations of the real and complex numbers in which the normal operations of arithmetic are definable, though, not all of the normal rules apply. Specifically, there is an identification of elements via the modulo operation that turns regular arithmetic into modular arithmetic. Once the modular arithmetic is suitably restricted, to avoid zero having nonzero factorizations and similar problems, by defining equivalence to be with respect to the modulo operation involving a prime number of the power of a prime number, spaces containing only a finite number of elements, but having many of the usual properties of the real numbers, can be constructed. The sizes of the spaces are essentially determined by the primes and powers chosen for the modulo relation. See Ref. ([57]) for a complete introduction to finite fields.

A property of lengths on these spaces that Nambu noted, while long known in mathematics, became the centerpiece for our analysis. Namely, as a consequence of Fermat's Little Theorem:

$$(a+b)^p = a + b = a^p + b^p \mod p \ , \tag{1.64}$$

which looks similar to the attempted modified norm in Ref. [50], discussed earlier.

As will be explained at length in Chapter 3, to try to implement this norm in as simple of a way as possible, we took the Galois fields to be the base number space on which vector fields are defined. Using these vector fields to replace the normal Hilbert spaces, we were able to construct toy models that 1) contained the discreteness of the underlying number field, 2) had large degeneracies in the phase structure arising from the modular arithmetic, and not surprising 3) have to be interpreted carefully in order to yield a theory that could be called both physical and quantum.

The resulting models lead to some surprising conclusions. In the simplest models, the CHSH correlations had a maximum value of 2, even though the predictions it generates can be argued to be not reproducible by classical theories. This line of arguments follows those set out in the Kochen-Specker theorem [58] and developed in the context of correlations by Hardy [59] and Greenberger, Horne, Shimony, and Zeilinger [60]; the gist of which is that the entanglement of variables in quantum

mechanics lead to predictions that are logically inconsistent from a classical perspective. Thus, the roles of the Bell/CHSH bound and the Cirel'son bound as indicators for what is a classical or quantum theory are called into question.

In a slightly less simple model, the base number field of the vector spaces is extended to include numbers that are analogous to complex numbers. Concepts similar to Hermiticity and unitarity are uncovered, though, difficulty is had in interpreting the predictions of these models in terms of probabilities, though, this difficulty is addressed by forgoing a rigidly probabilistic interpretation. These models are also logically distinguishable from classical theories and have states whose CHSH correlator value is 4. Extending the mathematical structures encountered in these particular models to function spaces is currently in progress, with the hope of recovering the previous results while making connections to 'real' systems, as opposed to abstracted, toy systems.

Chapter 2

Minimal Length through Modified Commutation Relations

2.1 Background

The beginnings of the following analysis can be traced to the work of Kempf during the 90's. Specifically, while studying Bargmann-Fock representations of quantum group symmetric Heisenberg algebras [23], he demonstrated that the deformation of the commutation relations between position and momentum operators that is induced by the quantum group deformation of the Heisenberg algebra leads to minimum values of the uncertainties of those operators.

In that paper, Kempf begins by constructing q-deformed creation and annihilation operators, $\hat{a}$ and $\hat{a}^\dagger$, and then, by ansatz, writes the position and momentum operators as particular linear combinations of $\hat{a}$ and $\hat{a}^\dagger$. In one dimension, these look like

$$\hat{x} = L(\hat{a} + \hat{a}^\dagger),\ \hat{p} = K(\hat{a} - \hat{a}^\dagger) \tag{2.1}$$

where

$$K = \frac{\hbar}{4L}(q^2 + 1). \tag{2.2}$$

The minimum values of the uncertainties of these operators are found to be

$$\Delta x_0 = L\sqrt{(q^2-1)/q^2},\ \Delta p_0 = K\sqrt{(q^2-1)/q^2}. \tag{2.3}$$

With this identification, and the assumption that the product $\Delta x_0 \Delta p_0$ is significantly

smaller than $\hbar/2$, the commutation relation between $\hat{x}$ and $\hat{p}$ can be written

$$[\hat{x}, \hat{p}] = i\hbar + \frac{4i}{\hbar}\left(\hat{x}^2(\Delta p_0)^2 + \hat{p}^2(\Delta x_0)^2)\right). \tag{2.4}$$

This was followed by Kempf, Mangano, and Mann [18], in which the authors began by finding a Hilbert space representation for the position and momentum operators that obeyed the assumed relation

$$[\,\hat{x},\,\hat{p}\,] \;=\; i\hbar(1+\beta\hat{p}^2). \tag{2.5}$$

As can be seen by comparing Eq. (2.4) and Eq. (2.5), Δp_0 is expected to be zero and Δx_0 is expected to be proportional to $\hbar\sqrt{\beta}$.

This modification allows for the modeling of systems which obey the minimal length uncertainty relation (MLUR), as described in [19]:

$$\Delta x \;\geq\; \frac{\hbar}{2}\left(\frac{1}{\Delta p} + \beta\,\Delta p\right)\;. \tag{2.6}$$

The exact form of the momentum space representations used are as follows:

$$\begin{aligned} \hat{x} &= i\hbar\,(1+\beta p^2)\,\frac{\partial}{\partial p}\;, \\ \hat{p} &= p\;. \end{aligned} \tag{2.7}$$

They then calculated the energy eigenvalues and eigenstates for a 1-d harmonic oscillator and found them to be

$$E_n = \hbar\omega\left(n+\frac{1}{2}\right)\left(\frac{1}{4\sqrt{r}} + \sqrt{1+\frac{1}{16r}}\right) + \hbar\omega\frac{n^2}{4\sqrt{r}} \tag{2.8}$$

and

$$\psi_n(p) \propto \frac{1}{(1+\beta p^2)^{\sqrt{q+r}_n}} F\left(a_n, -n; c_n; \frac{1}{2} + i\frac{\sqrt{\beta}}{2}p\right) \tag{2.9}$$

where

$$\begin{aligned} r &= (4m^2\omega^2\hbar^2\beta^2)^{-1}, \\ \sqrt{q+r}_n &= \frac{1}{2}(n+\frac{1}{2}) + \frac{1}{4}\sqrt{1+16r}, \\ a_n &= -n - \sqrt{1+16r}, \\ c_n &= 1 - 2\sqrt{q+r}_n, \end{aligned} \tag{2.10}$$

and $F()$ is a hypergeometric function.

Chang, Minic, Okamura, and Takeuchi were able to markedly simplify the solution from [18] and were thus able to extend it to an n-dimensional harmonic oscillator [64].

The analysis in the remainder of this chapter takes a detailed look at the 1-d case of the solution from [64]. We'll start by recalling pertinent details of the 1-d harmonic oscillator in canonical quantum mechanics. The solutions from [64] will then be given explicitly while being extended to the case of negative mass, the uncertainties in position and momentum will be calculated explicitly, and all results will be compared to their classical counterparts. The key findings from this analysis were published in [65].

This analysis was performed mainly to study the behavior of the uncertainty relations while they are under the influence of this particular form of minimal length scale. Specifically, we were looking to find states for which the uncertainties in position and momentum are proportional, as mentioned in the last chapter, and as could naively be expected from examination of Fig. 1.1.

An unexpected result was the appearance of physical bound states for an anharmonic oscillator, as there are not usually physical solutions for that potential in canonical quantum mechanics. Not only was their existence surprising, these states are precisely the states with the uncertainty behavior we were looking for. It will be exciting to study this relationship in the future.

2.2 Canonical Harmonic Oscillators

As stated in the introduction, we have modified the canonical commutation relations between $\hat{x}$ and $\hat{p}$ and then studied the effect this has in the context of the usual harmonic oscillator. Before we begin to look at the details of that study, we should refresh our memory on what happens in the canonical case. The following is a brief overview that can be found in any suitable introductory text on the subject, such as Shankar [61] or Schwabl [62].

In canonical quantum mechanics, the relation between the operators that represent position and momentum can be specified by the following commutation relation:

$$[\,\hat{x},\,\hat{p}\,] \;=\; i\hbar \tag{2.11}$$

We then recognize that suitable representations for these operators, when acting on a Hilbert space, are

$$\begin{aligned} \hat{x} &= x, \\ \hat{p} &= i\hbar \frac{\partial}{\partial x} \ . \end{aligned} \tag{2.12}$$

since

$$\begin{aligned} [\,\hat{x},\,\hat{p}\,]\psi(x) &= xi\hbar \frac{\partial}{\partial x}\psi(x) - i\hbar \frac{\partial}{\partial x}\, x\,\psi(x) \\ &= xi\hbar \frac{\partial}{\partial x}\psi(x) - i\hbar\,\psi(x) - i\hbar\, x\frac{\partial}{\partial x}\psi(x) \\ &= i\hbar\,\psi(x) \end{aligned} \tag{2.13}$$

The Schrödinger equation for a harmonic oscillator is then

$$\begin{aligned} E\,\psi(x) &= \left(\frac{\hat{p}^2}{2m} + \frac{k\hat{x}^2}{2}\right)\psi(x) \\ &= -\frac{\hbar^2}{2m}\frac{\partial^2}{\partial x^2}\psi(x) + \frac{kx^2}{2}\psi(x) \end{aligned} \tag{2.14}$$

where E is the total energy of the particle, m is the particle's mass, and k is the spring constant. Proceeding with the solution, we can write that

$$\begin{aligned} -\frac{2mE}{\hbar^2}\,\psi(x) &= \frac{\partial^2}{\partial x^2}\psi(x) - \frac{mkx^2}{\hbar^2}\psi() \\ -\epsilon\,\psi(x) &= \frac{\partial^2}{\partial x^2}\psi(x) - \frac{x^2}{a^4}\psi(x) \end{aligned} \tag{2.15}$$

where we have defined

$$\epsilon = \frac{2mE}{\hbar^2}\,,\ a \ = \ \left[\frac{\hbar^2}{k|m|}\right]^{1/4}. \tag{2.16}$$

Though the absolute value seems out of place, as the mass should never be negative, we'll use this definition in anticipation of later analysis. Collecting terms, we see that

$$\frac{\partial^2}{\partial x^2}\psi(x) + \left(-\frac{x^2}{a^4} + \epsilon\right)\psi(x) = \ 0 \tag{2.17}$$

By substituting $y = x/a$, the equation becomes

$$\frac{\partial^2}{\partial y^2}\psi(y) + (a^2\epsilon - y^2)\psi(y) = \ 0 \tag{2.18}$$

If we replace $\psi(y)$ with $\phi(y)e^{-y^2/2}$ and use a prime to indicate derivatives, this equation will transform into the eigenvalue equation

$$\psi''(y) - 2y\psi'(y) = -(a^2\epsilon - 1)\psi(y) \tag{2.19}$$

The equation has solutions when $a^2\epsilon - 1$ is an even integer and those solutions are the Hermite polynomials, $H_n(y)$:

$$\epsilon_n = \frac{2n+1}{a^2}\,,\ \psi_n(x) \propto e^{-x^2/2a^2} H_n(x/a) \tag{2.20}$$

Utilizing the orthogonality relation between the Hermite polynomials,

$$\int_{-\infty}^{+\infty} e^{-x^2} H_n(x) H_m(x) dx = 2^n n! \sqrt{\pi}\delta_{nm}, \tag{2.21}$$

we find that the normalized energy eigenstates are

$$\psi_n(x) = (2^n n! \sqrt{\pi} a)^{-1/2} e^{-x^2/2a^2} H_n(x/a). \tag{2.22}$$

To calculate the uncertainties in position and momentum, it is easiest to use the creation and annihilation operators, $\hat{a}$ and $\hat{a}^\dagger$, which in this case are given by:

$$\hat{a} = \frac{\sqrt{km}\hat{x} + i\hat{p}}{\sqrt{2\sqrt{km}\hbar}}, \quad \hat{a}^\dagger = \frac{\sqrt{km}\hat{x} - i\hat{p}}{\sqrt{2\sqrt{km}\hbar}} \tag{2.23}$$

These operators have the following effects on energy eigenstates:

$$\begin{aligned} \hat{a}^\dagger \psi_n(x) &= \sqrt{n+1}\ \psi_{n+1}(x), \\ \hat{a}\ \psi_n(x) &= \sqrt{n}\ \psi_{n-1}(x). \end{aligned} \tag{2.24}$$

Rewriting $\hat{a}$ and $\hat{a}^\dagger$ in terms of $\hat{x}$ and $\hat{p}$ yields

$$\hat{x} = \sqrt{\frac{\hbar}{2\sqrt{km}}}(\hat{a} + \hat{a}^\dagger),\ \hat{p} = -i\sqrt{\frac{\hbar\sqrt{km}}{2}}(\hat{a} - \hat{a}^\dagger). \tag{2.25}$$

Using Dirac notion, $\psi_n(x) = |n\rangle$, we see that the moments and uncertainty of $\hat{x}$ in an energy eigenstate are

$$\begin{aligned} \langle n|\,\hat{x}\,|n\rangle &= \sqrt{\frac{\hbar}{2\sqrt{km}}}\,\langle n|\,(\hat{a} + \hat{a}^\dagger)\,|n\rangle \\ &= \sqrt{\frac{\hbar}{2\sqrt{km}}}(\sqrt{n}\langle n|n-1\rangle + \sqrt{n+1}\langle n|n+1\rangle) \\ &= 0, \end{aligned} \tag{2.26}$$

$$\begin{aligned}
\langle n|\,\hat{x}^2\,|n\rangle &= \frac{\hbar}{2\sqrt{km}}\,\langle n|\,(\hat{a}^2+\hat{a}^\dagger\hat{a}+\hat{a}\hat{a}^\dagger+\hat{a}^{\dagger 2})\,|n\rangle \\
&= \frac{\hbar}{2\sqrt{km}}\Big(\sqrt{n}\sqrt{n-1}\langle n|n-2\rangle \\
&\qquad +((n+1)+n)\langle n|n\rangle+\sqrt{n+1}\sqrt{n+2}\langle n|n+2\rangle\Big) \\
&= \frac{\hbar}{2\sqrt{km}}(2n+1),
\end{aligned}$$

and

$$(\Delta x)^2=\langle x^2\rangle-\langle x\rangle^2=\frac{\hbar}{2\sqrt{km}}(2n+1). \tag{2.27}$$

Likewise, the moments and uncertainty of $\hat{p}$ in an energy eigenstate are

$$\begin{aligned}
\langle n|\,\hat{p}\,|n\rangle &= -i\sqrt{\frac{\hbar\sqrt{km}}{2}}\,\langle n|\,(\hat{a}-\hat{a}^\dagger)\,|n\rangle \\
&= -i\sqrt{\frac{\hbar\sqrt{km}}{2}}(\sqrt{n}\langle n|n-1\rangle-\sqrt{n+1}\langle n|n+1\rangle) \\
&= 0,
\end{aligned} \tag{2.28}$$

$$\begin{aligned}
\langle n|\,\hat{p}^2\,|n\rangle &= -\frac{\hbar\sqrt{km}}{2}\,\langle n|\,(\hat{a}^2-\hat{a}^\dagger\hat{a}-\hat{a}\hat{a}^\dagger+\hat{a}^{\dagger 2})\,|n\rangle \\
&= -\frac{\hbar\sqrt{km}}{2}\Big(\sqrt{n}\sqrt{n-1}\langle n|n-2\rangle \\
&\qquad -((n+1)+n)\langle n|n\rangle+\sqrt{n+1}\sqrt{n+2}\langle n|n+2\rangle\Big) \\
&= \frac{\hbar\sqrt{km}}{2}(2n+1),
\end{aligned}$$

and

$$(\Delta p)^2=\langle p^2\rangle-\langle p\rangle^2=\frac{\hbar\sqrt{km}}{2}(2n+1). \tag{2.29}$$

Note that when the mass or the spring constant are changed to be negative in Eq. (2.14), making the harmonic oscillator into an anharmonic one, the resulting differential equations are solved by complex-indexed parabolic cylinder functions. These functions are not square-integrable for real values of the energy, which implies that there are no physical states that correspond to these negative parameter variants of the harmonic oscillator potential in canonical quantum mechanics.

2.3 Energy Eigenstates of The Deformed Harmonic Oscillator

We begin the consideration of the effects of the modified commutation relations by starting with the same quadratic harmonic oscillator potential. The Schrödinger equation for the harmonic oscillator in the representation from Eq. (2.7) is

$$\begin{aligned} \hat{H}\,\Psi(p) = \left[\frac{k\hat{x}^2}{2} + \frac{\hat{p}^2}{2m}\right]\Psi(p) &= E\,\Psi(p), \\ \left[-\frac{\hbar^2 k}{2}\left\{(1+\beta p^2)\frac{\partial}{\partial p}\right\}^2 + \frac{p^2}{2m}\right]\Psi(p) &= E\,\Psi(p)\,. \end{aligned} \tag{2.30}$$

At this point, it is not assumed that $m > 0$, so the kinetic energy term can potentially contribute with either sign. While this seems an arbitrary thing to do, as has been mentioned before, it will be of interest shortly.

This differential equation is rendered manageable with the help of the following variable transformation from [64]: p maps to ρ via

$$\rho \equiv \frac{1}{\sqrt{\beta}}\arctan(\sqrt{\beta}p)\,, \tag{2.31}$$

which maps the region $-\infty < p < \infty$ to

$$-\frac{\pi}{2\sqrt{\beta}} < \rho < \frac{\pi}{2\sqrt{\beta}}\,. \tag{2.32}$$

The $\hat{x}$ and $\hat{p}$ operators are then

$$\begin{aligned} \hat{x} &= i\hbar\frac{\partial}{\partial\rho}\,, \\ \hat{p} &= \frac{1}{\sqrt{\beta}}\tan(\sqrt{\beta}\rho)\,, \end{aligned} \tag{2.33}$$

and the inner product in momentum space is

$$\langle\phi|\psi\rangle = \int_{-\pi/2\sqrt{\beta}}^{\pi/2\sqrt{\beta}} d\rho\;\phi^*(\rho)\,\psi(\rho)\,. \tag{2.34}$$

Note that $\hat{x}$ now resembles the usual representation of the momentum operator, but for ρ, and is thus the wave-number operator in ρ-space. This implies that the

Fourier coefficients of the wave-function in ρ-space may be interpreted as providing the probability amplitudes for a discretized x-space.

In ρ-space, Eq. (2.30) becomes:

$$\left[-\frac{\hbar^2 k}{2} \frac{\partial^2}{\partial \rho^2} + \frac{1}{2m\beta} \tan^2 \sqrt{\beta}\rho \right] \Psi(\rho) \;=\; E\, \Psi(\rho) \; . \tag{2.35}$$

Under this transformation, the usual potential energy term, $k\hat{x}^2/2$, effectively becomes the kinetic energy term, and the usual kinetic energy term, $\hat{p}^2/2m$, effectively becomes the potential energy term. Explicitly, we now have a tangent-squared potential which is 'inverted' when $1/m < 0$.

The following dimensionless parameters and dimensionless variable help to simplify later analysis:

$$\begin{aligned} \kappa &\equiv \left[\, \beta^2 \hbar^2 k |m| \,\right]^{1/4} \;=\; \frac{\Delta x_{\min}}{a} \; , \\ \varepsilon &\equiv \frac{2|m|E\beta}{\kappa^2} \; , \\ \xi &\equiv \frac{\sqrt{\beta}\rho}{\kappa} \; ; \end{aligned} \tag{2.36}$$

where the length-scale a was introduced in Eq. (2.16). As m is no longer assumed to be positive, the absolute value of m will be used for clarity. The constant κ is a ratio comparing the characteristic length of the harmonic oscillator to the minimal length while ε is the energy of the harmonic oscillator appropriately scaled by said ratio. The dimensionless variable ξ is the appropriately scaled kinematic variable, which is constrained to the range

$$-\frac{\pi}{2\kappa} < \xi < \frac{\pi}{2\kappa} \; . \tag{2.37}$$

The ξ-space inner product is

$$\langle \phi | \psi \rangle \;=\; \frac{\kappa}{\sqrt{\beta}} \int_{-\pi/2\kappa}^{\pi/2\kappa} d\xi \; \phi^*(\xi)\, \psi(\xi) \; . \tag{2.38}$$

Since the integral in the inner product in ξ-space is dimensionless, the dimension of the inner product is contained in the prefactor, $1/\sqrt{\beta}$.

After these substitutions, the Schrödinger equation is now

$$\left[\; \frac{\partial^2}{\partial \xi^2} \mp \frac{1}{\kappa^2} \tan^2 \kappa\xi + \varepsilon \; \right] \Psi(\xi) = 0 \; , \tag{2.39}$$

where the minus sign in front of the tangent-squared potential is for the case $m > 0$, and the plus sign for the case $m < 0$.

Let $\Psi(\xi) = c^\lambda f(s)$, where $s \equiv \sin\kappa\xi$, $c \equiv \cos\kappa\xi = \sqrt{1-s^2}$, and λ is a constant to be determined. The variable s is in the range

$$-1 < s < 1 \,, \tag{2.40}$$

with inner product given by

$$\langle\phi|\psi\rangle \;=\; \frac{1}{\sqrt{\beta}} \int_{-1}^{1} \frac{ds}{c}\; \phi^*(s)\, \psi(s) \,. \tag{2.41}$$

When written in terms of s and $f(s)$, Eq. (2.39) becomes

$$\begin{aligned} &(1-s^2) f'' - (2\lambda+1)\, s\, f' \\ &+ \left[\left\{ \frac{\varepsilon}{\kappa^2} - \lambda \right\} + \left\{ \lambda(\lambda-1) \mp \frac{1}{\kappa^4} \right\} \frac{s^2}{c^2} \right] f = 0 \,. \end{aligned} \tag{2.42}$$

The parameter λ can be determined by requiring that the coefficient of the tangent-squared term should vanish:

$$\lambda(\lambda-1) \mp \frac{1}{\kappa^4} = 0 \,. \tag{2.43}$$

This is done so that the tangent-squared term, and its singularity at $\kappa\xi = \pm\pi/2$, is removed from the equation. The solutions for λ are

$$\lambda \;=\; \begin{cases} \dfrac{1}{2} + \sqrt{\dfrac{1}{4} + \dfrac{1}{\kappa^4}} \;\equiv\; \lambda_+ & (m > 0) \,, \\[2ex] \dfrac{1}{2} + \sqrt{\dfrac{1}{4} - \dfrac{1}{\kappa^4}} \;\equiv\; \lambda_- & (m < 0) \,, \end{cases} \tag{2.44}$$

where we have chosen the branches for which $\lambda \geq 1/2$ to prevent the inner-product, Eq. (2.41), from becoming infinite at the domain boundaries.

Note that $1 < \lambda_+$ while $\frac{1}{2} \leq \lambda_- < 1$, and that $\lambda_\pm \to 1$ in the limit $\kappa^2 = \beta\hbar\sqrt{k|m|} \to \infty$. The dependence of $\lambda_\pm$ on κ^2 is shown in Fig. 2.1. The λ_- branch does not extend below $\kappa^2 = 2$.

Setting $\lambda = \lambda_+$ for $m > 0$, and $\lambda = \lambda_-$ for $m < 0$ simplifies Eq. (2.42) to

$$(1-s^2)\, f'' - (\,2\lambda+1\,)\, s\, f' + \left(\frac{\varepsilon}{\kappa^2} - \lambda \right) f = 0 \,, \tag{2.45}$$

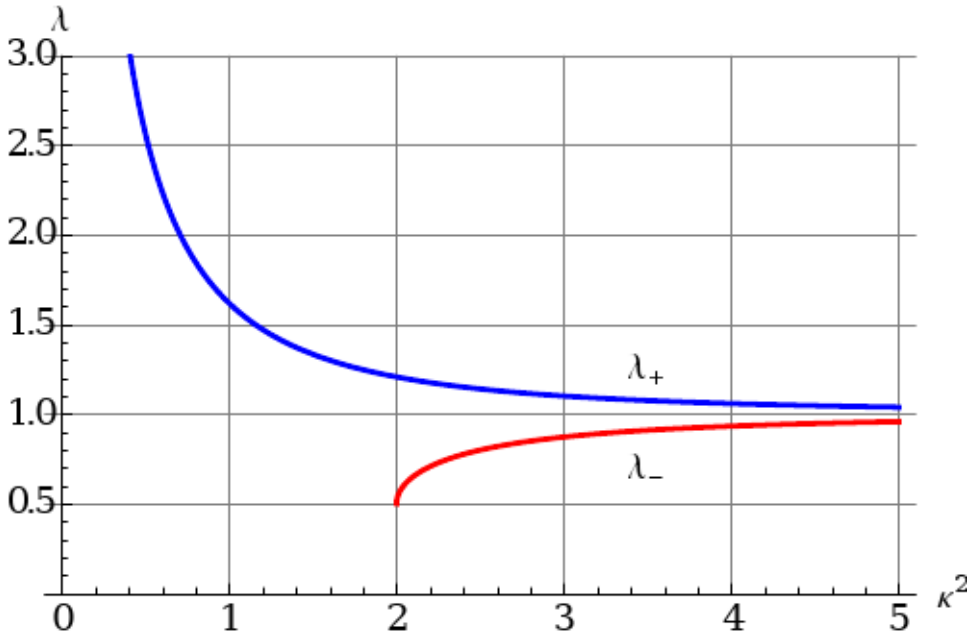

Figure 2.1: Plots of λ_+ (blue) and λ_- (red), Eq. (2.44), as functions of $\kappa^2 = \beta\hbar\sqrt{k|m|}$.

the sign of m being encoded in the value of λ. Since $f(s)$ should be non-singular at $s = \pm 1$, we demand a polynomial solution to Eq. (2.45). This requirement imposes the following condition on the coefficient of f:

$$\frac{\varepsilon}{\kappa^2} - \lambda = n\,(\,n + 2\lambda\,)\,, \tag{2.46}$$

where n is a non–negative integer [67].

Eq. (2.45) becomes

$$(1 - s^2)f'' - (\,2\lambda + 1\,)\,s\,f' + n\,(\,n + 2\lambda\,)\,f = 0\,, \tag{2.47}$$

the solution of which is given by the Gegenbauer polynomial:

$$f(s) \;=\; C_n^{\lambda}(s)\,. \tag{2.48}$$

The Gegenbauer polynomials satisfy the following orthogonality relation:

$$\int_{-1}^{1} c^{2\lambda-1}\,C_n^{\lambda}(s)\,C_m^{\lambda}(s)\,ds \;=\; \frac{2\pi\,\Gamma(n+2\lambda)}{[\,2^{\lambda}\Gamma(\lambda)\,]^2\,n!\,(n+\lambda)}\,\delta_{nm}\,. \tag{2.49}$$

The energy eigenvalues follow from the condition Eq. (2.46). Replacing λ with $\lambda_\pm$, we find

$$\begin{aligned}
\varepsilon_n^{(\pm)} &= \kappa^2 \left[n^2 + (2n+1)\lambda_\pm \right] \\
&= \frac{n^2 + (2n+1)\lambda_\pm}{\sqrt{\lambda_\pm |\lambda_\pm - 1|}} \\
&= \kappa^2 \left(n^2 + n + \frac{1}{2} \right) + (2n+1) \sqrt{\frac{\kappa^4}{4} \pm 1} \,,
\end{aligned} \tag{2.50}$$

or in the original dimensionful units,

$$\begin{aligned}
E_n^{(\pm)} &= \frac{1}{2\beta|m|} \frac{n^2 + (2n+1)\lambda_\pm}{\lambda_\pm |\lambda_\pm - 1|} \\
&= \hbar\omega \left[\left(n + \frac{1}{2} \right) \sqrt{\frac{\beta^2 m^2 \hbar^2 \omega^2}{4} \pm 1} \right. \\
&\qquad \left. + \left(n^2 + n + \frac{1}{2} \right) \frac{\beta |m| \hbar \omega}{2} \right] \\
&= \frac{k}{2} \left[\left(n + \frac{1}{2} \right) \sqrt{(\Delta x_{\min})^4 \pm 4a^4} \right. \\
&\qquad \left. + \left(n^2 + n + \frac{1}{2} \right) (\Delta x_{\min})^2 \right] ,
\end{aligned} \tag{2.51}$$

where $\omega = \sqrt{k/|m|}$.

For the $m > 0$ case, we can take the limit $\Delta x_{\min} = \hbar\sqrt{\beta} \to 0$, and we recover

$$\lim_{\Delta x_{\min} \to 0} E_n^{(+)} \;=\; ka^2 \left(n + \frac{1}{2} \right) \;=\; \hbar\omega \left(n + \frac{1}{2} \right) \tag{2.52}$$

as was found earlier in the chapter for the canonical harmonic oscillator.

For the $m < 0$ case, it is clear that we must have $\Delta x_{\min} \geq \sqrt{2}a$ for the square-root in Eq. (2.51) to remain real. Therefore, the limit $\Delta x_{\min} = \hbar\sqrt{\beta} \to 0$ cannot be taken in this case for non-zero a.

The two cases converge when $|m| \to \infty$, at which $a = 0$, and we find that the energy levels in that limit are

$$\lim_{|m| \to \infty} E_n^{(\pm)} \;=\; \frac{k}{2} (\Delta x_{\min})^2 (n+1)^2 \,. \tag{2.53}$$

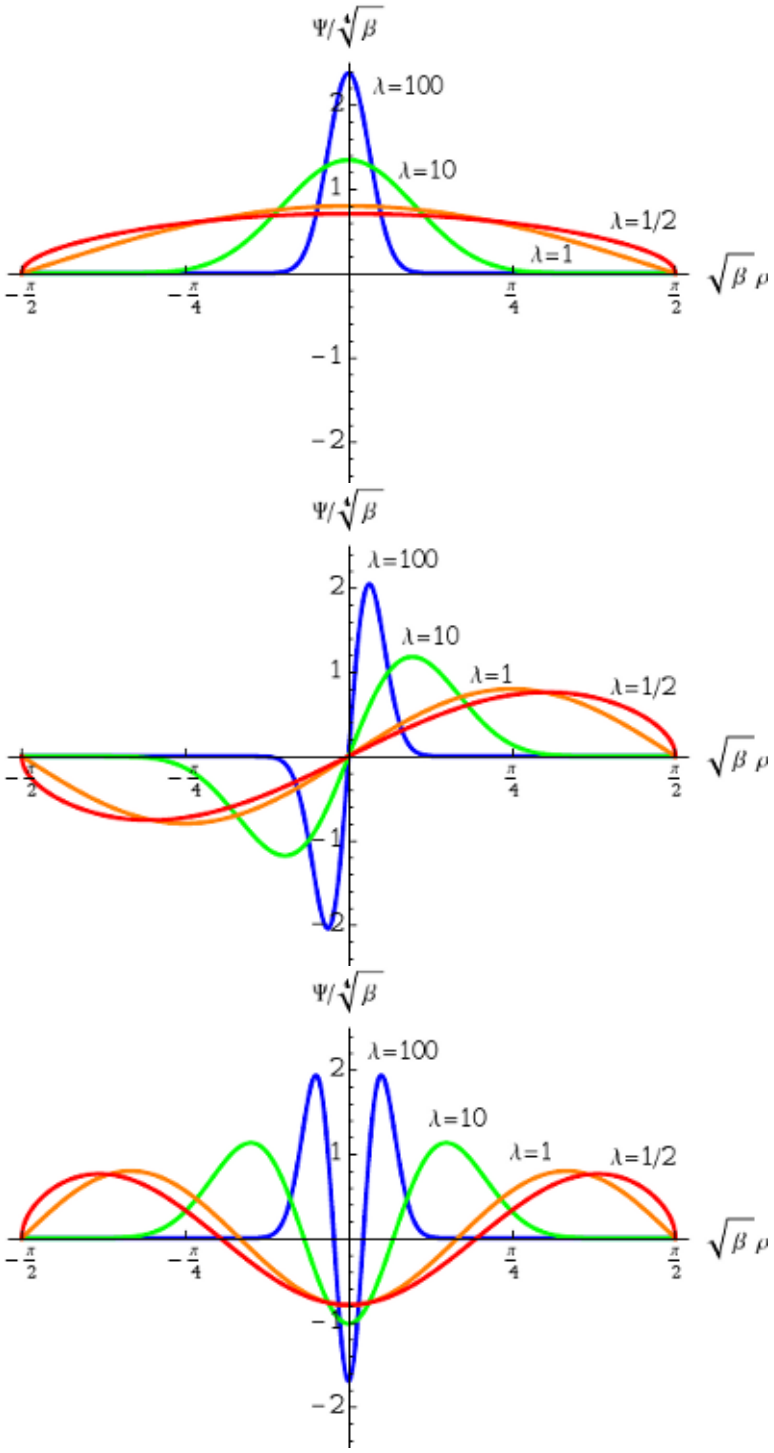

Figure 2.2: λ-dependence of the wave-functions of the first few energy eigenstates. The $\lambda > 1$ values correspond to $m > 0$, while the $\frac{1}{2} \leq \lambda < 1$ values correspond to $m < 0$. The $\lambda = 1$ case corresponds to the limit $|m| \to \infty$.

Thus, the $1/m > 0$ and $1/m < 0$ cases connect smoothly at $1/m = 0$.

The normalized energy eigenfunctions are thus given by:

$$\Psi_n^{(\lambda)}(p) \;=\; N_n^{(\lambda)}\, c^\lambda\, C_n^\lambda(s)\;, \tag{2.54}$$

where

$$\begin{aligned} N_n^{(\lambda)} &= \sqrt[4]{\beta}\left[2^\lambda \Gamma(\lambda)\sqrt{\frac{n!\,(n+\lambda)}{2\pi\,\Gamma(n+2\lambda)}}\right]\;, \\ c &= \cos\sqrt{\beta}\rho \;=\; \frac{1}{\sqrt{1+\beta p^2}}\;, \\ s &= \sin\sqrt{\beta}\rho \;=\; \frac{\sqrt{\beta}p}{\sqrt{1+\beta p^2}}\;. \end{aligned} \tag{2.55}$$

The wave-functions for the first few energy eigenstates for several representative values of λ are shown in Figs. 2.2.

Comparing Eq. (2.51) and Eq. (2.54) with Eq. (2.8) and Eq. (2.9) show how much simplification is achieved through the variable transformation in Eq. (2.31).

Using the wave-functions derived above, and the formula provided in the appendix, the expectation values of $\hat{x}$, $\hat{p}$, $\hat{x}^2$, and $\hat{p}^2$ for the energy eigenstates are found to be

$$\begin{aligned} \langle n,\lambda|\,\hat{x}\,|n,\lambda\rangle &= 0\;, \\ \langle n,\lambda|\,\hat{p}\,|n,\lambda\rangle &= 0\;, \\ \langle n,\lambda|\,\hat{x}^2\,|n,\lambda\rangle &= (\hbar^2\beta)\frac{(\lambda+n)\big[(2\lambda-1)n+\lambda\big]}{(2\lambda-1)}\;, \\ \langle n,\lambda|\,\hat{p}^2\,|n,\lambda\rangle &= \frac{1}{\beta}\left(\frac{2n+1}{2\lambda-1}\right)\;, \end{aligned} \tag{2.56}$$

giving the uncertainties in $\langle\hat{x}\rangle$ and $\langle\hat{p}\rangle$ as

$$\begin{aligned} \Delta x_n &= \Delta x_{\min}\sqrt{\frac{(\lambda+n)\big[(2\lambda-1)n+\lambda\big]}{(2\lambda-1)}}\;, \\ \Delta p_n &= \frac{1}{\sqrt{\beta}}\sqrt{\frac{2n+1}{2\lambda-1}}\;. \end{aligned} \tag{2.57}$$

For fixed n and fixed β, Δx_n is a monotonically decreasing function of λ in the range $\frac{1}{2} < \lambda < 1$, and a monotonically increasing one in the range $1 < \lambda$. On the other

hand, Δp_n is a monotonically decreasing function of λ throughout. Eliminating λ from the above expressions, we find

$$\begin{aligned} \frac{\Delta x_n}{\Delta x_{\min}} &= \frac{1}{2\sqrt{\beta}\Delta p_n}\sqrt{\left[1+\beta\Delta p_n^2\right]\left[(2n+1)^2+\beta\Delta p_n^2\right]} \\ &\geq \frac{1}{2}\left(\frac{1}{\sqrt{\beta}\Delta p_n}+\sqrt{\beta}\Delta p_n\right) , \end{aligned} \tag{2.58}$$

where the equality in the second line is saturated for the $n = 0$ case only. The first line gives the curve on the Δp-Δx plane that the point $(\Delta p_n, \Delta x_n)$ follows as λ is varied.

Differentiating with respect to Δp_n we find

$$\begin{aligned} &\frac{d}{d(\Delta p_n)}\left[\frac{\Delta x_n}{\Delta x_{\min}}\right] \\ &= \frac{\beta^2\Delta p_n^4-(2n+1)^2}{2\sqrt{\beta}\Delta p_n^2\sqrt{\left[1+\beta\Delta p_n^2\right]\left[(2n+1)^2+\beta\Delta p_n^2\right]}} , \end{aligned} \tag{2.59}$$

indicating that the curve is flat at the $\lambda = 1$ point where $\Delta p_n = \sqrt{(2n+1)/\beta}$ and Δx_n reaches its minimum of $\Delta x_{\min}(n+1)$. Therefore, the $\lambda = 1$ point is the turn-around point where the uncertainties switch from the $\Delta x \sim 1/\Delta p$ behavior to the $\Delta x \sim \Delta p$ behavior. To go from one branch to another one must flip the sign of the mass m.

Eliminating n from Eq. (2.57), we find

$$\frac{\Delta x_n}{\Delta x_{\min}} = \frac{1}{2}\sqrt{(1+\beta\Delta p_n^2)\left[1+(2\lambda-1)^2\beta\Delta p_n^2\right]} . \tag{2.60}$$

This gives the curve on which the points $(\Delta p_n, \Delta x_n)$ fall on for constant λ. In particular, for $\lambda = 1$ this reduces to

$$\frac{\Delta x_n}{\Delta x_{\min}} = \frac{1+\beta\Delta p_n^2}{2} , \tag{2.61}$$

and gives the $1/m = 0$ boundary between the $1/m > 0$ and $1/m < 0$ regions in Δx-Δp space. These properties of the uncertainties have been plotted in Fig. 2.3.

As shown in Fig. 2.3, the value of λ determines where the uncertainties $(\Delta p_n, \Delta x_n)$ are along their trajectories given by Eq. (2.58), with $\lambda > 1$ keeping the uncertainties

on the $\Delta x \sim 1/\Delta p$ branch of the trajectory, while $\frac{1}{2} < \lambda < 1$ keeping them on the $\Delta x \sim \Delta p$ branch. Let us consider a few limiting values of λ to see the behavior of the solutions there.

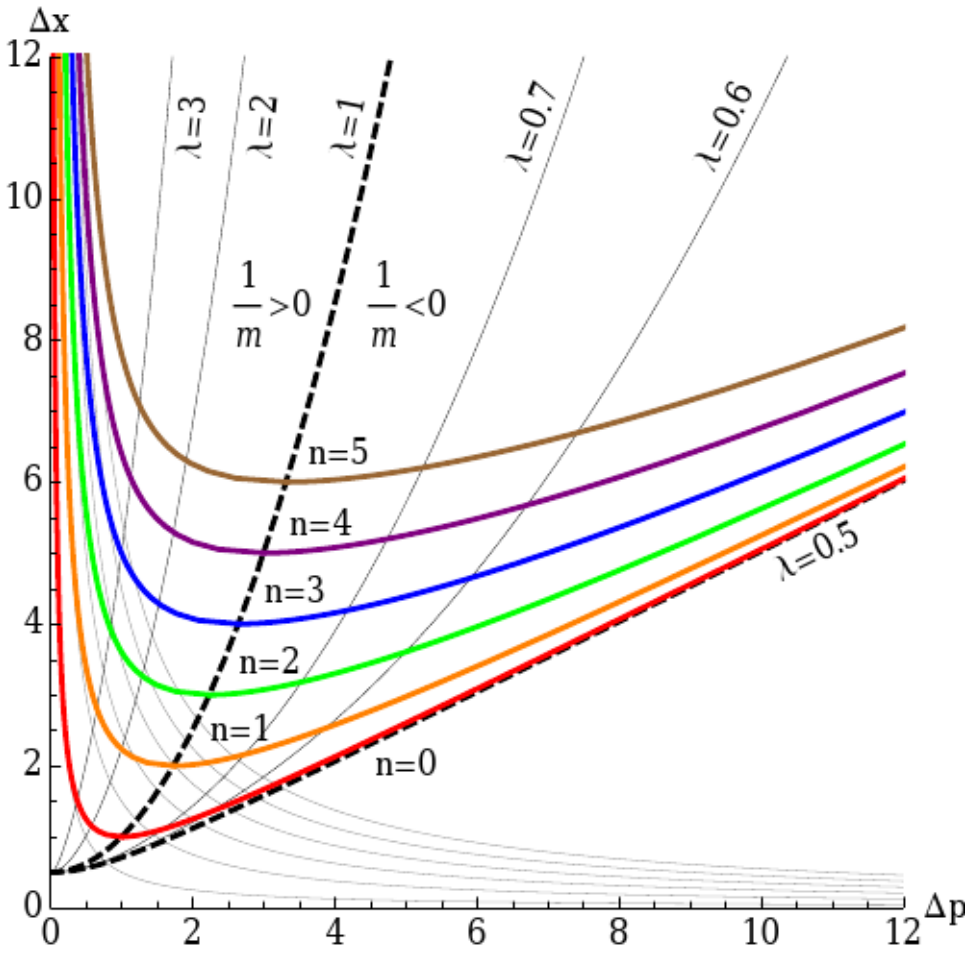

Figure 2.3: Δp versus Δx for the lowest six energy eigenstates of the harmonic oscillator. Δx is in units of $\Delta x_{\min} = \hbar\sqrt{\beta}$, while Δp is in units of $1/\sqrt{\beta} = \hbar/\Delta x_{\min}$. The location of the state along the curves shown is determined by the value of λ defined in Eq. (2.44). The $\lambda = 1$ points correspond to the case $1/m = 0$. As $1/m$ is increased to the positive side, the value of λ will increase away from one and the state will move toward the left along the $\Delta x \sim 1/\Delta p$ branch. If $1/m$ is decreased into the negative, the value of λ will decrease toward $1/2$, and the state will move toward the right along the $\Delta x \sim \Delta p$ branch. The $n = 0$ curve (shown in red) corresponds to the minimal length uncertainty bound, Eq. (2.6).

2.4 Limiting Cases: $\lambda \to \infty$

The $\beta \to 0$ limit only exists for the $m > 0$ case where $\lambda = \lambda_+$. As $\beta \to 0$, the parameter λ_+ diverges to infinity as

$$\lambda \;=\; \lambda_+ \;\sim\; \frac{1}{m\hbar\omega\beta} \;\xrightarrow{\beta\to 0}\; \infty\,, \tag{2.62}$$

where $\omega = \sqrt{k/m}$. In that limit, the Gegenbauer polynomials become Hermite polynomials:

$$\lim_{\lambda\to\infty} n!\,\lambda^{-n/2}\,C_n^{\lambda}(x/\sqrt{\lambda}) \;=\; H_n(x)\,. \tag{2.63}$$

Noting that as $\beta \to 0$, we have

$$s \;\sim\; \sqrt{\beta}p \;\sim\; \frac{p}{\sqrt{\lambda m\hbar\omega}}\,, \tag{2.64}$$

we can conclude that

$$\lim_{\lambda\to\infty} n!\,\lambda^{-n/2}\,C_n^{\lambda}(s) \;=\; H_n\!\left(\frac{p}{\sqrt{m\hbar\omega}}\right)\,. \tag{2.65}$$

Similarly,

$$\lim_{\lambda\to\infty} c^{\lambda} \;=\; \lim_{\lambda\to\infty}\left(1-\frac{p^2}{\lambda m\hbar\omega}\right)^{\lambda/2} \;=\; \exp\!\left(-\frac{p^2}{2m\hbar\omega}\right)\,. \tag{2.66}$$

Using Stirling's formula

$$\Gamma(z) \;\sim\; \sqrt{2\pi}\,e^{-z}z^{z-(1/2)} + \cdots \tag{2.67}$$

the normalization constant can be shown to converge to

$$\begin{aligned}
&\lim_{\lambda\to\infty} N_n^{(\lambda)}\,\frac{\lambda^{n/2}}{n!}\\
&\quad= \lim_{\lambda\to\infty} \sqrt[4]{\beta}\left[2^{\lambda}\Gamma(\lambda)\sqrt{\frac{n!\,(n+\lambda)}{2\pi\,\Gamma(n+2\lambda)}}\,\frac{\lambda^{n/2}}{n!}\right]\\
&\quad= \lim_{\lambda\to\infty} \sqrt[4]{\frac{1}{\mu\hbar\omega\lambda}}\sqrt{\frac{2^{2\lambda-1}\lambda^n\,(n+\lambda)\big[\,\Gamma(\lambda)\,\big]^2}{n!\,\pi\,\Gamma(n+2\lambda)}}\\
&\quad= \lim_{\lambda\to\infty} \frac{1}{\sqrt[4]{\mu\hbar\omega}}\sqrt{\frac{2^{2\lambda-1}\lambda^{n-(1/2)}\,(n+\lambda)\Big[\,\sqrt{2\pi}\,e^{-\lambda}\lambda^{\lambda-(1/2)}\,\Big]^2}{n!\,\pi\,\sqrt{2\pi}\,e^{-n-2\lambda}(n+2\lambda)^{n+2\lambda-(1/2)}}}
\end{aligned}$$

$$
\begin{aligned}
&= \lim_{\lambda\to\infty} \frac{1}{\sqrt[4]{\mu\hbar\omega}} \sqrt{\frac{2^{2\lambda-(1/2)}\lambda^{n+2\lambda-(3/2)}\,(n+\lambda)}{n!\,\sqrt{\pi}\,e^{-n}(n+2\lambda)^{n+2\lambda-(1/2)}}} \\
&= \frac{1}{\sqrt{2^n n!\,e^{-n}}} \frac{1}{\sqrt[4]{\mu\hbar\omega\pi}} \lim_{\lambda\to\infty} \sqrt{\frac{(1+n/\lambda)}{(1+n/2\lambda)^{n+2\lambda-(1/2)}}} \\
&= \frac{1}{\sqrt{2^n n!\,e^{-n}}} \frac{1}{\sqrt[4]{\mu\hbar\omega\pi}} \sqrt{\frac{1}{e^n}} \\
&= \frac{1}{\sqrt{2^n n!}} \frac{1}{\sqrt[4]{m\hbar\omega\pi}}\,. \qquad (2.68)
\end{aligned}
$$

Therefore,

$$
\begin{aligned}
&\lim_{\lambda\to\infty} \Psi_n^{(\lambda)}(p) \\
&\quad = \frac{1}{\sqrt{2^n n!}} \frac{1}{\sqrt[4]{m\hbar\omega\pi}} \exp\left(-\frac{p^2}{2m\hbar\omega}\right) H_n\left(\frac{p}{\sqrt{m\hbar\omega}}\right)\,, \qquad (2.69)
\end{aligned}
$$

which are just the usual harmonic oscillator wave-functions in momentum space, as shown earlier in the chapter. The energy eigenvalues reduce to the usual ones given in Eq. (2.52).

Using Eq. (2.62), the uncertainties reduce to the canonical ones from earlier, as expected:

$$
\begin{aligned}
\Delta x_n &= \hbar\sqrt{\beta}\sqrt{\frac{(\lambda+n)\big[(2\lambda-1)n+\lambda\big]}{(2\lambda-1)}} \\
&= \hbar\sqrt{\frac{(\lambda\beta+n\beta)\big[(2\lambda\beta-\beta)n+\lambda\beta\big]}{(2\lambda\beta-\beta)}} \\
&\xrightarrow{\beta\to 0} \hbar\sqrt{\frac{(\lambda\beta)\big[(2\lambda\beta)n+\lambda\beta\big]}{(2\lambda\beta)}} = \sqrt{\frac{\hbar(2n+1)}{2m\omega}}, \\
\Delta p_n &= \frac{1}{\sqrt{\beta}}\sqrt{\frac{2n+1}{2\lambda+1}} \\
&\xrightarrow{\beta\to 0} \sqrt{\frac{\hbar m\omega(2n+1)}{2}}\,, \qquad (2.70)
\end{aligned}
$$

which satisfy

$$
\Delta x_n \Delta p_n \xrightarrow{\lambda\to\infty} \hbar\left(n+\frac{1}{2}\right) \geq \frac{\hbar}{2}\,. \qquad (2.71)
$$

2.5 Limiting Cases: $\lambda \to 1$

The limit $\lambda = 1$ is reached when β and k are kept constant while $|m|$ is taken to infinity. When $\lambda = 1$, the Gegenbauer polynomials become the Chebycheff polynomials of the second kind:

$$C_n^1(s) \;=\; U_n(s)\;, \tag{2.72}$$

where

$$U_n(\cos\theta) \;=\; \frac{\sin(n+1)\theta}{\sin\theta}\;, \tag{2.73}$$

while the normalization constant reduces to

$$N_n^{(\lambda)} \;\xrightarrow{\lambda\to 1}\; \sqrt[4]{\beta}\sqrt{\frac{2}{\pi}}\;. \tag{2.74}$$

Therefore,

$$\lim_{\lambda\to 1}\frac{\Psi_n^{(1)}(p)}{\sqrt[4]{\beta}} \;=\; \sqrt{\frac{2}{\pi}}\,c\,U_n(s)\;. \tag{2.75}$$

The orthonormality relation for the Chebycheff polynomials is

$$\int_{-1}^{1}\sqrt{1-x^2}\,U_n(x)\,U_m(x)\,dx \;=\; \frac{\pi}{2}\,\delta_{nm}\;, \tag{2.76}$$

and we can see that the correct normalization constant is obtained. Since the argument in our case is $s = \sin\sqrt{\beta}\rho$, it is more convenient to express the Chebycheff polynomials as

$$\begin{aligned} U_{2n}(\sin\theta) \;&=\; (-1)^n\frac{\cos[(2n+1)\theta]}{\cos\theta}\;,\\ U_{2n+1}(\sin\theta) \;&=\; (-1)^n\frac{\sin[(2n+2)\theta]}{\cos\theta}\;, \end{aligned} \tag{2.77}$$

for $n = 0, 1, 2, \cdots$. This will allow us to write

$$\begin{aligned} \lim_{\lambda\to 1}\frac{\Psi_{2n}^{(1)}(p)}{\sqrt[4]{\beta}} \;&=\; (-1)^n\sqrt{\frac{2}{\pi}}\cos\Big[(2n+1)\sqrt{\beta}\rho\Big]\;,\\ \lim_{\lambda\to 1}\frac{\Psi_{2n+1}^{(1)}(p)}{\sqrt[4]{\beta}} \;&=\; (-1)^n\sqrt{\frac{2}{\pi}}\sin\Big[(2n+2)\sqrt{\beta}\rho\Big]\;. \end{aligned} \tag{2.78}$$

The energy eigenvalues in this limit were given in Eq. (2.53). Here, our procedure of keeping the spring constant k fixed while taking $|m|$ to infinity maintains the finiteness of E_n, while taking the kinetic energy contribution to E_n to zero.

From the n-dependence of the energies, we can see that, in this limit, the problem reduces to that of an infinite square well potential, of width $\pi/\sqrt{\beta}$, in ρ-space. Indeed, the effective potential in ρ-space was

$$\frac{1}{2m\beta}\tan^2\bigl(\sqrt{\beta}\rho\bigr) \xrightarrow{m\to\infty} \begin{cases} 0 & \text{for } \rho \neq \pm\dfrac{\pi}{2\sqrt{\beta}}\ , \\ \infty & \text{at } \rho = \pm\dfrac{\pi}{2\sqrt{\beta}}\ . \end{cases} \tag{2.79}$$

This can also be seen from the form of the energy eigenfunctions, which have reduced to simple sines and cosines. We will see in the next section that the classical solution also behaves as that of a particle in an infinite square well potential in ρ-space in the same limit.

The uncertainties become

$$\begin{aligned} \Delta x_n &\xrightarrow{\lambda\to 1} \Delta x_{\min}\bigl(n+1\bigr)\ , \\ \Delta p_n &\xrightarrow{\lambda\to 1} \sqrt{\frac{(2n+1)}{\beta}}\ , \end{aligned} \tag{2.80}$$

as was shown in Fig. 2.3. Note that

$$\begin{aligned} \frac{\hbar}{2}\left[\frac{1}{\Delta p_n} + \beta\Delta p_n\right] &= \Delta x_{\min}\,\frac{n+1}{\sqrt{2n+1}} \\ &\leq \Delta x_{\min}\bigl(n+1\bigr) \;=\; \Delta x_n\ , \end{aligned} \tag{2.81}$$

the bound being saturated only for the ground state $n = 0$.

2.6 Limiting Cases: $\lambda \to \frac{1}{2}$

The $\lambda \to \frac{1}{2}$ limit is reached as $\Delta x_{\min} \to \sqrt{2}a$ when $m < 0$. In this limit, the Gegenbauer polynomials become the Legendre polynomials, $C_n^{1/2}(s) = P_n(s)$, while the normalization constant reduces to

$$N_n^{(\lambda)} \xrightarrow{\lambda \to \frac{1}{2}} \sqrt[4]{\beta}\sqrt{\frac{2n+1}{2}} \ . \tag{2.82}$$

The wavefunctions are

$$\frac{\Psi_n^{(1/2)}(p)}{\sqrt[4]{\beta}} \ = \ \sqrt{\frac{2n+1}{2}}\sqrt{c}\, P_n(s) \ . \tag{2.83}$$

Note that the orthonormality relation for the Legendre polynomials is

$$\int_{-1}^{1} P_n(x)\, P_m(x)\, dx \ = \ \frac{2}{2n+1}\, \delta_{nm} \ , \tag{2.84}$$

so these wave-functions are properly normalized. The integrals for $\langle \hat{x}^2 \rangle$ and $\langle \hat{p}^2 \rangle$ diverge in this limit, so both Δx_n and Δp_n are divergent for all n. However, the energy, which is the difference between $k\langle \hat{x}^2 \rangle/2$ and $\langle \hat{p}^2 \rangle/2|m|$, stays finite:

$$E_n^- \ = \ \frac{k}{2}(\Delta x_{\rm min})^2 \left(n^2 + n + \frac{1}{2} \right) \ . \tag{2.85}$$

2.7 The Classical Equations of Motion

As we have seen above, for values of β which maintain the inequality $\Delta x_{\rm min} = \hbar\sqrt{\beta} > \sqrt{2}a$, the harmonic oscillator Hamiltonian admits an infinite ladder of positive energy eigenstates even when $m < 0$. Furthermore, these are states with finite Δx and Δp, implying that the particle is 'bound' close to the phase space origin, just as in the $m > 0$ case. But how can a particle be 'bound' for an 'inverted' harmonic oscillator? To gain insight into this question, we solve the corresponding classical equation of motion.

We assume that the classical limit of our commutation relation, Eq. (2.5), is obtained by the usual correspondence between commutators and Poisson brackets:

$$\frac{1}{i\hbar}[\, \hat{A},\, \hat{B}\,] \ \to \ \{A,\, B\,\} \ . \tag{2.86}$$

Therefore, we assume

$$\{\, x,\, x\,\} \ = \ 0 \ ,$$

$$\begin{aligned} \{\, p,\, p \,\} &= 0 \,, \\ \{\, x,\, p \,\} &= (1 + \beta p^2) \,. \end{aligned} \tag{2.87}$$

Then, the equations of motion for the harmonic oscillator with Hamiltonian given by

$$H = \frac{1}{2} k x^2 + \frac{1}{2m} p^2 \,, \tag{2.88}$$

are

$$\begin{aligned} \dot{x} &= \{\, x,\, H \,\} = \frac{1}{m}(1 + \beta p^2)\, p \,, \\ \dot{p} &= \{\, p,\, H \,\} = -k(1 + \beta p^2)\, x \,. \end{aligned} \tag{2.89}$$

We allow m to take on either sign: if $m > 0$, then $\dot{x}$ and p will have the same sign; if $m < 0$ they will have opposite sign. Note that, even though the equations of motion of x and p have changed, the total energy will still be conserved. Consequently, the time-evolution of x and p in phase space will be along the trajectory given by $H =$ constant. For the $m > 0$ case this will be an ellipse, while for the $m < 0$ case this will be a hyperbola.

To solve these equations, we change the variable p to ρ, which was introduced in Eq. (2.31) for the quantum case. Then, the equations become

$$\begin{aligned} \dot{x} &= \frac{1}{m\sqrt{\beta}} \left[\frac{\tan(\sqrt{\beta}\rho)}{\cos^2(\sqrt{\beta}\rho)} \right] = \frac{1}{2m\beta} \frac{d}{d\rho} \left[\tan^2(\sqrt{\beta}\rho) \right] \,, \\ \dot{\rho} &= -kx \,. \end{aligned} \tag{2.90}$$

Therefore,

$$\ddot{\rho} = -k\dot{x} = -\frac{k}{2m\beta} \frac{d}{d\rho} \left[\tan^2(\sqrt{\beta}\rho) \right] \,, \tag{2.91}$$

Multiplying both sides of the equation with $\dot{\rho}$, we obtain

$$\dot{\rho}\ddot{\rho} = -\frac{k}{2m\beta}\, \dot{\rho} \frac{d}{d\rho} \left[\tan^2(\sqrt{\beta}\rho) \right] \,, \tag{2.92}$$

which can be rewritten as

$$\frac{1}{2} \frac{d}{dt} \left[\dot{\rho}^2 \right] = -\frac{k}{2m\beta} \frac{d}{dt} \left[\tan^2(\sqrt{\beta}\rho) \right] \,, \tag{2.93}$$

and thus,

$$\dot{\rho}^2 = -\frac{k}{m\beta} \left[\tan^2\big(\sqrt{\beta}\rho\big) - C \right] \,, \tag{2.94}$$

where C is the integration constant. Since we must have $\dot{\rho}^2 > 0$, the range of allowed values of C will depend on whether $m > 0$ or $m < 0$. We will consider the two cases separately.

2.7.1 $m > 0$ case

When $m > 0$, we introduce the angular frequency

$$\omega \;=\; \sqrt{\frac{k}{m}} \tag{2.95}$$

as usual. Then, Eq. (2.94) becomes

$$\beta\,\dot{\rho}^2 \;=\; \omega^2\Big[\,C - \tan^2\big(\sqrt{\beta}\rho\big)\Big]\,, \tag{2.96}$$

and taking the square-root, we obtain

$$\sqrt{\beta}\,\dot{\rho} \;=\; \pm\omega\sqrt{C - \tan^2(\sqrt{\beta}\rho)}\,. \tag{2.97}$$

In this case, we must have $C > 0$ for the content of the square-root to be positive. Separating variables, we obtain

$$\frac{\sqrt{\beta}\,d\rho}{\sqrt{C - \tan^2\big(\sqrt{\beta}\rho\big)}} \;=\; \pm\omega\,dt\,. \tag{2.98}$$

The left-hand side integrates to

$$\begin{aligned}\int &\frac{\sqrt{\beta}\,d\rho}{\sqrt{C - \tan^2(\sqrt{\beta}\rho)}} \\ &= \;\frac{1}{\sqrt{1+C}}\,\arcsin\left[\sqrt{\frac{1+C}{C}}\,\sin\big(\sqrt{\beta}\rho\big)\right]\,.\end{aligned} \tag{2.99}$$

Therefore,

$$\begin{aligned}&\sqrt{\beta}\rho(t) \\ &= \;\arcsin\left[\sqrt{\frac{C}{1+C}}\,\sin\Big\{\pm\sqrt{1+C}\,\omega(t-t_0)\Big\}\right]\end{aligned}$$

(2.100)

where t_0 is the integration constant. Without loss of generality, we can choose the sign inside the braces to be 'plus'. Setting $t_0 = 0$, we obtain:

$$\begin{aligned}
\sqrt{\beta mk}\, x(t) &= -\frac{\sqrt{\beta}}{\omega}\,\dot{\rho} \\
&= -\frac{\sqrt{C(1+C)}\,\cos\!\big(\sqrt{1+C}\,\omega t\big)}{\sqrt{1+C\,\cos^2\!\big(\sqrt{1+C}\,\omega t\,\big)}}\,, \\
\sqrt{\beta}\, p(t) &= \tan(\sqrt{\beta}\rho) \\
&= \frac{\sqrt{C}\,\sin\!\big(\sqrt{1+C}\,\omega t\big)}{\sqrt{1+C\,\cos^2\!\big(\sqrt{1+C}\,\omega t\,\big)}}\,,
\end{aligned} \tag{2.101}$$

and the energy is given by

$$\begin{aligned}
E &= \frac{k}{2}\,x(t)^2 + \frac{p(t)^2}{2m} \\
&= \frac{1}{2\beta m}\left[\sqrt{\beta mk}\,x(t)\right]^2 + \frac{1}{2\beta m}\left[\sqrt{\beta}\,p(t)\right]^2 \\
&= \frac{C}{2\beta m} \;>\; 0\,.
\end{aligned} \tag{2.102}$$

The period of oscillation T is no longer equal to $2\pi/\omega$ when $\beta \neq 0$. It is now

$$T \;=\; \frac{2\pi}{\omega}\,\frac{1}{\sqrt{1+C}}\,. \tag{2.103}$$

If we let

$$A \;\equiv\; \sqrt{\frac{C}{\beta mk}}\,, \tag{2.104}$$

then

$$E \;=\; \frac{1}{2}kA^2\,, \tag{2.105}$$

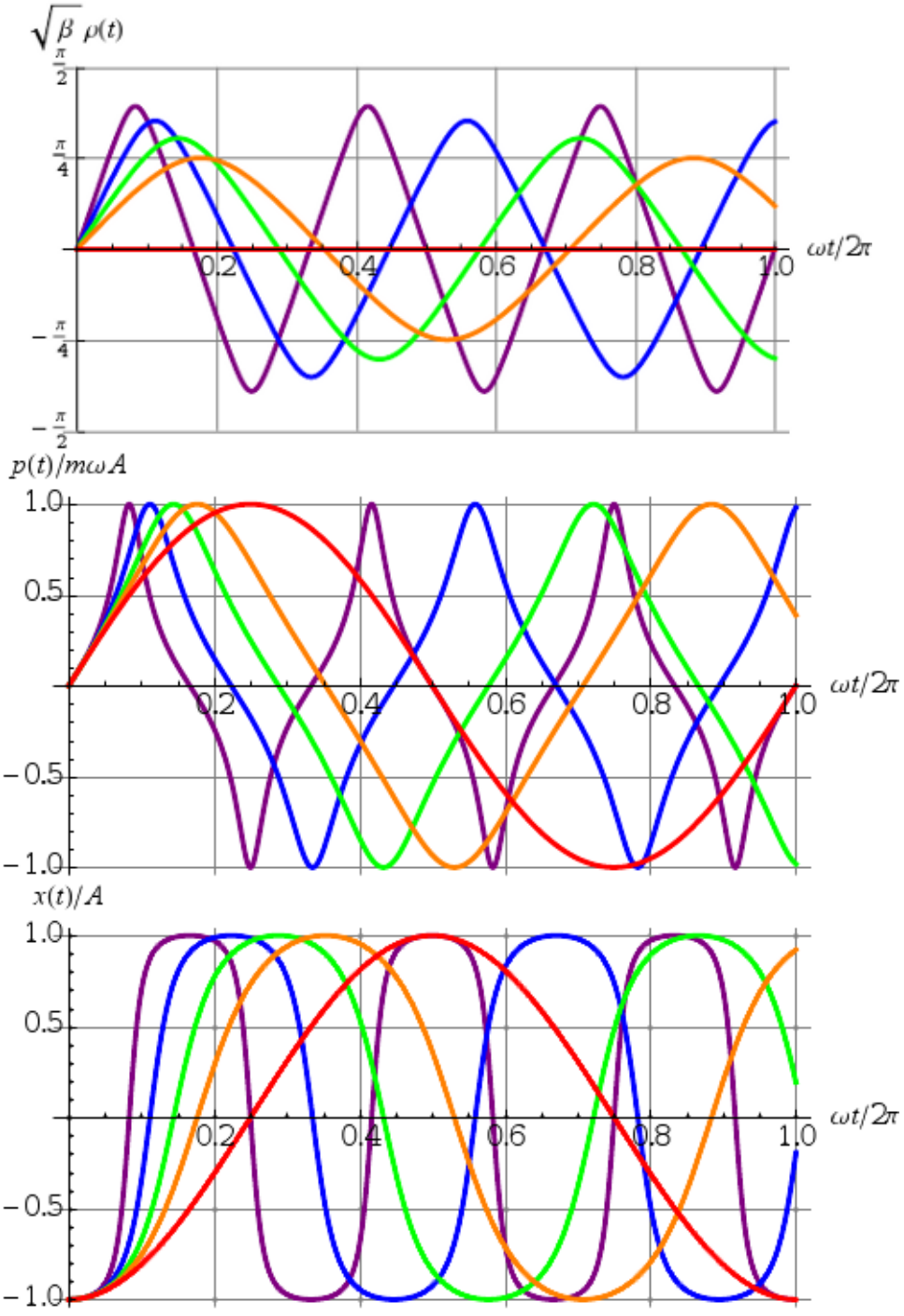

Figure 2.4: The dependence of the classical behavior of a positive mass particle in a harmonic oscillator potential on the parameter $C = 2mE\beta = \beta m^2\omega^2 A^2$, where E is the particle's energy, and A is the amplitude of the oscillation in x. The undeformed $\beta = 0$ case is shown in red. The other four cases are $C = 1$ (orange), $C = 2$ (green), $C = 4$ (blue), and $C = 8$ (purple).

If we take the limit $\beta \to 0$ while keeping A fixed, we find:

$$\begin{aligned} x(t) &\xrightarrow{\beta\to 0} -A\cos(\omega t)\ , \\ p(t) &\xrightarrow{\beta\to 0} Am\omega\sin(\omega t)\ , \end{aligned} \tag{2.106}$$

which shows that the canonical behavior is recovered in this limit. The behavior of the solution when $\beta \neq 0$ is compared with the $\beta = 0$ limit for several representative values of C in Fig. 2.4.

Another interesting limit is obtained by setting $C = 2mE\beta$ and letting $m \to \infty$ while keeping E and β fixed. In that limit,

$$\sqrt{1+C}\,\omega \quad \xrightarrow{m\to\infty} \quad \sqrt{2E\beta k} \;=\sqrt{\beta}kA \;\equiv\; \omega_0\ , \tag{2.107}$$

and we find

$$\begin{aligned} \sqrt{\beta}\,\rho(t) &\xrightarrow{m\to\infty} \arcsin\Big[\sin(\omega_0 t)\Big]\ , \\ \sqrt{\beta}\,p(t) &\xrightarrow{m\to\infty} +\frac{\sin(\omega_0 t)}{|\cos(\omega_0 t)|}\ , \\ x(t)/A &\xrightarrow{m\to\infty} -\frac{\cos(\omega_0 t)}{|\cos(\omega_0 t)|}\ . \end{aligned} \tag{2.108}$$

The behavior of the solution in this limit is shown in Fig. 2.5. The motion of a particle in an infinite square well potential (in ρ-space) is reproduced, in correspondence to the quantum $\lambda \to 1$ limit.

2.7.2 $m < 0$ Case

For the $m < 0$ case, by an abuse of notation, let us set

$$\omega \;=\; \sqrt{\frac{k}{|m|}}\ . \tag{2.109}$$

Then, Eq. (2.94) becomes

$$\beta\,\dot{\rho}^2 \;=\; \omega^2\bigg[\,\tan^2\!\big(\sqrt{\beta}\rho\big) - C\,\bigg]\ . \tag{2.110}$$

The integration constant C can have either sign in this case. We will consider the three cases $C < 0$, $C > 0$, and $C = 0$ separately.

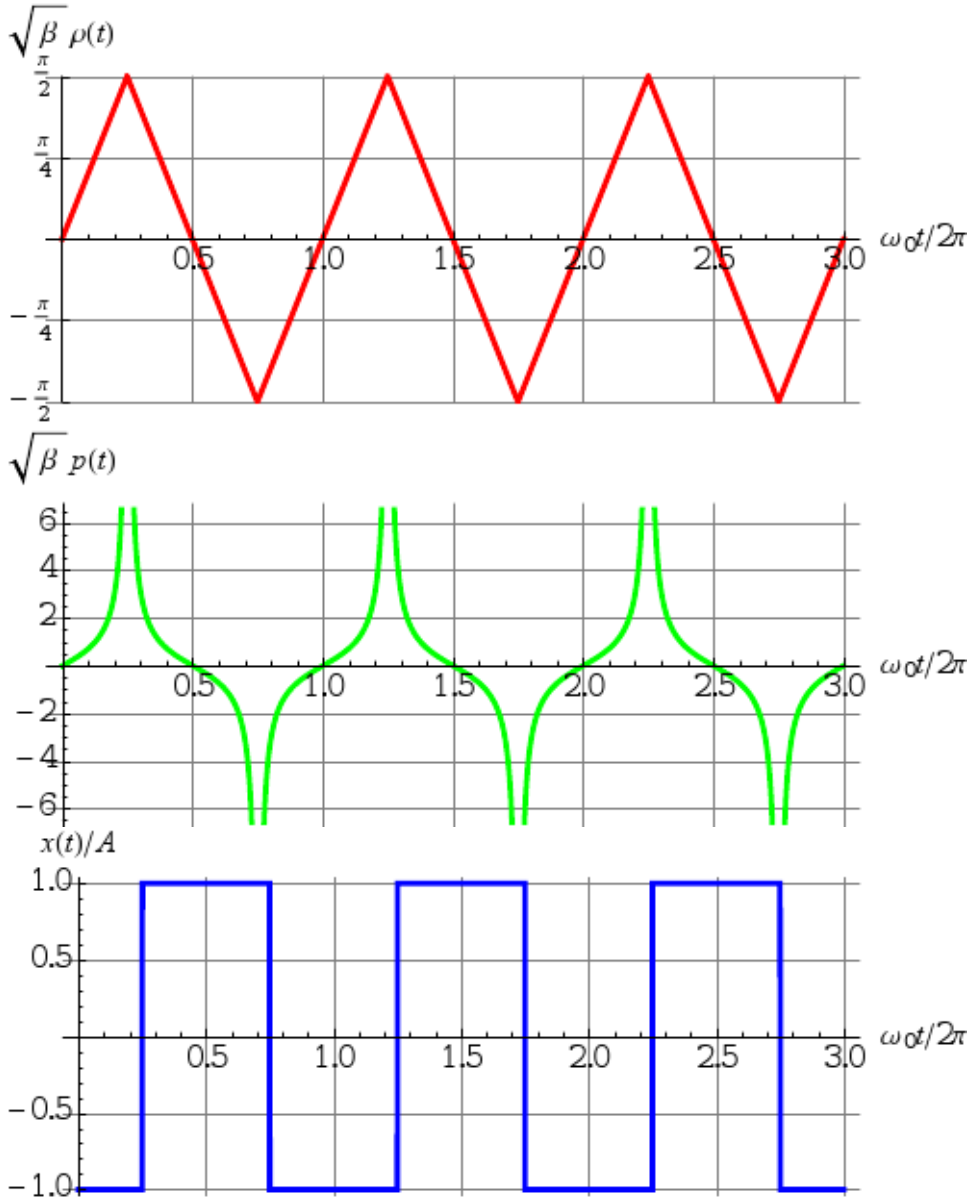

Figure 2.5: The classical behavior of a positive mass particle in a harmonic oscillator potential with modified Poisson brackets, Eq. (2.87), in the limit $m \to \infty$ with $C = 2mE\beta$ where E and β are kept fixed. $\rho(t)$ and $x(t)$ take on the behavior of the position and momentum of a particle in an infinite square well.

$C < 0$ (positive energy) case

For the $C < 0$ case, the square-root of Eq. (2.110) gives us

$$\sqrt{\beta}\,\dot{\rho} \;=\; \pm\,\omega\sqrt{\tan^2(\sqrt{\beta}\rho) + |C|}\,. \tag{2.111}$$

Therefore,

$$\frac{\sqrt{\beta}\,d\rho}{\sqrt{\tan^2\!\big(\sqrt{\beta}\rho\big) + |C|}} \;=\; \pm\,\omega\,dt\,. \tag{2.112}$$

The left-hand side integrates to

$$\begin{aligned}
&\int \frac{\sqrt{\beta}\,d\rho}{\sqrt{\tan^2(\sqrt{\beta}\rho) + |C|}} \\
&\quad= \begin{cases}
\dfrac{1}{\sqrt{|C|-1}}\,\arcsin\left[\sqrt{\dfrac{|C|-1}{|C|}}\,\sin\big(\sqrt{\beta}\rho\big)\right] & \big(|C|>1\big) \\
\sin\big(\sqrt{\beta}\rho\big) & \big(|C|=1\big) \\
\dfrac{1}{\sqrt{1-|C|}}\,\operatorname{arcsinh}\left[\sqrt{\dfrac{1-|C|}{|C|}}\,\sin\big(\sqrt{\beta}\rho\big)\right] & \big(|C|<1\big)
\end{cases}
\end{aligned} \tag{2.113}$$

Therefore,

$$\begin{aligned}
&\sin\big(\sqrt{\beta}\rho(t)\big) \\
&\quad= \begin{cases}
\sqrt{\dfrac{|C|}{|C|-1}}\;\sin\Big[\pm\sqrt{|C|-1}\;\omega(t-t_0)\Big] & \big(|C|>1\big) \\
\pm\,\omega(t-t_0) & \big(|C|=1\big) \\
\sqrt{\dfrac{|C|}{1-|C|}}\;\sinh\Big[\pm\sqrt{1-|C|}\;\omega(t-t_0)\Big] & \big(|C|<1\big)
\end{cases}
\end{aligned} \tag{2.114}$$

where t_0 is the integration constant, which we will set to zero in the following. From this, we find:

$$\sqrt{\beta|m|k}\;x(t) \;=\; -\frac{\sqrt{\beta}}{\omega}\,\dot{\rho}$$

$$
\begin{aligned}
&= \begin{cases} \mp \dfrac{\sqrt{|C|(|C|-1)}\,\cos\!\big(\pm\sqrt{|C|-1}\,\omega\,t\big)}{\sqrt{|C|\cos^2\!\big(\pm\sqrt{|C|-1}\,\omega\,t\,\big)-1}} & \big(|C|>1\big) \\ \mp \dfrac{1}{\sqrt{1-(\omega\,t)^2}} & \big(|C|=1\big) \\ \mp \dfrac{\sqrt{|C|(1-|C|)}\,\cosh\!\big(\pm\sqrt{1-|C|}\,\omega\,t\big)}{\sqrt{1-|C|\cosh^2\!\big(\pm\sqrt{1-|C|}\,\omega\,t\,\big)}} & \big(|C|<1\big) \end{cases} \\
\sqrt{\beta}\,p(t) &= \tan(\sqrt{\beta}\rho) \\
&= \begin{cases} \dfrac{\sqrt{|C|}\,\sin\!\big(\pm\sqrt{|C|-1}\,\omega\,t\big)}{\sqrt{|C|\cos^2\!\big(\pm\sqrt{|C|-1}\,\omega\,t\,\big)-1}} & \big(|C|>1\big) \\ \pm \dfrac{\omega\,t}{\sqrt{1-(\omega\,t)^2}} & \big(|C|=1\big) \\ \dfrac{\sqrt{|C|}\,\sinh\!\big(\pm\sqrt{1-|C|}\,\omega\,t\big)}{\sqrt{1-|C|\cosh^2\!\big(\pm\sqrt{1-|C|}\,\omega\,t\,\big)}} & \big(|C|<1\big) \end{cases}
\end{aligned}
\tag{2.115}
$$

In all three cases, we have

$$
\begin{aligned}
E &= \frac{k}{2}\,x(t)^2 - \frac{p(t)^2}{2|m|} \\
&= \frac{1}{2\beta|m|}\Big[\sqrt{\beta|m|k}\;x(t)\Big]^2 - \frac{1}{2\beta|m|}\Big[\sqrt{\beta}\,p(t)\Big]^2 \\
&= \frac{|C|}{2\beta|m|} \;>\; 0\;.
\end{aligned}
\tag{2.116}
$$

Let

$$
B \;\equiv\; \sqrt{\frac{|C|}{\beta|m|k}}\;. \tag{2.117}
$$

Then

$$
E \;=\; \frac{1}{2}kB^2\;, \tag{2.118}
$$

and we can identify B as the distance of closest approach to the origin (aka impact parameter).

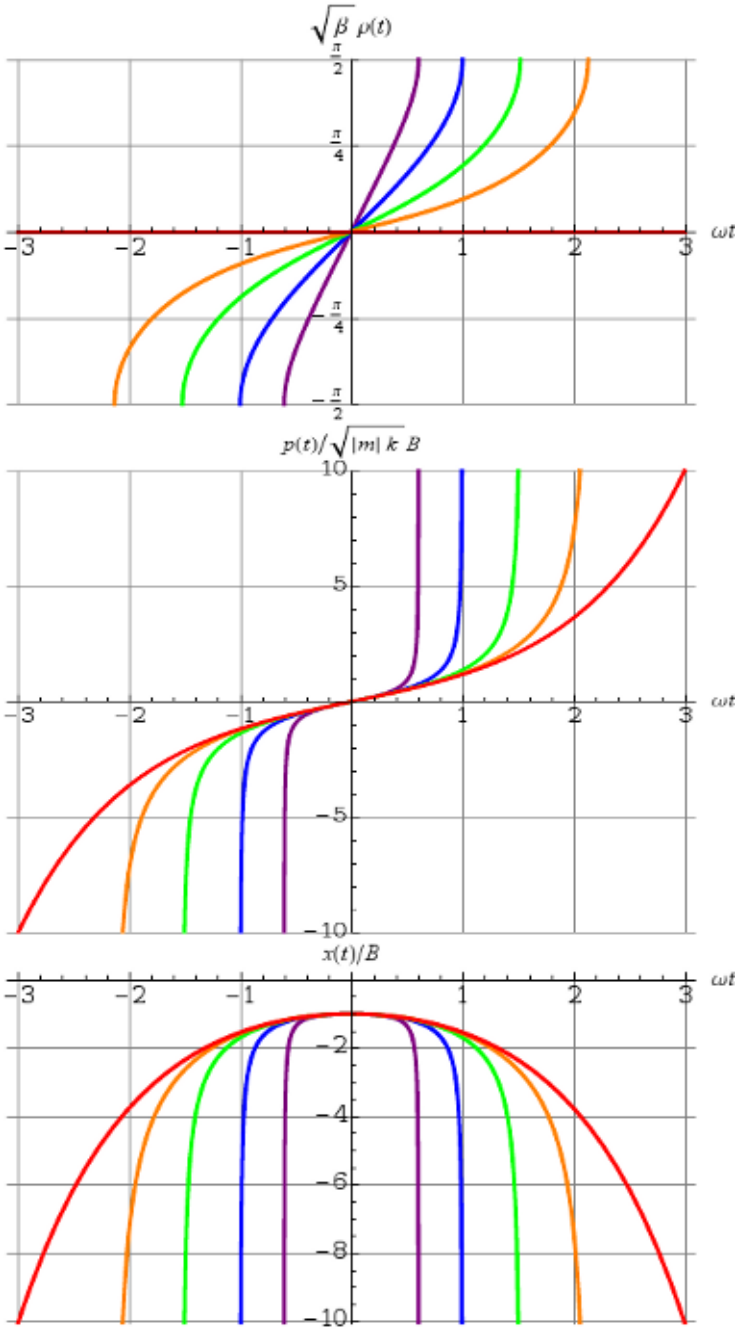

Figure 2.6: The dependence of the classical behavior of a negative mass particle in a harmonic oscillator potential on the parameter $C = -2\mu E\beta = -\beta|m|kB^2$, where E is the particle's energy, and B is the distance of closest approach to the origin in x-space. Note that due to the negative mass, $p(t)$ is negative when $\dot{x}(t)$ is positive, and vice versa. The undeformed $\beta = 0$ case is shown in red. The other three cases are $C = -\frac{1}{16}$ (orange), $C = -\frac{1}{4}$ (green), $C = -1$ (blue), and $C = -4$ (purple).

Taking the limit $\beta \to 0$ while keeping B fixed, we find:

$$\begin{aligned} x(t) &\xrightarrow{\beta\to 0} \mp B\cosh(\pm\omega t)\ , \\ p(t) &\xrightarrow{\beta\to 0} B|m|\omega\sinh(\pm\omega t)\ , \end{aligned} \tag{2.119}$$

which recovers the canonical solution. This behavior of $x(t)$ and $p(t)$ for the $\beta = 0$ case is compared with that in the $\beta \neq 0$ case for several representative values of C in Fig. 2.6.

It should be noted that for any finite value of $C < 0$, it only takes a finite amount of time for the particle to get from $(x, p) = (\pm\infty, \pm\infty)$ to $(x, p) = (\pm\infty, \mp\infty)$, or equivalently, for $\sqrt{\beta}\rho$ to evolve from $\mp\pi/2$ to $\pm\pi/2$. We will call this time $T/2$ for reasons that will become clear later. T is given by:

$$T = \frac{4}{\omega} \times \begin{cases} \dfrac{1}{\sqrt{|C|-1}}\ \arccos\dfrac{1}{\sqrt{|C|}} & \big(|C| > 1\big) \\ 1 & \big(|C| = 1\big) \\ \dfrac{1}{\sqrt{1-|C|}}\ \operatorname{arccosh}\dfrac{1}{\sqrt{|C|}} & \big(|C| < 1\big) \end{cases} \tag{2.120}$$

This dependence on $C < 0$ is shown in Fig. 2.7.

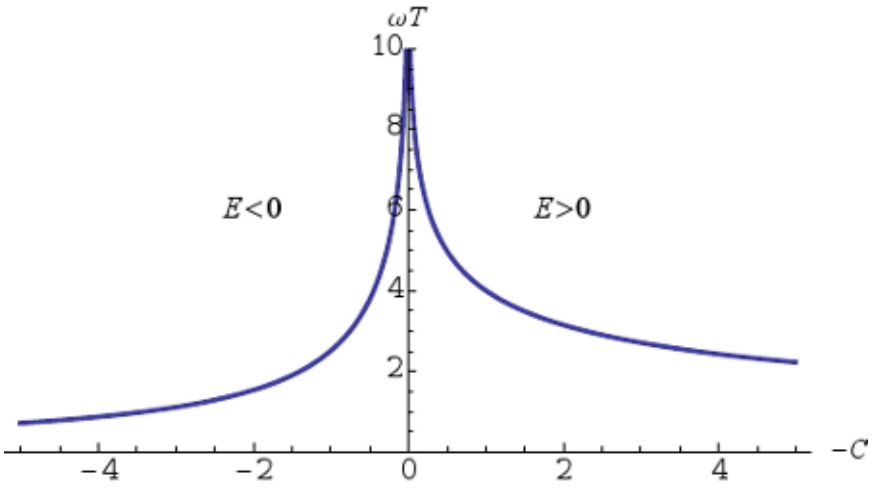

Figure 2.7: ωT as a function of $-C = 2|m|E\beta$, where $\omega = \sqrt{k/|m|}$, and E is the particle's energy. $T/2$ is the time it takes for the particle to traverse the entire trajectory.

$C > 0$ (negative energy) case

For the $C > 0$ case, taking the square-root of Eq. (2.110) yields

$$\sqrt{\beta}\,\dot{\rho} \;=\; \pm\,\omega\,\sqrt{\tan^2\!\big(\sqrt{\beta}\rho\big) - C}\,. \tag{2.121}$$

Therefore,

$$\frac{\sqrt{\beta}\,d\rho}{\sqrt{\tan^2\!\big(\sqrt{\beta}\rho\big) - C}} \;=\; \pm\,\omega\,dt\,. \tag{2.122}$$

The left-hand side integrates to

$$\begin{aligned}\int \frac{\sqrt{\beta}\,d\rho}{\sqrt{\tan^2(\sqrt{\beta}\rho) - C}} \\ =\;\; \frac{1}{\sqrt{1+C}}\,\operatorname{arccosh}\!\left|\sqrt{\frac{1+C}{C}}\,\sin\!\big(\sqrt{\beta}\rho\big)\right|\,.\end{aligned} \tag{2.123}$$

Therefore,

$$\begin{aligned}&\sin\!\big(\sqrt{\beta}\rho(t)\big) \\ &\quad=\;\; \pm\sqrt{\frac{C}{1+C}}\;\cosh\!\Big[\pm\sqrt{1+C}\;\omega(t-t_0)\Big]\end{aligned} \tag{2.124}$$

where t_0 is the integration constant, which we will set to zero in the following. The sign on the argument of the hyperbolic cosine is also irrelevant so we will set it to plus. From this, we find:

$$\begin{aligned}\sqrt{\beta|m|k}\,x(t) \;&=\; -\frac{\sqrt{\beta}}{\omega}\,\dot{\rho} \\ &=\; \mp\,\frac{\sqrt{C(1+C)}\,\sinh\!\big(\sqrt{1+C}\,\omega\,t\big)}{\sqrt{1 - C\sinh^2\!\big(\sqrt{1+C}\,\omega\,t\,\big)}} \\ \sqrt{\beta}\,p(t) \;&=\; \tan(\sqrt{\beta}\rho) \\ &=\; \pm\frac{\sqrt{C}\,\cosh\!\big(\sqrt{1+C}\,\omega\,t\big)}{\sqrt{1 - C\sinh^2\!\big(\sqrt{1+C}\,\omega\,t\,\big)}}\end{aligned} \tag{2.125}$$

and

$$\begin{aligned} E &= \frac{k}{2}\,x(t)^2 - \frac{p(t)^2}{2|m|} \\ &= \frac{1}{2\beta|m|}\left[\sqrt{\beta|m|k}\,x(t)\right]^2 - \frac{1}{2\beta|m|}\left[\sqrt{\beta}\,p(t)\right]^2 \\ &= -\frac{C}{2\beta|m|} \;<\; 0\,. \end{aligned} \tag{2.126}$$

Let

$$p_{\min} \;\equiv\; \sqrt{\frac{C}{\beta}}\,. \tag{2.127}$$

Then

$$E \;=\; -\frac{p_{\min}^2}{2|m|}\,, \tag{2.128}$$

and we can identify $p_{\min}$ as the magnitude of the momentum that the particle has at the origin $x = 0$. Taking the limit $\beta \to 0$ while keeping $p_{\min}$ constant, we find

$$\begin{aligned} x(t) &\xrightarrow{\beta\to 0} \mp\,\frac{p_{\min}}{|m|\omega}\,\sinh(\pm\omega t)\,, \\ p(t) &\xrightarrow{\beta\to 0} \pm\,p_{\min}\,\cosh(\pm\omega t)\,. \end{aligned} \tag{2.129}$$

As in the $C < 0$, the time $T/2$ it takes for the particle to travel from $x = \mp\infty$ to $x = \pm\infty$ is finite. T is given by:

$$T \;=\; \frac{4}{\omega\sqrt{1+C}}\,\operatorname{arcsinh}\frac{1}{\sqrt{C}}\,. \tag{2.130}$$

This dependence on $C > 0$ is also shown in Fig. 2.7.

$C = 0$ (zero energy) case

For $C = 0$, Eq. (2.110) leads to

$$\sqrt{\beta}\,\dot{\rho} \;=\; \pm\,\omega\,\tan\!\big(\sqrt{\beta}\rho\big)\,, \tag{2.131}$$

or

$$\frac{\sqrt{\beta}\,d\rho}{\tan\big(\sqrt{\beta}\rho\big)} \;=\; \pm\,\omega\,dt\,, \tag{2.132}$$

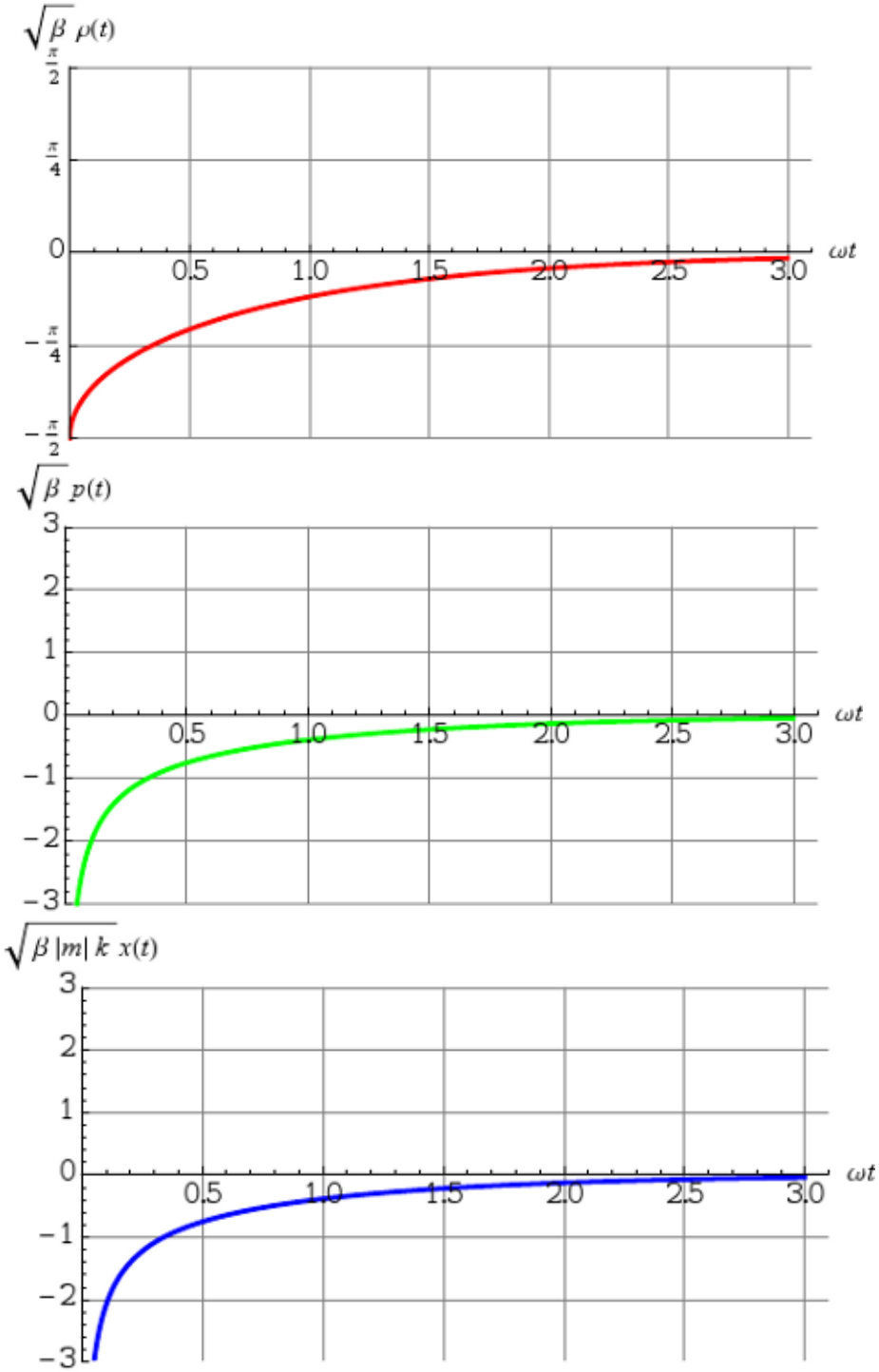

Figure 2.8: The classical behavior of a zero-energy particle with negative mass in a harmonic oscillator potential. The particle starts out at $x = -\infty$ at time $t = 0$ and asymptotically approaches the origin.

which can be integrated easily to yield

$$\ln\Big|\sin\big(\sqrt{\beta}\rho\big)\Big| \;=\; \pm\,\omega\,(t-t_0)\;, \tag{2.133}$$

or

$$\sin\big(\sqrt{\beta}\rho\big) \;=\; \pm\,e^{\,\pm\,\omega\,(t-t_0)}\;\;, \tag{2.134}$$

with all combinations of signs allowed. Set $t_0 = 0$. The solutions for the $t > 0$ region are

$$\begin{aligned} \sqrt{\beta|m|k}\;x(t) \;&=\; -\frac{\sqrt{\beta}}{\omega}\,\dot{\rho} \;\;\;\;\;\;=\; \pm\frac{1}{\sqrt{e^{2\omega t}-1}}\;, \\ \sqrt{\beta}\,p(t) \;&=\; \tan\big(\sqrt{\beta}\rho\big) \;=\; \pm\frac{1}{\sqrt{e^{2\omega t}-1}}\;. \end{aligned} \tag{2.135}$$

The particle starts out at $(x,p) = (\pm\infty, \pm\infty)$ and asymptotically approaches the origin, taking an infinite amount of time to get there. This behavior is show in Fig. 2.8.

2.8 Compactification

As we have seen, when $m < 0$ and $\beta \neq 0$, it only takes a finite amount of time for the particle to traverse the entire classical trajectory as long as the energy of the particle is non-zero. This means that we must specify what happens to the particle after it reaches infinity. For this, we could either compactify x-space so that the particle which reaches $x = \pm\infty$ will return from $x = \mp\infty$, in which case the momentum of the particle will bounce back from infinite walls at $p = \pm\infty$, or we could compactify p-space so that the particle which reaches $p = \pm\infty$ will return from $p = \mp\infty$, in which case the position of the particle will bounce back from infinite walls at $x = \pm\infty$.

Here, we choose to compactify x-space so that the $|m| \to \infty$ limit of the $m < 0$, $C < 0$ solution will match the $m \to \infty$ limit of the $m > 0$, $C > 0$ solution. This choice also agrees with the boundary condition we imposed in the quantum case, in which the wave-function in ρ was demanded to vanish at the domain boundaries $\rho = \pm\pi/2\sqrt{\beta}$, which corresponds to placing infinite potential walls there. The $m > 0$, $C > 0$ solution was given by Eq. (2.108). Taking the $|m| \to \infty$ limit of Eq. (2.115) while keeping B fixed, we find

$$\sqrt{|C|-1}\,\omega \quad\xrightarrow{m\to\infty}\quad \sqrt{2E\beta k} \;=\sqrt{\beta}kB \;\equiv\; \omega_0\;, \tag{2.136}$$

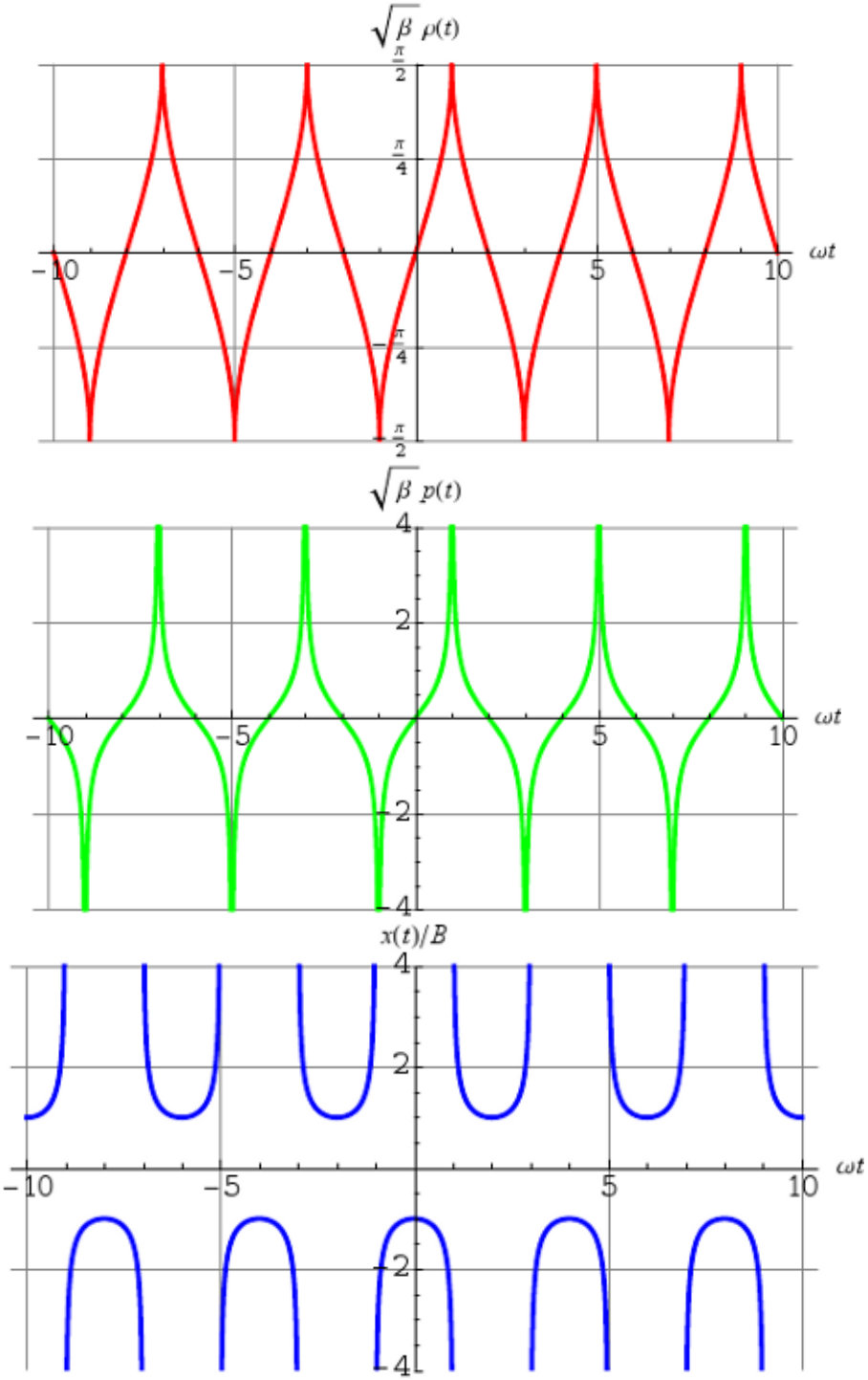

Figure 2.9: The periodic behavior of the negative-mass particle in a harmonic oscillator potential in compactified x-space. The example shown is for $C = -1$.

and

$$\begin{aligned}
\sqrt{\beta}\,\rho(t) &\xrightarrow{|m|\to\infty} \arcsin\Big[\sin(\pm\omega_0 t)\Big]\,, \\
\sqrt{\beta}\,p(t) &\xrightarrow{|m|\to\infty} +\frac{\sin(\pm\omega_0 t)}{|\cos(\pm\omega_0 t)|}\,, \\
x(t)/B &\xrightarrow{|m|\to\infty} \mp\frac{\cos(\pm\omega_0 t)}{|\cos(\pm\omega_0 t)|}\,.
\end{aligned} \tag{2.137}$$

which formally agrees with Eq. (2.108), and if graphed will lead to a figure similar to Fig. 2.5. The one significant difference is, however, that when the particle jumps from $x = \pm A$ to $x = \mp A$ in the $m > 0$ case it goes through $x = 0$, while when it jumps from $x = \pm B$ to $x = \mp B$ in the $m < 0$ case, it must go through $x = \infty$.

By compactifying x-space, all motion when $E \neq 0$ will become oscillatory through $x = \infty$, and the T calculated above becomes the oscillatory period. As an example, we plot the x-compactified solution for $C = -1$ in Fig. 2.9, for which the period is $T = 4/\omega$. Note that the period for the $m < 0$, $C < 0$ solution in the limit of $|m| \to \infty$ becomes

$$\lim_{|m|\to\infty} T \;=\; \lim_{|m|\to\infty} \frac{4}{\omega\sqrt{|C|^2-1}} \arccos\frac{1}{\sqrt{|C|}} \;=\; \frac{2\pi}{\omega_0}\,, \tag{2.138}$$

the arccosine providing a $\pi/2$.

2.9 Classical Probablities

Consider the $m < 0$, $C = -2|m|E\beta < 0$ case. $\sqrt{\beta}\rho$ evolves from $-\pi/2$ to $\pi/2$ in time $T/2$, that is:

$$\begin{aligned}
\frac{T}{2} &= \int_{-T/4}^{T/4} dt \;=\; \int_{-\pi/2\sqrt{\beta}}^{\pi/2\sqrt{\beta}} \frac{dt}{d\rho}\,d\rho \;=\; \int_{-\pi/2\sqrt{\beta}}^{\pi/2\sqrt{\beta}} \frac{d\rho}{\dot\rho} \\
&= \frac{1}{\omega}\int_{-\pi/2\sqrt{\beta}}^{\pi/2\sqrt{\beta}} \frac{\sqrt{\beta}\,d\rho}{\sqrt{\tan^2\big(\sqrt{\beta}\rho\big)+|C|}}\,.
\end{aligned} \tag{2.139}$$

Thus, we can identify

$$P(\rho) \;=\; \frac{2}{\omega T}\,\frac{\sqrt{\beta}}{\sqrt{\tan^2\big(\sqrt{\beta}\rho\big)+|C|}} \tag{2.140}$$

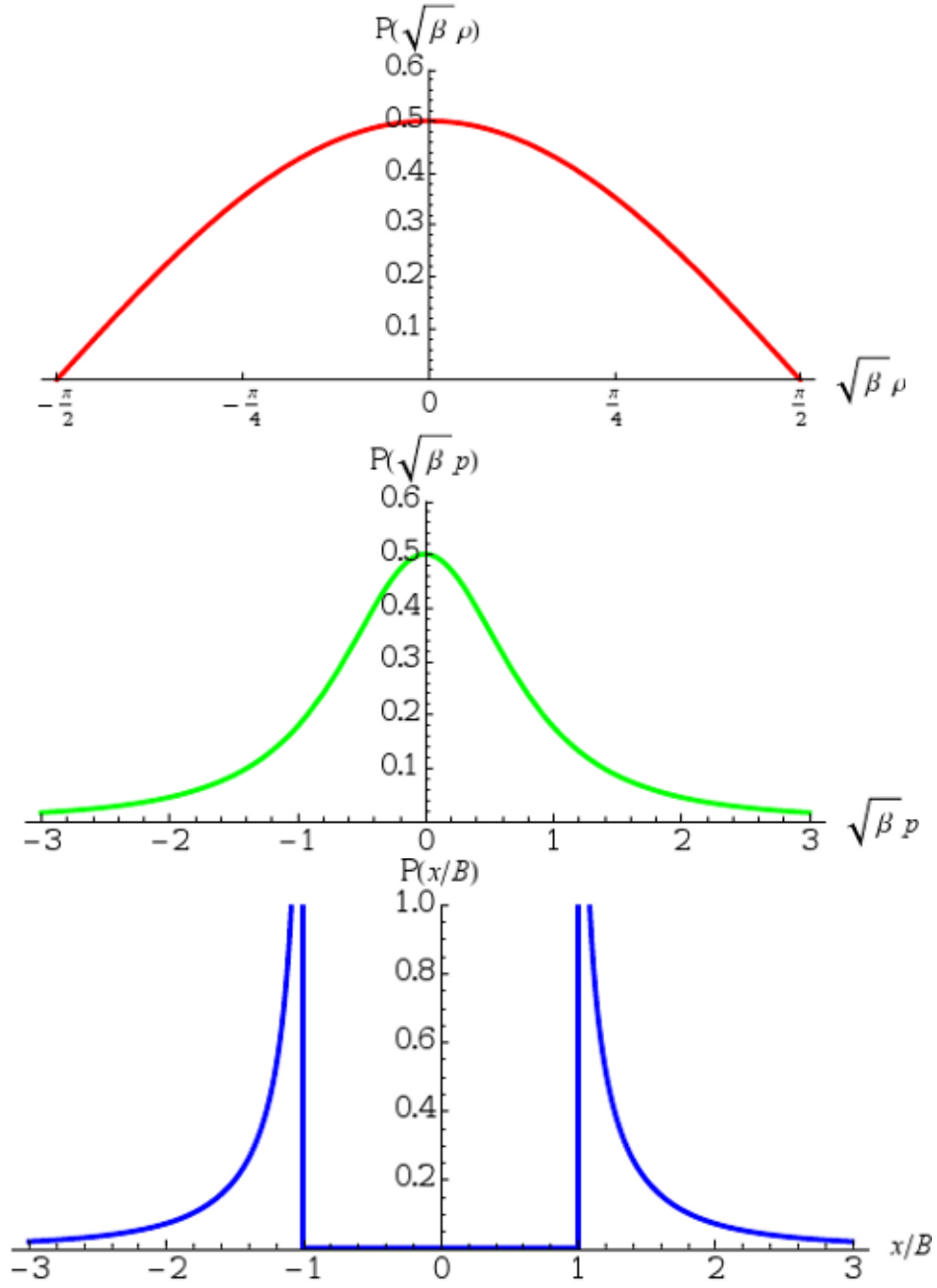

Figure 2.10: Classical probabilities in ρ-, p-, and x-spaces of a negative mass particle in a harmonic oscillator potential for the case $C = -2|m|E\beta = -1$. The time dependence of this solution was shown in Fig. 2.9. Though the trajectory of the particle is not confined to a finite region of phase space, the classical probabilities of finding the particle near the phase-space-origin is still finite due to the finiteness of the time it takes for the particle to traverse the entire trajectory.

as the classical probability density of the particle in ρ-space. The classical probablity in p- and x-spaces can be defined in a similar manner:

$$\begin{aligned} P(p) &= P(\rho)\,\frac{d\rho}{dp} \\ &= \frac{2}{\omega T}\,\frac{\sqrt{\beta}}{(1+\beta p^2)\sqrt{|C|+\beta p^2}}\,, \\ P(x) &= P(\rho)\,\frac{d\rho}{dx} \\ &= \frac{2}{T}\frac{\sqrt{\beta}|m|}{\sqrt{\beta|m|kx^2-|C|}\Big(\beta|m|k^2x^2-|C|+1\Big)} \\ &= \frac{2}{\omega T}\frac{B^2}{\sqrt{x^2-B^2}\Big[\,|C|(x^2-B^2)+B^2\,\Big]}\,. \end{aligned} \tag{2.141}$$

These probability functions are plotted in Fig. 2.10 for the case $C=-2|m|E\beta=-1$.

Comparing the energies of the quantum and classical solutions given in Eqs. (2.51) and (2.116), we can conclude that the correspondence is given by the relation

$$-C \;=\; \frac{n^2+(2n+1)\lambda}{\lambda(1-\lambda)}\,, \qquad \frac{1}{2}<\lambda<1\,. \tag{2.142}$$

We expect the quantum and classical probabilities to match for large n. As an example, we take $\lambda=\frac{3}{4}$ and $n=30$, which correspond to:

$$\begin{aligned} C &= -5044\,, \\ \kappa &= \frac{\Delta x_{\min}}{a} \;=\; \frac{1}{\sqrt[4]{\lambda(1-\lambda)}} \;=\; \frac{2}{\sqrt[4]{3}} \;\approx\; 1.52, \\ B &= \frac{\sqrt{|C|}}{\kappa^2}\,\Delta x_{\min} \overset{1\ll n}{\approx}\; n\,\Delta x_{\min} \;=\; 30\,\Delta x_{\min}\,. \end{aligned} \tag{2.143}$$

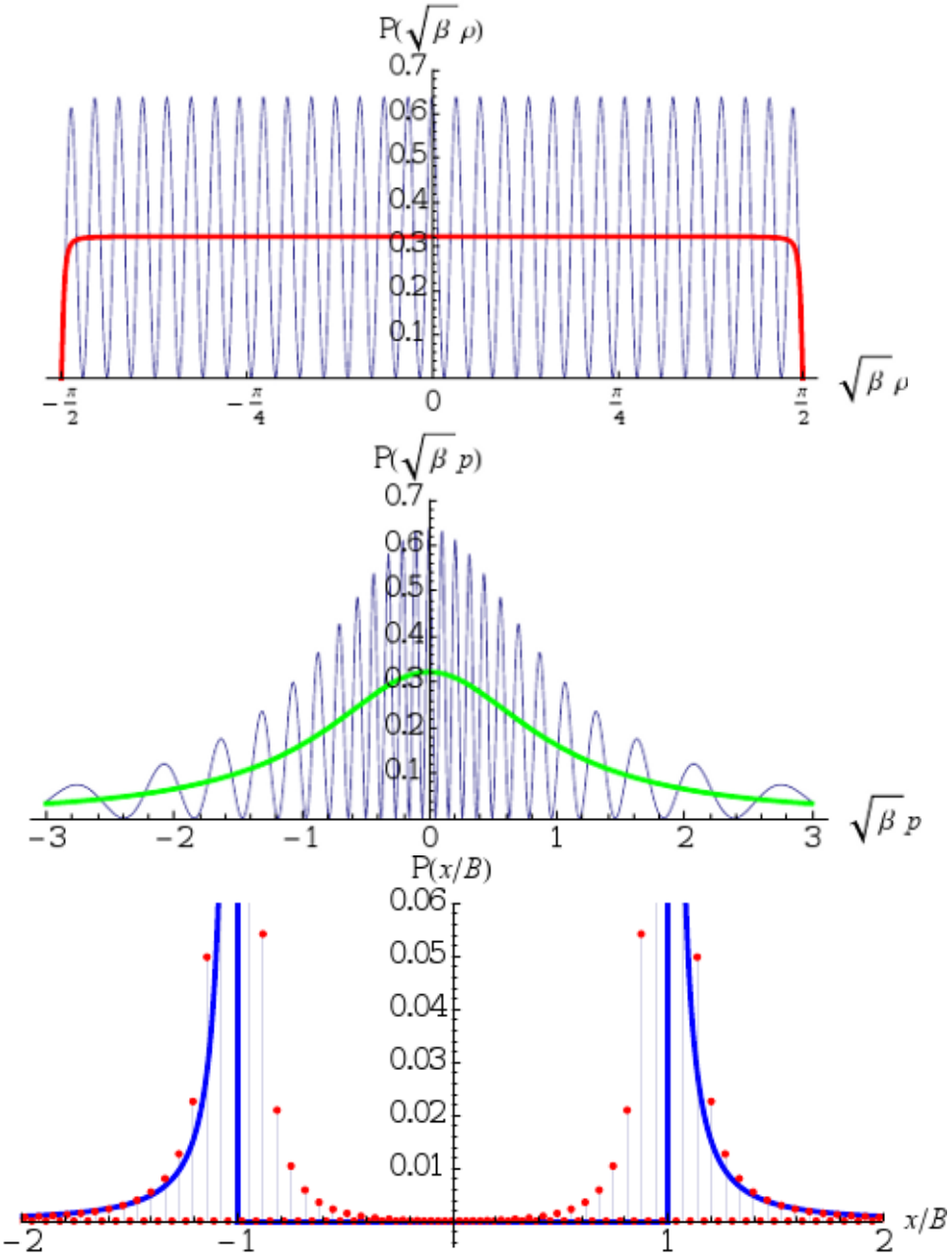

Figure 2.11: Comparison of quantum and classical probabilities in ρ-, p-, and x-spaces for a negative mass particle in a harmonic oscillator potential for the case $\lambda = \frac{3}{4}$ and $n = 30$, which corresponds to the classical $C = -2|m|E\beta = -5044$. The quantum distribution in x-space is discrete due to the existence of the minimal length. There is also some seepage of the probability into classically forbidden regions in x-space as is expected of quantum probabilities.

The comparison of the quantum and classical probabilities for this case in ρ-, p-, and x-spaces are shown in Fig. 2.11. If we average out the bumps in the quantum case, it is clear that the distributions agree, up to the typical quantum mechanical phenomenon of seepage of the probability into energetically forbidden regions. Thus, the existence of 'bound' states with a finite Δx and Δp in the quantum case can be associated with the fact that the particle spends a finite amount of time near the phase space origin in the classical limit.

2.10 Further Discussion

We have solved for the eigenstates of the harmonic oscillator hamiltonian under the assumption of the deformed commutation relation between $\hat{x}$ and $\hat{p}$ as given in Eq. (2.5), and successfully calculated the uncertainties in position and momentum without encountering any analytic incongruities. Though none were expected, as the analytic structure of the employed representation was shown by Kempf [18] to be free from anomalies, it is always nice to see the details check out.

To reiterate, for the normal harmonic oscillator with positive mass ($1/m > 0$), the eigenstates are found on the $\Delta x \sim 1/\Delta p$ branch of the MLUR, where decreasing $1/m$ leads to larger Δp, and thus smaller Δx; the behavior seen in canonical quantum systems. This leads us to think that we are dealing with a perfectly reasonable, small-parameter deformation to canonical quantum mechanics.

The question of possible experimental tests has been addressed by Benczik, Chang, Minic, and Takeuchi in [66] where they analyze the energy eigenstates of the hydrogen atom under a similar modification of the commutation relations. Unfortunately, that system provides poor bounds on the size of the minimal length under current modeling assumptions.

Somewhat surprisingly, $1/m$ can be decreased through zero into the negative, thereby 'inverting' the harmonic oscillator, while still maintaining an infinite ladder of positive energy eigenstates so long as the condition $\Delta x_{\min}/\sqrt{2} > a \equiv [\,\hbar^2/k|m|\,]^{1/4}$ is satisfied. There, the eigenstates are found on the $\Delta x \sim \Delta p$ branch of the MLUR, where decreasing $1/m$ away from zero further into the negative leads to larger Δp, and thus larger Δx, with both diverging as a approaches the above bound from below. The $1/m = 0$ line separating the $\Delta x \sim 1/\Delta p$ and $\Delta x \sim \Delta p$ regions is given by Eq. (2.61).

One way to understand why the negative mass solutions are being stabilized, is

by considering what happens to the phase space volume when the commutation relations are modified. As we saw in Chapter 1, the density of states in the phase space becomes momentum dependent. As the momentum increases, the density of states decreases, attenuating the contribution from the high momentum states. This attenuation is apparently sufficient to allow for the states to be normalizable.

Though the states in the negative mass case have $\Delta x \sim \Delta p$, they are separated from the $\Delta x \sim 1/\Delta p$ states by the sign of the mass parameter, and so there seems to be no interaction between them. This would have been required to study possible mechanisms of jamming, and is currently being searched for in other potentials. There are indications that both states are simultaneously accessible in the free particle case, but the subtleties of that situation have yet to be explored.

Taking the classical limit by replacing our deformed commutator with a deformed Poisson bracket, we solved the corresponding classical equations of motion and find that the solutions for the 'inverted' harmonic oscillator are such that the particle only takes a finite amount of time to traverse its entire trajectory. This leads to a finite classical probability density of finding the particle near the phase space origin, and provides another explanation of why 'bound' states with discrete energy levels can be expected in the quantum case. Although compactification was used to make sense of this 'bound' behavior, it would be interesting to see if angular motion in a 2D or 3D case could allow for similar 'bound' behavior in regular space.

One significant difference between the classical and quantum cases is, however, that the classical system has no restriction on the sign of the energy, whereas the quantum system only allows for positive energy eigenstates. The latter is guaranteed by the above mentioned condition on $\Delta x_{\min}$ and a. Indeed, the condition is equivalent to

$$E \;=\; \frac{k}{2}(\Delta x)^2 - \frac{1}{2|m|}(\Delta p)^2 \;>\; 0\,, \tag{2.144}$$

when one assumes $\Delta x \sim (\hbar\beta/2)\Delta p$.

Another interesting thing to consider would be the relativistic implications of modified commutation relations. In our case, when the mass was negative, the classical equations of motion calls for the particle to move at arbitrarily large speeds. We are also assuming that Eq. (2.5) embodies the non-relativistic limit of some relativistic theory with a minimal length. From that perspective, the infinite speed that the negative-mass particle attains seems problematic.

Chapter 3

Galois Fields as State Spaces

3.1 Background

One of the centerpieces of canonical quantum mechanics is the use of Hilbert spaces for the state spaces of the theory. This has been formally the case since von Neumann's work, especially after landmark explanations of the foundations of quantum mechanics [68]. In this chapter we will explore the use of spaces other than Hilbert spaces for use as the state space of a quantum theory and will see that many features of the canonical theory can be recovered.

Before we begin the process of modifying this aspect of the theory, we will take a look at some key features of Hilbert spaces and see how they are used in the canonical quantum theory. This information can be found in any introductory text on analysis, such as Kolmogorov and Fomin [69].

A Hilbert space is a real, or complex, inner product space that is also a complete metric space. Completeness in this sense means that all Cauchy sequences in the space converge to an element of the space, where the convergence is with respect to the metric defined by the inner product. We can thus treat convergent series, such as Fourier series, simply, as the limit is guaranteed to be an element of the space. It also allows us to avoid major issues in defining derivatives and other useful operations. If we also assume that the Hilbert spaces we will use are also separable, as is often done, then there is guaranteed to exist some countable orthogonal basis for the space.

For a given Hilbert space, $\mathcal{H}$, the space of linear functionals, often called the *dual*

space, of $\mathcal{H}$ is isomorphic to $\mathcal{H}$, and that these spaces are linked through the inner product on $\mathcal{H}$. This correspondence is the result of the Riesz representation theorem. A further consequence of this theorem is that a bounded linear operator, $\hat{A}$, acting on $\mathcal{H}$ can be identified with a bounded linear operator, $\hat{A}^\dagger$, acting on the dual space of $\mathcal{H}$. $\hat{A}^\dagger$ is called the adjoint of $\hat{A}$. An operator that is equal to it's own adjoint is called self-adjoint, or Hermitian. These operators have real eigenvalues and their eigenvectors form orthogonal bases for the Hilbert space.

Linear operators that preserve the inner product between any two elements of a Hilbert space are called unitary operators and they correspond to basis transformations between orthonormal bases. These act as canonical coordinate transforms do in classical theories (as can be seen in Goldstein, Safko, and Poole [70] or Landau and Lifshitz [71]).

In canonical quantum mechanics, spaces such as the space of square integrable functions over some interval, $L_2[a, b]$, or the usual space of sequences of elements of $\mathbb{R}^N$, are important examples of Hilbert spaces. The function spaces are useful when dealing with solutions to differential equations, particularly the Schrödinger equation and sequence spaces aid in the Fourier analysis of these solutions.

Now that we have recalled the basic mathematical structures of Hilbert spaces, let's take a step-by-step look at how these structures can be associated with elements of a physical system, thus creating a physical theory. For more details, see any graduate level quantum mechanics text, like Shankar [61] of Schwabl [62].

Quantum descriptions of physical systems can begin with the introduction of a vector space, generally defined over the complex number field, $\mathbb{C}$, or over a space of complex functions. Elements of the space are then associated with states of the physical system under consideration. Such a space, in the canonical approach, is assumed to be a Hilbert space $\mathcal{H}$ and, in the case of N-level systems, with which we will be most interested in considering, these spaces are explicitly $\mathcal{H} = \mathbb{C}^N$.

The Hilbert space, by definition, $\mathcal{H}$ possesses an inner product $\mathcal{H} \times \mathcal{H} \to \mathbb{C}$, which we denote

$$\big(||\alpha\rangle\rangle \, , ||\beta\rangle\rangle \big) \, \in \, \mathbb{C} \, , \qquad |\alpha\rangle \, , \, |\beta\rangle \, \in \, \mathcal{H} \, . \tag{3.1}$$

As specified by the Reisz representation theorem, we can associate with each vector $|\alpha\rangle \in \mathcal{H}$, a similarly labeled dual-vector $\langle\alpha| \in \mathcal{H}^*$, via

$$\langle\alpha| \; = \; \big(||\alpha\rangle\rangle \, , | \quad \rangle \big) \, , \tag{3.2}$$

so that

$$\langle\alpha|\beta\rangle \; = \; \big(||\alpha\rangle\rangle \, , ||\beta\rangle\rangle \big) \, . \tag{3.3}$$

The presence of the inner product allows for us to define for each linear operator acting on the vector space, $\hat{A}$, the Hermitian conjugate, $\hat{A}^\dagger$, of that operator via

$$\left(||\alpha\rangle\rangle \, , \left| \hat{A} \, |\beta\rangle \right\rangle \right) \; = \; \left(\left| \hat{A}^\dagger \, |\alpha\rangle \right\rangle , ||\beta\rangle\rangle \right) \, , \tag{3.4}$$

Linear operators that satisfy the relation $\hat{A}^\dagger = \hat{A}$ are said to be Hermitian, or as before, self-adjont, operators.

Having an inner product also allows for the definition of unitary operators via

$$\left(\left| \hat{U} \, |\alpha\rangle \right\rangle , \left| \hat{U} \, |\beta\rangle \right\rangle \right) \; = \; \left(||\alpha\rangle\rangle \, , ||\beta\rangle\rangle \right) \, . \tag{3.5}$$

These operators, by definition, are those that leave the inner product unchanged. Specifically, they will not alter the 'magnitude' of a vector, defined by the norm that is induced by the inner product. This will be advantageous as we want this magnitude to represent an absolutely unchangeable value.

We will now consider two ways for quantum descriptions using these mathematical structures to make contact with physical experiments. In canonical quantum mechanics, these different ways provide equivalent predictions for measurements of the properties of a given system.

In the first approach, possible outcomes of a measurement of an observable property of a system , A, are assumed to be identifiable with the eigenvalues of a Hermitian linear operator, $\hat{A}$. Let us denote an eigenvector of some observable, $\hat{A}$, that is associated with eigenvalue α by $|\alpha\rangle$:

$$(\hat{A} - \alpha \hat{I}) \, |\alpha\rangle \; = \; 0 \, . \tag{3.6}$$

When the system is in the state represented by the vector $|\psi\rangle \in \mathcal{H}$, the probability of obtaining the outcome $\alpha \in \mathbb{R}$ as a result of a measurement of $\hat{A}$ is given by

$$P(\alpha|\psi) \; = \; \frac{\left|\langle \alpha|\psi\rangle\right|^2}{\sum_\beta \left|\langle \beta|\psi\rangle\right|^2} \, , \tag{3.7}$$

where the sum in the denominator runs over all the eigenvalues of $\hat{A}$. The hermiticity of $\hat{A}$ ensures that its eigenvalues are all real, and that the eigenvectors are mutually orthogonal and form a complete basis of the state space.

If the vector representing the state of the system and the eigenvectors of $\hat{A}$ are normalized,

$$\langle \psi|\psi\rangle = 1 \, , \qquad \langle \alpha|\beta\rangle \; = \; \delta_{\alpha\beta} \, , \tag{3.8}$$

the above expression for the probability simplifies to the usual form of the Born rule: $P(\alpha|\psi) = |\langle\alpha|\psi\rangle|^2$. Since the eigenvectors of $\hat{A}$ form an orthonormal basis, the requirement that a state is normalized forces the sum of the probabilities of all of the possible measurement outcomes to be 1.

Another consequence of $\hat{A}$ having normalized, orthogonal eigenstates is that it can be represented as a sum of projection operators:

$$\hat{A} = \sum_{\alpha} \alpha \, |\alpha\rangle \, \langle\alpha| \, , \tag{3.9}$$

where, again, the sum is over the possible eigenvalues of $\hat{A}$.

From their definition in Eq. (3.5), it is clear to see that unitary operators acting on the state space will leave the inner product invariant. Thus, unitary transformations of the state space will act as basis transformations as well as guaranteeing that the sum of the probabilities of all the possible measurement outcomes will remain 1. This makes them useful in describing dynamic changes to the system, such as time evolution.

Thus, given states in a Hilbert space and Hermitian linear operators, we can predict the probabilities of the outcomes of measurements. One can then bring the tools statistics to bear on these probability distributions; calculating quantities such as expectation values and uncertainties.

Instead of defining a formula for the probabilities of measurement outcomes, there is an alternative way of making contact with experiment. Let's begin this time with the quantity

$$E\left(\hat{A}, |\psi\rangle\right) = \frac{\langle\psi| \, \hat{A} \, |\psi\rangle}{\langle\psi|\psi\rangle} \, , \tag{3.10}$$

which is real for hermitan $\hat{A}$, and interpret the result as the expectation value for repeated measurement of the associated observable in the state $|\psi\rangle$. If $\langle\psi|\psi\rangle = 1$, the expression reduces to $\langle\psi| \, \hat{A} \, |\psi\rangle$.

As an aside, though this is not the approach typically used in ordinary quantum mechanics, it is the standard approach in Quantum Field Theory (QFT), a much more advanced version of quantum mechanics, in which all physical predictions are expressed in terms of N-point correlation functions, *i.e.*, the vacuum expectation values of the products of N field operators. This is most explicit in the path integral formulation of QFT, as detailed in Feynman and Hibbs [72].

To recover the probabilistic interpretation of the first approach, one asserts that the probability for obtaining the outcome α for the measurement of $\hat{A}$ on the state $|\psi\rangle$ is given by

$$P(\alpha|\psi) \;=\; \frac{\langle\psi|\;\delta(\hat{A}-\alpha)\;|\psi\rangle}{\langle\psi|\psi\rangle}\,. \tag{3.11}$$

Here the delta function is evaluated heuristically: its value is 1 if $\hat{A}$ and a have the same effect on $|\psi\rangle$ and is 0 otherwise. No absolute values are invoked, and attention is shifted to moments of the relevant observable operator in the state in question. In particular, we need the expectation values of several powers of the operator in order to determine all of the probabilities that correspond to a generic state.

For canonical quantum descriptions using the Hilbert space $\mathcal{H}$, these two starting points lead to identical results. That is because the linearity that is required to form an expectation value through the probability-weighted sum of measurement outcomes is guaranteed by the use of the inner product in defining both, as we will see in detail shortly. This situation however changes when the underlying space is not a Hilbert space. Indeed, for spaces for which the inner product is ill-defined, one can expect different outcomes for these two approaches.

The main goal of this chapter is to explore the consequences of choosing for a state space a space that cannot have an inner product while retaining as much of the usual structure as we can. The states spaces that we will use will be formed by discretizing the number fields over which the vector space is defined. We then impose the physical interpretation provided by one of the two approaches mentioned above: the first approach being the direct definition of probabilities via Eq. (3.7) and the second approach being the direct definition of expectation values via Eq. (3.10).

Replacing the field of the state space has been done or suggested before, in various contexts. Several authors have attempted to extend canonical quantum mechanics by using the quaternions as the base number field. Reviews of these attempts can be found in various works by Finkelstein [73]. As they are non-commutative, they do provide for a richer mathematical structure, though, many of the physical predictions turn out to be the same as for complex quantum mechanics. In Ref. [56], Nambu suggests that one could replace the usual continuous position and momentum spaces by Galois fields. The purpose behind this would be to study the special form of the norm that these spaces have. As mentioned in the first chapter, this was a major inspiration for the current analysis. From a quantum computation perspective, Schumacher and Westmoreland [74], consider replacing the base field with the simplest Galois field, GF(2). They then study the logical and computational structure of that

theory. The current analysis of the probability approach extends their work, though, it focuses on correlations and symmetry, as opposed to qubits and logic gates.

The fields we consider are finite Galois fields $GF(p^n)$, where $n \in \mathbb{N}$ and p is a prime number. For the $n = 1$ case, they are $GF(p) = \mathbb{Z}_p = \mathbb{Z}/p\mathbb{Z}$. Vector spaces over $GF(p^n)$ do not have inner products since $GF(p^n)$ is not an ordered field; ordered fields being fields on which an ordering can be imposed that respects both addition and multiplication. This prevents any bilinear map to $GF(p^n)$ from being positive-definite (or non-negative) in a natural way.

However, for either Eq. (3.7) or Eq. (3.10) to make sense, the dual-vectors that appear in the expression only need to constitute a basis for the dual-vector space and have a possible outcome of a measurement associated with each one. The usual pairing of dual-vectors with vectors via the inner product is inessential. Indeed, all the inner product does, in a sense, is connect the two approaches via the property

$$\langle\psi|\alpha\rangle \;=\; \big(\,||\psi\rangle\rangle\,,||\alpha\rangle\rangle\big) \;=\; \big(\,||\alpha\rangle\rangle\,,||\psi\rangle\rangle\big)^* \;=\; \langle\alpha|\psi\rangle^*\,, \tag{3.12}$$

so that we can write,

$$\begin{aligned}\sum_\alpha \alpha P(\alpha|\psi) \;&=\; \frac{\sum_\alpha \alpha\big|\langle\alpha|\psi\rangle\big|^2}{\sum_\beta\big|\langle\beta|\psi\rangle\big|^2} \;=\; \frac{\sum_\alpha\langle\alpha|\psi\rangle^*\alpha\langle\alpha|\psi\rangle}{\sum_\beta\langle\beta|\psi\rangle^*\langle\beta|\psi\rangle}\\ &=\; \frac{\sum_\alpha\langle\psi|\alpha\rangle\alpha\langle\alpha|\psi\rangle}{\sum_\beta\langle\psi|\beta\rangle\langle\beta|\psi\rangle} \;=\; \frac{\langle\psi|\,\hat{A}\,|\psi\rangle}{\langle\psi|\psi\rangle}\,,\end{aligned} \tag{3.13}$$

where we have made the identification

$$\hat{A} \;=\; \sum_\alpha \alpha\,|\alpha\rangle\,\langle\alpha|\;. \tag{3.14}$$

Thus, we will avoid defining inner products, and instead, once a basis of the dual-vector space and the associated set of outcomes is specified, we will use those to define 'observables'.

To make contact with the outcome of measurements and probability distributions, we need a map from the Galois field to that of non-negative real numbers. It is essential that this map preserves not only scalar products, which is necessary to distinguish entangled states from product ones, but also the actions of symmetry groups, our version of unitary transformation, on the Galois field.

This connection is achieved in the first approach through the use of an absolute value function. Eq. (3.7) can be used as is to define the probability of each outcome via

the absolute value function from $GF(p^n)$ to $\mathbb{R}$ given by

$$|\,\underline{k}\,| \;=\; \begin{cases} 0 & \text{if } \underline{k} = \underline{0}\,, \\ 1 & \text{if } \underline{k} \neq \underline{0}\,. \end{cases} \tag{3.15}$$

Here, numbers and symbols with underlines are used to denote elements of $GF(p^n)$, to distinguish them from elements of $\mathbb{R}$. Note that this function is a product preserving as $|\underline{k}\underline{\ell}| = |\underline{k}||\underline{\ell}|$, making it a group homomorphism. This property is essential for the probabilities of product states to factorize, which is essential for two particles to be considered distinct, as we will see later.

Applying this formalism to 2-level systems, we will construct spin-like observables for which the measurement outcomes are $\pm 1 \in \mathbb{R}$, and calculate the Clauser-Horne-Shimony-Holt (CHSH) [43] bound for the model, as motivated and described in the first chapter. In the first approach, it is found that the CHSH bound for spin-like systems over Galois fields cannot be larger than 2.

It will also be shown that the predictions that this theory make are not obtainable from classical theories with suitable restrictions. The arguments used will be similar to those used by Hardy [59] and Greenberger, Horne, Shimony, and Zeilinger [60] in the case of canonical quantum mechanics.

The major results from this analysis have been accepted for publication (pre-prints of those articles can be found on the arXIv: [75] and [76]).

We will then explore the consequences of the second approach to interpretation, namely, the direct definition of expectation values via Eq. (3.10). Again, we consider vector spaces over the finite Galois field $GF(p^n)$, which do not have inner products.

The concepts of normalizability of states, hermiticity of operators, and that of a dual-vector being a Hermitian conjugate of a vector, must all be reexamined before we can apply Eq. (3.10). Furthermore, working in a vector space over $GF(p^n)$, the expression $\langle\psi|\,\hat{A}\,|\psi\rangle$ = (row vector)·(matrix)·(column vector) will generically lead to an element of $GF(p^n)$, which must be mapped to an element of $\mathbb{R}$ if the result is to represent the expectation value of a measurement of a physical observable.

These issues are addressed one by one and we will look at the specific implications of these definitions on vector spaces over the fields $GF(3) = \mathbb{Z}_3$ and then $GF(9) = \mathbb{Z}_3[\,\underline{i}\,]$, where $\underline{i}$ is the solution to the equation $\underline{x}^2 + \underline{1} \;=\; \underline{0}$ (which is irreducible in $GF(3)$). In these cases, we will find that $\langle\psi|\,\hat{A}\,|\psi\rangle \in GF(3)$ by construction, which will determine an appropriate mapping to a number in $\mathbb{R}$. Because we are looking at the expectation values of observables, the range of this map need not be restricted

to the non-negative reals as in the case of the absolute value function. It will be shown that the requirement that this map be a group homomorphism and invariant under the actions of the relevant symmetry groups determines the map uniquely. It is the use of this map for expectation values, instead of the absolute value function on brackets, that leads to the markedly different results between the two approaches.

It is also shown below that the connection to probabilities given by Eq. (3.11) for canonical QM is no longer valid. In fact, individual probability distributions are not fixed in this approach, giving rise to indeterminacies beyond those of canonical QM.

We will find that in this approach, the predictions again go beyond those of classical theories, as will be shown with a GHSZ/Hardy type argument. Lastly, we will find that the CHSH bound for the $GF(3)$ case is also 2, while for the $GF(9)$ case, however, the CHSH bound violates the Cirel'son bound [40] and is found to be 4; the maximum possible value.

While the major results of this analysis are currently under review for publication, a preprint can be found on the arXiv: Ref. [77].

3.2 The Probability Path

3.2.1 Preliminaries

The essential modification in this chapter is the replacement of the Hilbert space of an N-level quantum system, $\mathcal{H}_{\mathbb{C}} = \mathbb{C}^N$, with a discrete vector space over a finite field: $\mathcal{H}_q = \mathbb{Z}_q^N$. Here, $\mathbb{Z}_q$ denotes the Galois field $GF(q)$, where $q = p^n$ with p prime and $n \in \mathbb{N}$.

Once this choice is made, as we saw in the last section, there are two paths that can be taken towards creating the modified theory. In this section, the consequences of preserving the canonical probability rule will be explored.

To begin, we'll need to identify the various parts of (3.7) with elements of $\mathcal{H}_q$ or associated spaces. Mirroring the canonical case, we'll assume that the states of the system are represented by vectors $|\psi\rangle \in \mathcal{H}_q$. The dual-vectors, $\langle x| \in \mathcal{H}_q^*$, will be used to represent the outcomes of measurements, though, as will be explained later, the particular outcome represented can and shall depend on the context of the measurement.

Observables are associated with a choice of basis of $\mathcal{H}_q^*$, each dual-vector in each basis representing a different outcome. The probability of obtaining the outcome represented by $\langle x|$ when a measurement of the observable is performed on the state represented by $|\psi\rangle$ is given by the canonical form

$$P(x|\psi) \;=\; \frac{\big|\langle x|\psi\rangle\big|^2}{\sum_y \big|\langle y|\psi\rangle\big|^2}\,, \tag{3.16}$$

where the sum in the denominator is taken over the basis of the dual space corresponding to the observable and the bracket $\langle x|\psi\rangle \in \mathbb{Z}_q$ is converted into a non-negative real number $|\langle x|\psi\rangle| \in \mathbb{R}$ via the absolute value function:

$$|\,\underline{k}\,| \;=\; \begin{cases} 0 & \text{if } \underline{k} = \underline{0}\,, \\ 1 & \text{if } \underline{k} \neq \underline{0}\,. \end{cases} \tag{3.17}$$

Here, underlined numbers and symbols represent elements of $\mathbb{Z}_q$, to distinguish them from elements of $\mathbb{R}$ or $\mathbb{C}$.

As all non-zero elements of $\mathbb{Z}_q$ are assigned an absolute value of 1, they may act like the phases of canonical quantum mechanics, which share this same property. Since $\mathbb{Z}_q\backslash\{\underline{0}\}$ is a cyclic multiplicative group, this definition of absolute value is consistent with the requirement that

$$|\underline{k}\underline{l}| \;=\; |\underline{k}||\underline{l}|\,, \tag{3.18}$$

which is necessary for the probabilities of product states to factorize, as will be important when we discuss two particle state spaces.

There is one other finite subset of $\mathbb{R}$ that is a cyclic group with respect to multiplication that could be used, in some cases, to build an alternate, absolute value like function; the set $\{-1, 1\}$. Since the result of the absolute value is squared in the probability formula, there will be no ultimate difference if it is used instead of $\{1\}$, so we will take (3.17) as our absolute value function. In the second approach, this will not be the case, and the use of $\{-1, 1\}$ will have interesting consequences.

Note that we now have only two possible measurement outcomes. This does not conceptually pose a problem for the current scheme as we are mainly concerned with the description of spin-like systems.

Since the multiplication of $|\psi\rangle$ with a non-zero element of $\mathbb{Z}_q$ will not affect the probability as defined above, vectors that differ by a non-zero multiplicative constant are identified as representing the same physical state, thus endowing the state space with

a finite projective geometry (for more information about finite projective geometry, these texts are recommended [78, 79, 80]).

$$PG(N-1,q) \;=\; (\,\mathbb{Z}_q^N \backslash \{\underline{\mathbf{0}}\}\,) \,/\, (\,\mathbb{Z}_q \backslash \{\underline{0}\}\,) \tag{3.19}$$

The group of all possible basis transformations in this space is the projective group $PGL(N,q)$:

$$PGL(N,q) \;=\; GL(N,q) \,/\, Z(N,q)\;. \tag{3.20}$$

Here, $GL(N,q)$ is the general linear group of $\mathbb{Z}_q^N$, and $Z(N,q)$, the $N \times N$ unit matrices multiplied by elements of $\mathbb{Z}_q \backslash \{\underline{0}\}$, is the center of $GL(N,q)$. As a reminder, the center of a given group is the subset of its elements that commute with all elements of the group.

Effectively, the elements of $PGL(N,q)$ lead to permutations of the states in $PG(N-1,q)$, and is thus a subgroup of the symmetric group of all possible state permutations. Physically, basis transformations usually correspond to a change of detector settings, such as the rotation of the polarization axis of a spin-measuring device. This interpretation will be seen later to be justified in this discrete context as well.

Let us denote the model resulting from this procedure as $DQM(N,q)$, where 'DQM' stands for discrete quantum mechanics. Spin-like systems, those with two possible outcomes ± 1, can be constructed on the space $V_q \equiv \mathbb{Z}_q^2$ as $DQM(2,q)$, and two-particle spin-like systems on $V_q \otimes V_q = \mathbb{Z}_q^2 \otimes \mathbb{Z}_q^2 = \mathbb{Z}_q^4$ as $DQM(4,q)$. We will consider the cases $q = 2$, 3, 4, and 5 as concrete examples of this procedure, so that we may gain some intuition about these systems.

3.2.2 $\mathbb{Z}_2$ Quantum Mechanics

One-Particle Spin

As the smallest prime is 2, the first concrete example is $q = 2$. The spin-like system $DQM(2,2)$ is perhaps the simplest quantum system imaginable as it is constructed on the finite field consisting of only two elements, $GF(2) = \mathbb{Z}_2 = \mathbb{Z}/2\mathbb{Z} = \{\underline{0}, \underline{1}\}$, with the following addition and multiplication tables:

$+$	$\underline{0}$	$\underline{1}$
$\underline{0}$	$\underline{0}$	$\underline{1}$
$\underline{1}$	$\underline{1}$	$\underline{0}$

$\times$	$\underline{0}$	$\underline{1}$
$\underline{0}$	$\underline{0}$	$\underline{0}$
$\underline{1}$	$\underline{0}$	$\underline{1}$

As stated above, numbers with underlines indicate elements of $\mathbb{Z}_2$ in order to distinguish them from elements of $\mathbb{R}$ or $\mathbb{C}$. Since $\mathbb{Z}_2\backslash\{\underline{0}\} = \{\underline{1}\}$ is trivial, there are no phases to deal with. Therefore, each physical state is represented by a unique non-zero vector in $V_2 = \mathbb{Z}_2^2$.

There are only $2^2 - 1 = 3$ non-zero vectors in V_2, which we denote:

$$|a\rangle = \begin{bmatrix} \underline{1} \\ \underline{0} \end{bmatrix}, \quad |b\rangle = \begin{bmatrix} \underline{0} \\ \underline{1} \end{bmatrix}, \quad |c\rangle = \begin{bmatrix} \underline{1} \\ \underline{1} \end{bmatrix}, \tag{3.21}$$

and thus, there are 3 possible states of the system. Since these states are related by

$$\begin{aligned} |a\rangle &= |b\rangle + |c\rangle \ , \\ |b\rangle &= |c\rangle + |a\rangle \ , \\ |c\rangle &= |a\rangle + |b\rangle \ , \end{aligned} \tag{3.22}$$

any pair of them can be used as a basis for V_2. A change of basis in V_2 would permute the above column representations among the three vectors, or equivalently, permute the vector labels a, b, and c on the three column vectors. Since all permutations of the three vectors are possible, the group of basis transformations on V_2 is $S_3 \cong PGL(2,2)$.

The dual vector space V_2^* is the space of all linear maps from V_2 to $\mathbb{Z}_2$. There are $2^2 - 1 = 3$ non-zero dual vectors in V_2^*, and we denote them as:

$$\begin{aligned} \langle\bar{a}| &= \begin{bmatrix} \underline{0} & \underline{1} \end{bmatrix}, \\ \langle\bar{b}| &= \begin{bmatrix} \underline{1} & \underline{0} \end{bmatrix}, \\ \langle\bar{c}| &= \begin{bmatrix} \underline{1} & \underline{1} \end{bmatrix}. \end{aligned} \tag{3.23}$$

With this choice of labeling, the result of dual vectors acting on vectors can be written as:

$$\langle\bar{r}|s\rangle = \begin{cases} \underline{0} & \text{if } r = s, \\ \underline{1} & \text{if } r \neq s, \end{cases} \tag{3.24}$$

and consequently,

$$|\langle\bar{r}|s\rangle| = 1 - \delta_{rs} \ . \tag{3.25}$$

This 'anti-orthogonality' relation pairs up vectors with dual-vectors in a somewhat non-standard way, and leads to the various consequences of the current model. A different labeling could have been chosen, but this labeling highlights the symmetry of the actions of the dual vectors since each dual vector yields $\underline{0}$ once and $\underline{1}$ twice when acting on the vectors in V_2. To maintain Eq.(3.25), we assume that a relabeling of vectors in V_2 is always accompanied by the corresponding relabeling of dual-vectors in V_2^*.

Observables are associated with a *choice of basis* in V_2^*. There are six possible choices:

$$A_{rs} \;=\; \{\, \langle \bar{r}|\,,\, \langle \bar{s}|\,\}\,, \tag{3.26}$$

with $rs \in \{ab,\, ba,\, bc,\, cb,\, ca,\, ac\}$. Each of the dual vectors in each basis represents an *outcome* which could occur as the result of a measurement of the observable represented by that basis. That is, the measurement of the observable A_{rs} would result in one of the two outcomes, the one represented by $\langle \bar{r}|$ or the one represented by $\langle \bar{s}|$. For reference, in [74], Schumacher and Westmoreland referred to these as *effects* instead of *outcomes*.

Although elements of V_2^* map elements of V_2 onto $\mathbb{Z}_2$, the outcomes they represent need not be elements of $\mathbb{Z}_2$ themselves. We can assign the numerical values ± 1 to the two outcomes represented by the ordered pair of dual vectors in each basis: $+1$ to the first dual vector, and -1 to the second dual vector. Thus, $\langle \bar{r}|$ represents the outcome $+1$ when A_{rs} is measured, while $\langle \bar{s}|$ represents the outcome -1 when A_{rs} is measured. If the ordering of the dual vectors is reversed, to $\{\, \langle \bar{s}|\,,\, \langle \bar{r}|\,\}$, then this pair corresponds to $-A_{rs}$. Thus $A_{sr} = -A_{rs}$, and we can consider A_{rs} and A_{sr} to be essentially the same observable. So the number of distinct observables in our system is three; namely A_{ab}, A_{bc}, and A_{ca}.

The above assignment of outcomes allows us to view the A_{rs} as being spin-like observables, with the ordered pair of indices rs being analogous to the direction of the spin axis. Ref. [74] labels them as:

$$X \;=\; A_{bc}\,, \quad Y \;=\; A_{ca}\,, \quad Z \;=\; A_{ab}\,. \tag{3.27}$$

Indeed, if we look at their transformation properties under the group of basis transformations, S_3, we find:

$$\begin{array}{lll}
(ab)X \;=\; A_{ac} \;=\; -Y\,, & (ab)Y \;=\; A_{cb} \;=\; -X\,, & (ab)Z \;=\; A_{ba} \;=\; -Z\,, \\
(bc)X \;=\; A_{cb} \;=\; -X\,, & (bc)Y \;=\; A_{ba} \;=\; -Z\,, & (bc)Z \;=\; A_{ac} \;=\; -Y\,, \\
(ca)X \;=\; A_{ba} \;=\; -Z\,, & (ca)Y \;=\; A_{ac} \;=\; -Y\,, & (ca)Z \;=\; A_{cb} \;=\; -X\,, \\
(abc)X \;=\; A_{ca} \;=\; +Y\,, & (abc)Y \;=\; A_{ab} \;=\; +Z\,, & (abc)Z \;=\; A_{bc} \;=\; +X\,, \\
(acb)X \;=\; A_{ab} \;=\; +Z\,, & (acb)Y \;=\; A_{bc} \;=\; +X\,, & (acb)Z \;=\; A_{ca} \;=\; +Y\,,
\end{array} \tag{3.28}$$

which can all be considered $SO(3)$ rotations of the mutually orthogonal X, Y, and Z axes as shown in Fig. 3.1. The six basis transformations in S_3 can be mapped onto the six rotations of the dihedral group D_3 which keep the equilateral triangle abc in Fig 3.1 invariant. Thus, our spin-like states transform in an analogous way to canonical spin states under basis transformations, which are analogous to rotations of the canonical spin axes.

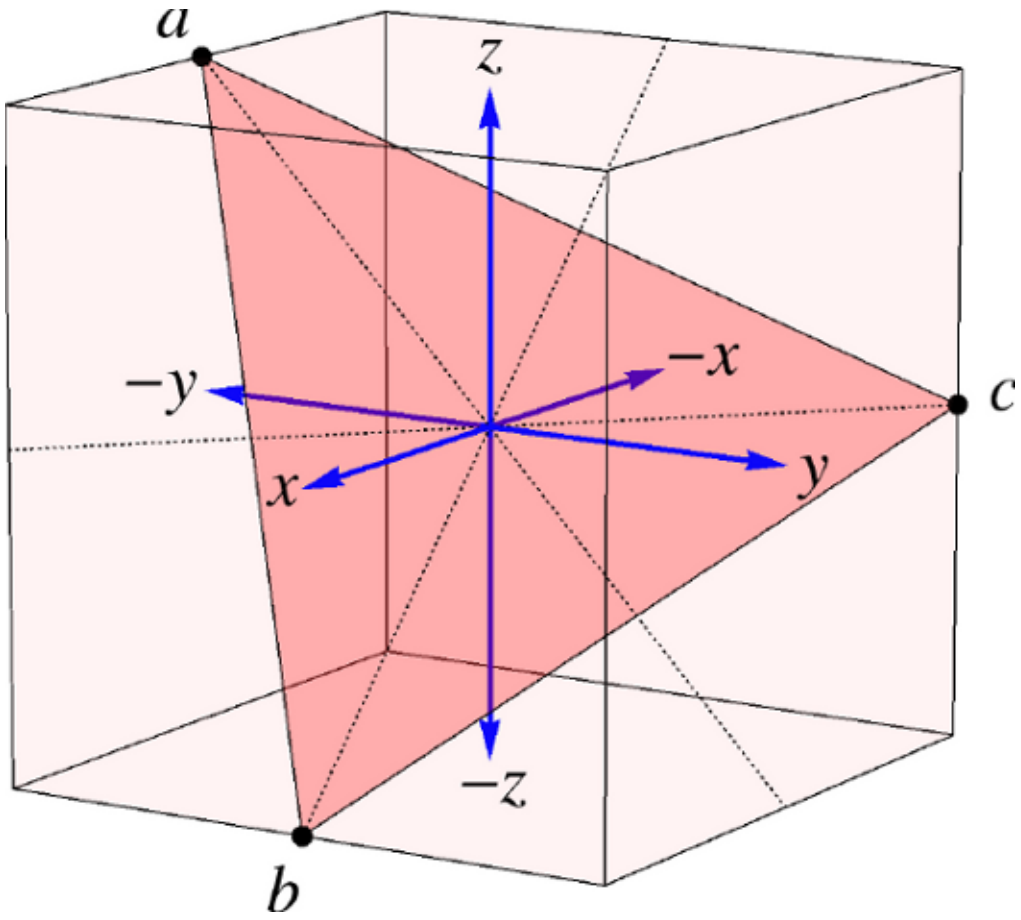

Figure 3.1: The 6 spin-like directions of $DQM(2,2)$. Allowed $SO(3)$ rotations are those that rotate the equilateral triangle abc onto itself.

Despite this similarity, a significant difference exists: the same dual vector can represent different outcomes of different observables. In addition to the outcome of $+1$ when A_{ab} is measured, $\langle\bar{a}|$ represents the outcome -1 when A_{ca} is measured. Similarly, $\langle\bar{b}|$ represents the outcome -1 when A_{ab} is measured and $+1$ when A_{bc} is measured. Therefore, what outcome each dual vector represents depends on the observable under consideration.

The probabilities of outcomes are calculated with Eq. (3.7). For the measurement of the observable $Z = A_{ab}$, for instance, we find:

$$\begin{aligned}
P(A_{ab}\,;+\,|\,a) &= \frac{\left|\langle\bar{a}|a\rangle\right|^2}{\left|\langle\bar{a}|a\rangle\right|^2+\left|\langle\bar{b}|a\rangle\right|^2} = 0\,,\\
P(A_{ab};-\,|\,a) &= \frac{\left|\langle\bar{b}|a\rangle\right|^2}{\left|\langle\bar{a}|a\rangle\right|^2+\left|\langle\bar{b}|a\rangle\right|^2} = 1\,,\\
P(A_{ab};+\,|\,b) &= \frac{\left|\langle\bar{a}|b\rangle\right|^2}{\left|\langle\bar{a}|b\rangle\right|^2+\left|\langle\bar{b}|b\rangle\right|^2} = 1\,,\\
P(A_{ab};-\,|\,b) &= \frac{\left|\langle\bar{b}|b\rangle\right|^2}{\left|\langle\bar{a}|b\rangle\right|^2+\left|\langle\bar{b}|b\rangle\right|^2} = 0\,,\\
P(A_{ab};+\,|\,c) &= \frac{\left|\langle\bar{a}|c\rangle\right|^2}{\left|\langle\bar{a}|c\rangle\right|^2+\left|\langle\bar{b}|c\rangle\right|^2} = \frac{1}{2}\,,\\
P(A_{ab};-\,|\,c) &= \frac{\left|\langle\bar{b}|c\rangle\right|^2}{\left|\langle\bar{a}|c\rangle\right|^2+\left|\langle\bar{b}|c\rangle\right|^2} = \frac{1}{2}\,.
\end{aligned} \tag{3.29}$$

The expectation values of $Z = A_{ab}$ on the three states, being calculated in the usual way, are:

$$\begin{aligned}
\langle A_{ab}\rangle_a &= (+1)\times 0 + (-1)\times 1 = -1\,,\\
\langle A_{ab}\rangle_b &= (+1)\times 1 + (-1)\times 0 = +1\,,\\
\langle A_{ab}\rangle_c &= (+1)\times \frac{1}{2} + (-1)\times \frac{1}{2} = 0\,.
\end{aligned} \tag{3.30}$$

When measuring A_{ab} with the system in the state $|a\rangle$, the probability of measuring -1 is 1 and the expectation value is also -1. The same goes for $|b\rangle$ and the outcome $+1$. Thus, $|a\rangle$ and $|b\rangle$ take on the role of the eigenstates of A_{ab}, while $|c\rangle$ is the superposition of the two with a 50-50 chance of obtaining either $+1$ or -1. The probabilities and expectation values of all other observables can be calculated in a similar fashion and the results are listed in Table 3.1.

The probabilities for $X = A_{bc}$ and $Y = A_{ca}$ can also be calculated by 'rotating' the results for $Z = A_{ab}$ via Eq.(3.28). For instance, since $(abc)A_{ab} = A_{bc}$, we can conclude that

$$\begin{aligned}
P(A_{bc};+\,|\,b) &= (abc)\,P(A_{ab};+\,|\,a) = 0\,,\\
P(A_{bc};-\,|\,b) &= (abc)\,P(A_{ab};-\,|\,a) = 1\,.
\end{aligned} \tag{3.31}$$

Note that, due to our construction, states $|r\rangle$ and $|s\rangle$ act as eigenstates of A_{rs} for any rs. However, in our approach, observables are not linear Hermitian maps from

observable	state	$P(+)$	$P(-)$	Expectation Value
A_{ab}	a	0	1	-1
	b	1	0	$+1$
	c	$\frac{1}{2}$	$\frac{1}{2}$	0
A_{bc}	a	$\frac{1}{2}$	$\frac{1}{2}$	0
	b	0	1	-1
	c	1	0	$+1$
A_{ca}	a	1	0	$+1$
	b	$\frac{1}{2}$	$\frac{1}{2}$	0
	c	0	1	-1

Table 3.1: The probabilities of the two outcomes + and − for all combinations of observables and states in $DQM(2,2)$.

V_2 to V_2 as is the case in canonical quantum mechanics, and thus we do not have eigenstates in the usual sense of the term.

Also note that each state acts as an eigenstate of two observables at a time: $|a\rangle$ of A_{ab} and A_{ca}, $|b\rangle$ of A_{bc} and A_{ab}, and $|c\rangle$ of A_{ca} and A_{bc}. This is due to each of the three dual vectors appearing in two distinct observables. Thus, despite the resemblance to spins existing along the x, y, and z directions of canonical quantum mechanics, the spin-like nature of this discrete quantum system is quite distinct.

3.2.3 Two Particle States

Two particle states are expressed as vectors in the space formed by the tensor product $V_2 \otimes V_2 = \mathbb{Z}_2^4$. This system is denoted $DQM(4,2)$. There are $2^4 - 1 = 15$ non-zero vectors in this space, of which nine are product states and six are entangled states.

The nine product states are:

$$\begin{array}{lllll}
|aa\rangle & = & |a\rangle \otimes |a\rangle & = & \left[\, \underline{1}\ \underline{0}\ \underline{0}\ \underline{0} \,\right]^{\mathrm{T}}, \\
|ab\rangle & = & |a\rangle \otimes |b\rangle & = & \left[\, \underline{0}\ \underline{1}\ \underline{0}\ \underline{0} \,\right]^{\mathrm{T}}, \\
|ba\rangle & = & |b\rangle \otimes |a\rangle & = & \left[\, \underline{0}\ \underline{0}\ \underline{1}\ \underline{0} \,\right]^{\mathrm{T}}, \\
|bb\rangle & = & |b\rangle \otimes |b\rangle & = & \left[\, \underline{0}\ \underline{0}\ \underline{0}\ \underline{1} \,\right]^{\mathrm{T}}, \\
|ac\rangle & = & |a\rangle \otimes |c\rangle & = & \left[\, \underline{1}\ \underline{1}\ \underline{0}\ \underline{0} \,\right]^{\mathrm{T}}, \\
|bc\rangle & = & |b\rangle \otimes |c\rangle & = & \left[\, \underline{0}\ \underline{0}\ \underline{1}\ \underline{1} \,\right]^{\mathrm{T}}, \\
|ca\rangle & = & |c\rangle \otimes |a\rangle & = & \left[\, \underline{1}\ \underline{0}\ \underline{1}\ \underline{0} \,\right]^{\mathrm{T}}, \\
|cb\rangle & = & |c\rangle \otimes |b\rangle & = & \left[\, \underline{0}\ \underline{1}\ \underline{0}\ \underline{1} \,\right]^{\mathrm{T}}, \\
|cc\rangle & = & |c\rangle \otimes |c\rangle & = & \left[\, \underline{1}\ \underline{1}\ \underline{1}\ \underline{1} \,\right]^{\mathrm{T}}.
\end{array} \tag{3.32}$$

The six non-product, or 'entangled', states can be classified according to their transformation properties under global S_3 'rotations', as follows.

The first is a singlet which transforms into itself under S_3, the set of all permutations of the labels a, b, and c:

$$\big|S\big\rangle \;=\; |aa\rangle + |bb\rangle + |cc\rangle \;=\; \left[\, \underline{0}\ \underline{1}\ \underline{1}\ \underline{0} \,\right]^{\mathrm{T}}. \tag{3.33}$$

This state is the closest analog to the spin singlet state $|0,0\rangle = \frac{1}{\sqrt{2}}\left(|\uparrow\downarrow\rangle - |\downarrow\uparrow\rangle\right)$ that exists in canonical quantum mechanics, as can be seen from the fact that $|S\rangle$ can also be written as

$$\big|S\big\rangle \;=\; |ab\rangle + |ba\rangle \;=\; |bc\rangle + |cb\rangle \;=\; |ca\rangle + |ac\rangle\ . \tag{3.34}$$

Unlike its canonical counterpart, this state is symmetric under the interchange of the two particles since there is no analog of -1 in $\mathbb{Z}_2$.

Three more states are symmetric under the interchange of the two particles. These three states transform into each other under S_3 and each state is labeled by the transformation under which that state is invariant:

$$\begin{array}{lllll}
\big|(ab)\big\rangle & = & |ab\rangle + |ba\rangle + |cc\rangle & = & \left[\, \underline{1}\ \underline{0}\ \underline{0}\ \underline{1} \,\right]^{\mathrm{T}}, \\
\big|(bc)\big\rangle & = & |aa\rangle + |bc\rangle + |cb\rangle & = & \left[\, \underline{1}\ \underline{1}\ \underline{1}\ \underline{0} \,\right]^{\mathrm{T}}, \\
\big|(ca)\big\rangle & = & |ac\rangle + |bb\rangle + |ca\rangle & = & \left[\, \underline{0}\ \underline{1}\ \underline{1}\ \underline{1} \,\right]^{\mathrm{T}}.
\end{array} \tag{3.35}$$

These would be the analogs of the spin-one triplet in canonical quantum mechanics.

The remaining two states are asymmetric under the interchange of the two particles:

$$\begin{array}{rcccl} \big|(abc)\big\rangle & = & |ab\rangle + |bc\rangle + |ca\rangle & = & \big[\ \underline{1}\ \ \underline{1}\ \ \underline{0}\ \ \underline{1}\ \big]^{\mathrm{T}}, \\ \big|(acb)\big\rangle & = & |ac\rangle + |cb\rangle + |ba\rangle & = & \big[\ \underline{1}\ \ \underline{0}\ \ \underline{1}\ \ \underline{1}\ \big]^{\mathrm{T}}. \end{array} \tag{3.36}$$

These transform as a doublet: they are invariant under even permutations, but transform into each other under odd permutations. There is a one-to-one correspondence between these entangled states and the elements of S_3, as well as a correspondence between the state multiplets and the conjugate classes of S_3.

3.2.4 Geometric Characterization

As mentioned previously, the space of the fifteen state vectors in $DQM(4,2)$ possesses the projective geometry $PG(3,2)$. In this geometry, the three points $|r\rangle$, $|s\rangle$, and $|t\rangle$ are on a line if they add up to the zero vector. The 15 points lie on 35 lines, with 7 lines crossing at each point. These 35 lines are contained in 15 planes, with 3 planes intersecting at each line.

In the current context, the nine product states are points that lie on six lines, no three of which are in the same plane, forming a non-planar grid:

$$\begin{array}{ccccc} |aa\rangle & = & |ab\rangle & = & |ac\rangle \\ \| & & \| & & \| \\ |ba\rangle & = & |bb\rangle & = & |bc\rangle \\ \| & & \| & & \| \\ |ca\rangle & = & |cb\rangle & = & |cc\rangle \end{array} \tag{3.37}$$

The six entangled states are each a sum of three product state points, no two of which lie on the same line of this grid. That is, no two states in the sum share the same row or column.

Beyond this, we have been unsuccessful in finding a geometric characterization of, or differentiation between, product and entangled states. It is unclear whether a similar characterization is possible in cases other than the current $q = 2$. The discovery of a geometrical understanding applicable to the generic $DQM(4,q)$ case with $PG(3,2)$ geometry could be enlightening.

3.2.5 Local Rotations

It will be useful to see how the six entangled states listed above transform into each other under basis transformations of either the first or the second particle, but not both. We find:

$$\begin{array}{rcrcrcrcl}
(ab)_1\,|S\rangle & = & (ab)_2\,|S\rangle & = & |ba\rangle + |ab\rangle + |cc\rangle & = & |(ab)\rangle & , \\
(bc)_1\,|S\rangle & = & (bc)_2\,|S\rangle & = & |aa\rangle + |cb\rangle + |bc\rangle & = & |(bc)\rangle & , \\
(ca)_1\,|S\rangle & = & (ca)_2\,|S\rangle & = & |ca\rangle + |bb\rangle + |ac\rangle & = & |(ca)\rangle & , \\
(acb)_1\,|S\rangle & = & (abc)_2\,|S\rangle & = & |ca\rangle + |ab\rangle + |bc\rangle & = & |(abc)\rangle & , \\
(abc)_1\,|S\rangle & = & (acb)_2\,|S\rangle & = & |ba\rangle + |cb\rangle + |ac\rangle & = & |(acb)\rangle & .
\end{array} \tag{3.38}$$

The transformation properties of the other states can be obtained from these relations, for instance:

$$(ab)_1\,|(bc)\rangle \;=\; (ab)_1(bc)_1\,|S\rangle \;=\; (abc)_1\,|S\rangle \;=\; |(acb)\rangle \;. \tag{3.39}$$

The fact that all six entangled states transform into each other this way, under what amounts to a simple relabeling of the states in the two one-particle vector spaces, means that they are all roughly equivalent and equally entangled.

3.2.6 Two Particle Observables

There are fifteen non-zero dual vectors in $V_2^* \otimes V_2^*$, but we will only be looking at the nine product observables constructed from the nine product dual vectors which are of the form

$$A_{rs}A_{tu} \;=\; \{\, \langle\bar{r}| \otimes \langle\bar{t}| \;,\; \langle\bar{r}| \otimes \langle\bar{u}| \;,\; \langle\bar{s}| \otimes \langle\bar{t}| \;,\; \langle\bar{s}| \otimes \langle\bar{u}| \,\} \;, \tag{3.40}$$

where the indices rs and tu are ab, bc, or ca. The four pairs of tensored dual vectors in this expression respectively represent the outcomes, $++$, $+-$, $-+$, and $--$ when $A_{rs}A_{tu}$ is measured. For reference, the row vector representations of all nine tensor products are as follows:

$$\begin{array}{rcl}
\langle\bar{a}| \otimes \langle\bar{a}| & = & \left[\underline{0}\;\;\underline{0}\;\;\underline{0}\;\;\underline{1}\right] , \\
\langle\bar{a}| \otimes \langle\bar{b}| & = & \left[\underline{0}\;\;\underline{0}\;\;\underline{1}\;\;\underline{0}\right] , \\
\langle\bar{a}| \otimes \langle\bar{c}| & = & \left[\underline{0}\;\;\underline{0}\;\;\underline{1}\;\;\underline{1}\right] , \\
\langle\bar{b}| \otimes \langle\bar{a}| & = & \left[\underline{0}\;\;\underline{1}\;\;\underline{0}\;\;\underline{0}\right] , \\
\langle\bar{b}| \otimes \langle\bar{b}| & = & \left[\underline{1}\;\;\underline{0}\;\;\underline{0}\;\;\underline{0}\right] ,
\end{array}$$

$$\begin{aligned}
\langle \bar{b}| \otimes \langle \bar{c}| &= \begin{bmatrix} \underline{1} & \underline{1} & \underline{0} & \underline{0} \end{bmatrix}, \\
\langle \bar{c}| \otimes \langle \bar{a}| &= \begin{bmatrix} \underline{0} & \underline{1} & \underline{0} & \underline{1} \end{bmatrix}, \\
\langle \bar{c}| \otimes \langle \bar{b}| &= \begin{bmatrix} \underline{1} & \underline{0} & \underline{1} & \underline{0} \end{bmatrix}, \\
\langle \bar{c}| \otimes \langle \bar{c}| &= \begin{bmatrix} \underline{1} & \underline{1} & \underline{1} & \underline{1} \end{bmatrix}.
\end{aligned} \tag{3.41}$$

Applying Eq. (3.7) to product observables, the probability of obtaining an outcome (x, y) represented by the product dual vector $\langle xy| = \langle x| \otimes \langle y|$ when observable O_1O_2 is measured on state $|\psi\rangle$ is given by:

$$P(O_1O_2\,;xy\,|\,\psi) \;=\; \frac{|\langle xy|\psi\rangle|^2}{\sum_{zw}|\langle zw|\psi\rangle|^2}\,. \tag{3.42}$$

For a product state $|\psi\rangle = |r\rangle \otimes |s\rangle \equiv |rs\rangle$, the brackets factorize:

$$\langle xy|rs\rangle \;=\; \big(\langle x| \otimes \langle y|\,\big)\big(\,|r\rangle \otimes |s\rangle\big) \;=\; \langle x|r\rangle\langle y|s\rangle\,, \tag{3.43}$$

and due to the condition Eq. (3.17) we imposed on the absolute values, we have

$$\big|\langle xy|rs\rangle\big| \;=\; \big|\langle x|r\rangle\big|\,\big|\langle y|s\rangle\big|\,. \tag{3.44}$$

Consequently, the probability also factorizes as

$$\begin{aligned}
P(O_1O_2\,;xy\,|\,rs) &= \frac{|\langle xy|rs\rangle|^2}{\sum_{zw}|\langle zw|rs\rangle|^2} \\
&= \frac{|\langle x|r\rangle|^2|\langle y|s\rangle|^2}{\sum_z\sum_w|\langle z|r\rangle|^2|\langle w|s\rangle|^2} \\
&= \left[\frac{|\langle x|r\rangle|^2}{\sum_z|\langle z|r\rangle|^2}\right]\left[\frac{\langle y|s\rangle|^2}{\sum_w|\langle w|s\rangle|^2}\right] \\
&= P(O_1\,;x\,|\,r)\,P(O_2\,;y\,|\,s)\,,
\end{aligned} \tag{3.45}$$

which is a property we would like to preserve for unentangled states. Otherwise, no isolated particle would be possible as a measurement performed on one particle of a product state could affect the outcome of a measurement on the other particle. Note the importance of Eq. (3.17) for this factorization to occur.

The expectation value of the product observable O_1O_2, *i.e.* the correlation between O_1 and O_2, will be

$$\langle O_1O_2\rangle_\psi \;=\; \sum_{xy} xy\; P(O_1O_2\,;xy\,|\,\psi)$$

$$= \frac{\sum_{xy} xy\,|\langle xy|\psi\rangle|^2}{\sum_{zw}|\langle zw|\psi\rangle|^2}\ , \tag{3.46}$$

which for product states factorizes as

$$\langle O_1 O_2\rangle_{rs} \ = \ \langle O_1\rangle_r \langle O_2\rangle_s\ . \tag{3.47}$$

Thus, the correlations for the nine product states will simply be products of those listed in Table 3.1.

The probabilities and expectation values of the nine product observables for all six entangled states are shown in Table 3.2, where we have used the notation $X = A_{bc}$, $Y = A_{ca}$, $Z = A_{ab}$. The entries can be rotated into each other via Eqs. (3.28) and (3.38) as before. For instance, since $-Y_1X_2 \ = \ (ab)_1 X_1 X_2$ and $(ab)_1\,|(ab)\rangle = |S\rangle$, we have

$$\begin{aligned} P(Y_1X_2;++,S) &= P(-Y_1X_2;-+,S) \\ &= (ab)_1 P(X_1X_2;-+,(ab)) \ = \ \frac{1}{3}\ . \end{aligned} \tag{3.48}$$

3.2.7 Entanglement and the Impossibility of Hidden Variables

It can now be demonstrated that a classical hidden variable theory cannot reproduce the probabilities and correlations predicted by this discrete quantum mechanics for entangled states. The argument used here is analogous to those of Hardy [59] and of Greenberger, Horne, Shimony, and Zeilinger [60], for canonical quantum mechanics.

Since all six entangled states are roughly equivalent, it suffices to consider only one, for which we will use the state $\big|S\big\rangle$. From Table 3.2, it is seen that

$$\begin{aligned} P(X_1X_2;++,S) &= P(X_1X_2;--,S) &= 0\ , \\ P(\,Y_1\,Y_2\,;++,S) &= P(\,Y_1\,Y_2\,;--,S) &= 0\ , \\ P(\,Z_1Z_2\,;++,S) &= P(\,Z_1Z_2\,;--,S) &= 0\ , \end{aligned} \tag{3.49}$$

which means that the pairs (X_1, X_2), (Y_1, Y_2), and (Z_1, Z_2) are all completely anti-correlated. That is to say, if any of those pairs of observables are measured with the sate of the system is $|S\rangle$, the outcomes for the observables in the pair must be opposites.

	state	++	+−	−+	−−	E.V.		state	++	+−	−+	−−	E.V.		state	++	+−	−+	−−	E.V.
X_1X_2	S	0	$\frac{1}{2}$	$\frac{1}{2}$	0	-1	Y_1X_2	S	$\frac{1}{3}$	0	$\frac{1}{3}$	$\frac{1}{3}$	$+\frac{1}{3}$	Z_1X_2	S	$\frac{1}{3}$	$\frac{1}{3}$	0	$\frac{1}{3}$	$+\frac{1}{3}$
	(ab)	$\frac{1}{3}$	$\frac{1}{3}$	$\frac{1}{3}$	0	$-\frac{1}{3}$		(ab)	$\frac{1}{2}$	0	0	$\frac{1}{2}$	$+1$		(ab)	0	$\frac{1}{3}$	$\frac{1}{3}$	$\frac{1}{3}$	$-\frac{1}{3}$
	(bc)	$\frac{1}{2}$	0	0	$\frac{1}{2}$	$+1$		(bc)	0	$\frac{1}{3}$	$\frac{1}{3}$	$\frac{1}{3}$	$-\frac{1}{3}$		(bc)	$\frac{1}{3}$	$\frac{1}{3}$	$\frac{1}{3}$	0	$-\frac{1}{3}$
	(ca)	0	$\frac{1}{3}$	$\frac{1}{3}$	$\frac{1}{3}$	$-\frac{1}{3}$		(ca)	$\frac{1}{3}$	$\frac{1}{3}$	$\frac{1}{3}$	0	$-\frac{1}{3}$		(ca)	$\frac{1}{2}$	0	0	$\frac{1}{2}$	$+1$
	(abc)	$\frac{1}{3}$	0	$\frac{1}{3}$	$\frac{1}{3}$	$+\frac{1}{3}$		(abc)	$\frac{1}{3}$	$\frac{1}{3}$	0	$\frac{1}{3}$	$+\frac{1}{3}$		(abc)	0	$\frac{1}{2}$	$\frac{1}{2}$	0	-1
	(acb)	$\frac{1}{3}$	$\frac{1}{3}$	0	$\frac{1}{3}$	$+\frac{1}{3}$		(acb)	0	$\frac{1}{2}$	$\frac{1}{2}$	0	-1		(acb)	$\frac{1}{3}$	0	$\frac{1}{3}$	$\frac{1}{3}$	$+\frac{1}{3}$
X_1Y_2	S	$\frac{1}{3}$	$\frac{1}{3}$	0	$\frac{1}{3}$	$+\frac{1}{3}$	Y_1Y_2	S	0	$\frac{1}{2}$	$\frac{1}{2}$	0	-1	Z_1Y_2	S	$\frac{1}{3}$	0	$\frac{1}{3}$	$\frac{1}{3}$	$+\frac{1}{3}$
	(ab)	$\frac{1}{2}$	0	0	$\frac{1}{2}$	$+1$		(ab)	0	$\frac{1}{3}$	$\frac{1}{3}$	$\frac{1}{3}$	$-\frac{1}{3}$		(ab)	$\frac{1}{3}$	$\frac{1}{3}$	$\frac{1}{3}$	0	$-\frac{1}{3}$
	(bc)	0	$\frac{1}{3}$	$\frac{1}{3}$	$\frac{1}{3}$	$-\frac{1}{3}$		(bc)	$\frac{1}{3}$	$\frac{1}{3}$	$\frac{1}{3}$	0	$-\frac{1}{3}$		(bc)	$\frac{1}{2}$	0	0	$\frac{1}{2}$	$+1$
	(ca)	$\frac{1}{3}$	$\frac{1}{3}$	$\frac{1}{3}$	0	$-\frac{1}{3}$		(ca)	$\frac{1}{2}$	0	0	$\frac{1}{2}$	$+1$		(ca)	0	$\frac{1}{3}$	$\frac{1}{3}$	$\frac{1}{3}$	$-\frac{1}{3}$
	(abc)	0	$\frac{1}{2}$	$\frac{1}{2}$	0	-1		(abc)	$\frac{1}{3}$	0	$\frac{1}{3}$	$\frac{1}{3}$	$+\frac{1}{3}$		(abc)	$\frac{1}{3}$	$\frac{1}{3}$	0	$\frac{1}{3}$	$+\frac{1}{3}$
	(acb)	$\frac{1}{3}$	0	$\frac{1}{3}$	$\frac{1}{3}$	$+\frac{1}{3}$		(acb)	$\frac{1}{3}$	$\frac{1}{3}$	0	$\frac{1}{3}$	$+\frac{1}{3}$		(acb)	0	$\frac{1}{2}$	$\frac{1}{2}$	0	-1
X_1Z_2	S	$\frac{1}{3}$	0	$\frac{1}{3}$	$\frac{1}{3}$	$+\frac{1}{3}$	Y_1Z_2	S	$\frac{1}{3}$	$\frac{1}{3}$	0	$\frac{1}{3}$	$+\frac{1}{3}$	Z_1Z_2	S	0	$\frac{1}{2}$	$\frac{1}{2}$	0	-1
	(ab)	0	$\frac{1}{3}$	$\frac{1}{3}$	$\frac{1}{3}$	$-\frac{1}{3}$		(ab)	$\frac{1}{3}$	$\frac{1}{3}$	$\frac{1}{3}$	0	$-\frac{1}{3}$		(ab)	$\frac{1}{2}$	0	0	$\frac{1}{2}$	$+1$
	(bc)	$\frac{1}{3}$	$\frac{1}{3}$	$\frac{1}{3}$	0	$-\frac{1}{3}$		(bc)	$\frac{1}{2}$	0	0	$\frac{1}{2}$	$+1$		(bc)	0	$\frac{1}{3}$	$\frac{1}{3}$	$\frac{1}{3}$	$-\frac{1}{3}$
	(ca)	$\frac{1}{2}$	0	0	$\frac{1}{2}$	$+1$		(ca)	0	$\frac{1}{3}$	$\frac{1}{3}$	$\frac{1}{3}$	$-\frac{1}{3}$		(ca)	$\frac{1}{3}$	$\frac{1}{3}$	$\frac{1}{3}$	0	$-\frac{1}{3}$
	(abc)	$\frac{1}{3}$	$\frac{1}{3}$	0	$\frac{1}{3}$	$+\frac{1}{3}$		(abc)	0	$\frac{1}{2}$	$\frac{1}{2}$	0	-1		(abc)	$\frac{1}{3}$	0	$\frac{1}{3}$	$\frac{1}{3}$	$+\frac{1}{3}$
	(acb)	0	$\frac{1}{2}$	$\frac{1}{2}$	0	-1		(acb)	$\frac{1}{3}$	0	$\frac{1}{3}$	$\frac{1}{3}$	$+\frac{1}{3}$		(acb)	$\frac{1}{3}$	$\frac{1}{3}$	0	$\frac{1}{3}$	$+\frac{1}{3}$

Table 3.2: Correlations of observables for the six entangled states.

Next, note that

$$P(X_1Z_2; +-, S) \;=\; 0\,, \tag{3.50}$$

which means that $X_1 = +1$ necessarily implies $Z_2 = +1$, while $Z_2 = -1$ necessarily implies $X_1 = -1$. Similarly,

$$P(Y_1Z_2; -+, S) \;=\; 0 \tag{3.51}$$

means that $Z_2 = +1$ necessarily implies $Y_1 = +1$, while $Y_1 = -1$ necessarily implies $Z_2 = -1$. Going through Table 3.2 in this fashion, we obtain the implication diagram shown in Fig. 3.2. As is clear from the diagram, no classical configuration exists which would be compatible with all of these constraints.

For instance, $X_1 = +1$ implies $Z_2 = +1$, which implies $Y_1 = +1$, which implies $X_2 = +1$, which contradicts the requirement that X_1 and X_2 are anti-correlated.

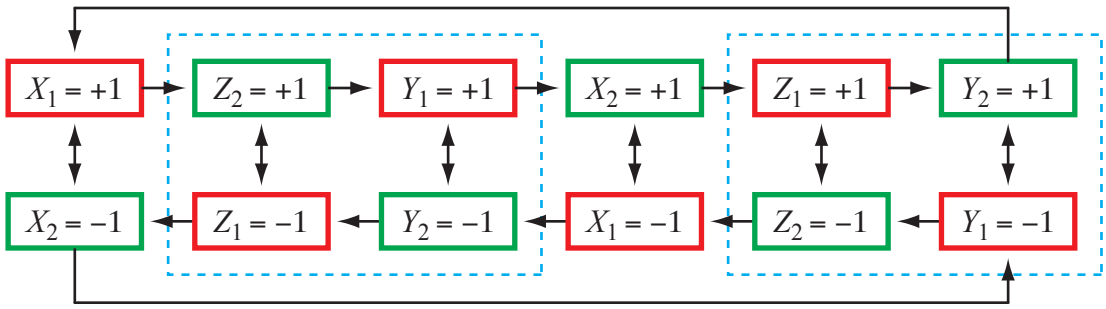

Figure 3.2: The implication chart for the state $|S\rangle$. Arrows point from the condition toward the implication. By tracing the arrows, it is easy to see that no classical configurations, and thus no hidden variable theory, can satisfy all of these requirements. If we ignore the observable X and look at only Y and Z, then the assignments within the dashed boxes are possible classical configurations. However, neither allow for the pairs $(Y_1 Z_2)$ and $(Z_1 Y_2)$ to be anti-correlated, which occurs with probability 1/3 in our toy quantum model.

While this seeming contradiction is not problematic for a quantum mechanical description, it is for a classical one, regardless of whether it has hidden variables or not, just as in [59] or [60].

It should be noted that even if we limit our attention to only two of the three observables available for each particle, hidden variables still cannot reproduce the quantum probabilities. For instance, consider only Y and Z for both particles. In this case, the selection of values within the dashed boxes on Fig. 3.2 give possible classical configurations. However, the combinations $(Y_1 Z_2) = (+-)$ and $(Z_1 Y_2) = (-+)$ cannot occur classically even though they are possible quantum mechanically.

By the fact that there exist states that cannot be reproduced classically, even with hidden variables, there is good reason to call this model 'quantum'.

3.2.8 The CHSH Bound

Let us now find the CHSH bound of our model, *i.e.* the upper bound of the absolute value of the CHSH correlator defined as

$$\langle A_1, A_2; B_1, B_2 \rangle \equiv \langle A_1 B_1 \rangle + \langle A_1 B_2 \rangle + \langle A_2 B_1 \rangle - \langle A_2 B_2 \rangle \,, \tag{3.52}$$

where the subscripts here refer to different possible generic choices of the operators A, acting on particle 1 (written on the left), and B, acting on particle 2 (written on

the right), not with any particular choice of those operators.

Owing to the equivalence of all entangled states, we only need to look at the correlations for one state for all possible observable combinations. That is, using Eqs. (3.28) and (3.38), we can convert the correlations for any entangled state into those for the state $|S\rangle$.

For instance:

$$\begin{aligned}\langle X_1, Y_1; X_2, Y_2\rangle_{(ab)} &= \langle X_1X_2\rangle_{(ab)} + \langle X_1Y_2\rangle_{(ab)} + \langle Y_1X_2\rangle_{(ab)} - \langle Y_1Y_2\rangle_{(ab)} \\ &= -\langle Y_1X_2\rangle_S - \langle Y_1Y_2\rangle_S - \langle X_1X_2\rangle_S + \langle X_1Y_2\rangle_S \\ &= -\langle Y_1, X_1; X_2, Y_2\rangle_S \end{aligned} \tag{3.53}$$

We also need not consider the negatives of the observables as long as all possible choices for A_1, A_2, B_1, and B_2 are considered since

$$\begin{aligned}&\langle A_1, A_2\,; B_1, B_2\rangle \\ &\quad= \langle A_1, -A_2\,; B_2, B_1\rangle \;=\; -\langle -A_1, A_2\,; B_2, B_1\rangle \\ &\quad= \langle A_2, A_1\,; B_1, -B_2\rangle \;=\; -\langle A_2, A_1\,; -B_1, B_2\rangle\,.\end{aligned} \tag{3.54}$$

Then, from simple inspection of Table 3.2, we can see that the maximum absolute value of the CHSH correlator is achieved for

$$\begin{aligned}\langle X, Y; Y, X\rangle_S &= -2\,, \\ \langle X, Z; Y, Z\rangle_S &= +2\,,\end{aligned} \tag{3.55}$$

with arbitrary permutations of the three observables leading to the same values. All the other correlators yield $\pm 2/3$. Thus, the CHSH bound for our model is 2, despite the fact that it is fully 'quantum' and does not allow for any hidden variables.

This result suggests that the non-violation of the CHSH inequality is not necessarily a robust indicator of whether a theory is classical or quantum. Stated more directly, the fact that this DQM(4,2) has a CHSH bound of 2 does not make it classical.

3.2.9 $\mathbb{Z}_3$ case

$DQM(2,3)$ is constructed on the field consisting of three elements, $GF(3) = \mathbb{Z}_3 = \mathbb{Z}/3\mathbb{Z} = \{\underline{0}, \underline{1}, \underline{2}\}$, with addition and multiplication tables given by

$+$	$\underline{0}$	$\underline{1}$	$\underline{2}$
$\underline{0}$	$\underline{0}$	$\underline{1}$	$\underline{2}$
$\underline{1}$	$\underline{1}$	$\underline{2}$	$\underline{0}$
$\underline{2}$	$\underline{2}$	$\underline{0}$	$\underline{1}$

$\times$	$\underline{0}$	$\underline{1}$	$\underline{2}$
$\underline{0}$	$\underline{0}$	$\underline{0}$	$\underline{0}$
$\underline{1}$	$\underline{0}$	$\underline{1}$	$\underline{2}$
$\underline{2}$	$\underline{0}$	$\underline{2}$	$\underline{1}$

In the following, we will write $\underline{2}$ as $-\underline{1}$. Since $\mathbb{Z}_3\backslash\{\underline{0}\} = \{\underline{1}, -\underline{1}\}$, each physical state will be represented by two vectors in $V_3 = \mathbb{Z}_3^2$ which differ by the multiplicative 'phase' $-\underline{1}$.

Therefore, of the $3^2 - 1 = 8$ non-zero vectors in V_3, there are pairs of vectors that are equivalent, and the inequivalent ones can be taken to be:

$$|a\rangle = \begin{bmatrix} \underline{1} \\ \underline{0} \end{bmatrix}, \quad |b\rangle = \begin{bmatrix} \underline{0} \\ \underline{1} \end{bmatrix}, \quad |c\rangle = \begin{bmatrix} -\underline{1} \\ \underline{1} \end{bmatrix}, \quad |d\rangle = \begin{bmatrix} \underline{1} \\ \underline{1} \end{bmatrix}. \tag{3.56}$$

Note that any pair of these states can be written as the sum and difference of the other two up to phases, *e.g.*

$$\begin{aligned} |c\rangle &= -|a\rangle + |b\rangle \ , \\ |d\rangle &= \ \ |a\rangle + |b\rangle \ . \end{aligned} \tag{3.57}$$

Thus, a basis transformation which interchanges a pair of states would leave the other two unaffected. In the above example, interchanging $|a\rangle$ and $|b\rangle$ would leave $|d\rangle$ unchanged, while $|c\rangle$ only acquires a physically insignificant phase factor of $-\underline{1}$.

Thus, single transpositions of the vector labels are possible, and the group generated by those transpositions would be $S_4 \cong PGL(2,3)$. That implies that all permutations of the vector labels are possible under basis transformations. This is the group of 'rotations' for $DQM(2,3)$.

The inequivalent dual-vectors of V_3^* can be taken to be

$$\begin{aligned} \langle\bar{a}| &= \begin{bmatrix} \underline{0} & -\underline{1} \end{bmatrix}, \\ \langle\bar{b}| &= \begin{bmatrix} \underline{1} & \underline{0} \end{bmatrix}, \\ \langle\bar{c}| &= \begin{bmatrix} \underline{1} & \underline{1} \end{bmatrix}, \\ \langle\bar{d}| &= \begin{bmatrix} \underline{1} & -\underline{1} \end{bmatrix}, \end{aligned} \tag{3.58}$$

The actions of these dual-vectors on the vectors are given by:

	$\|a\rangle$	$\|b\rangle$	$\|c\rangle$	$\|d\rangle$
$\langle\bar{a}\|$	$\underline{0}$	$-\underline{1}$	$-\underline{1}$	$-\underline{1}$
$\langle\bar{b}\|$	$\underline{1}$	$\underline{0}$	$-\underline{1}$	$\underline{1}$
$\langle\bar{c}\|$	$\underline{1}$	$\underline{1}$	$\underline{0}$	$-\underline{1}$
$\langle\bar{d}\|$	$\underline{1}$	$-\underline{1}$	$\underline{1}$	$\underline{0}$

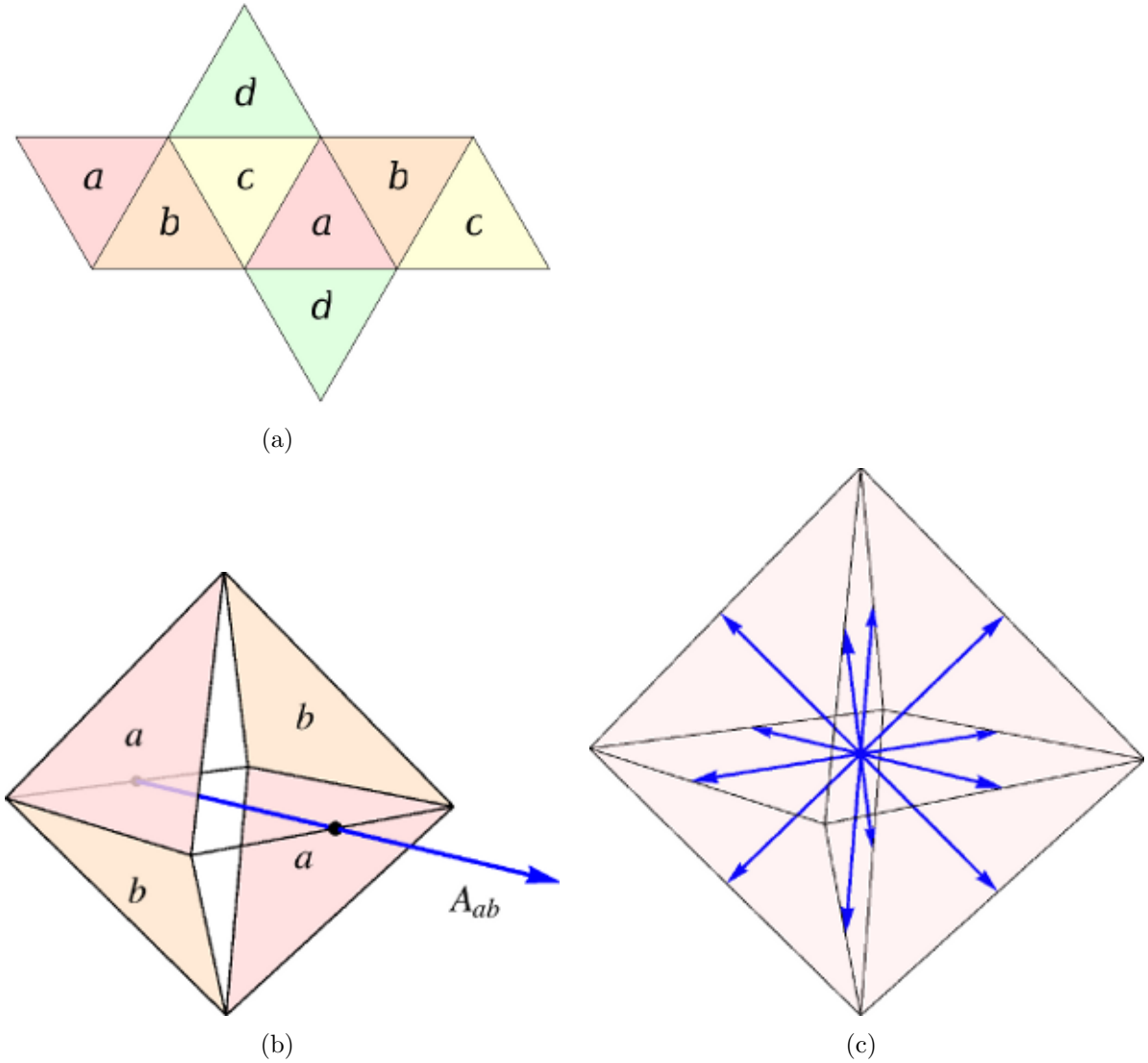

(a) (b) (c)

Figure 3.3: To map 'rotations' in $PGL(2,3) \cong S_4$ to rotations in $SO(3)$: (a) label the faces of an octahedron with four symbols as shown. Then, every permutation of the four labels *abcd* will correspond a rotation of the octahedral group. (b) The 'spin' observable A_{ab} in $DQM(2,3)$ can be mapped onto a direction in 3D space as shown. (c) The urchin diagram showing all 12 'spin' directions $DQM(2,3)$.

Thus,

$$\begin{aligned} \langle \bar{r}|s\rangle &= \underline{0} \quad \text{if } r = s, \\ &\neq \underline{0} \quad \text{if } r \neq s, \end{aligned} \tag{3.59}$$

and the relation $|\langle \bar{r}|s\rangle| = 1 - \delta_{rs}$ is obtained in this case as before. Maintaining this anti-orthogonality relation requires relabeling the dual vectors in the same way as the vectors under basis transformations.

From the set of four dual-vectors, we can define $4 \times 3 = 12$ observables with outcomes ± 1. If we count the 'spins' pointing in opposite directions as the same observable, we are left with 6 distinct observables. These 'spins' can be diagrammatically, not physically, associated with actual directions in 3-D, and their $PGL(2,3) \cong S_4$ transformations can be associated with rotations in $SO(3)$, as shown in Fig. 3.3 via the following procedure:

First, label the faces of an octahedron with four letters *abcd*, each letter appearing twice, on opposing faces as shown in Fig. 3.3a. The octahedral group O which rotates the octahedron onto itself consists of 24 elements. Each of these elements will permute the four letters on the faces of the octahedron. Thus, there exists a one-to-one correspondence between elements of the octahedral group and the 24 permutations of S_4. For more on octahedral groups, see [81] .

The 'direction' of the spin-like observable A_{ab} can be associated with the direction of the arrow shown in Fig. 3.3b. All 12 'spin directions' can be mapped this way, and Fig. 3.3c shows the resulting sea-urchin like array of spin-directions. These 12 'spins' transform into each other under $S_4 \cong O$ rotations.

3.2.10 $\mathbb{Z}_4$ case

$DQM(2,4)$ is constructed on the field consisting of four elements, $GF(4) = \mathbb{Z}_4 = \mathbb{Z}_2[\underline{\omega}] = \{\underline{0}, \underline{1}, \underline{\omega}, \underline{\omega}^2\}$, which is the Galois extension of $\mathbb{Z}_2 = \mathbb{Z}/2\mathbb{Z}$ by the solutions of the equation

$$\underline{x}^2 + \underline{x} + \underline{1} \;=\; \underline{0}\,, \tag{3.60}$$

which we denote $\underline{\omega}$ and $\underline{\omega}^2 = \underline{1} + \underline{\omega}$. The addition and multiplication tables of this field are:

$+$	$\underline{0}$	$\underline{1}$	$\underline{\omega}$	$\underline{\omega}^2$
$\underline{0}$	$\underline{0}$	$\underline{1}$	$\underline{\omega}$	$\underline{\omega}^2$
$\underline{1}$	$\underline{1}$	$\underline{0}$	$\underline{\omega}^2$	$\underline{\omega}$
$\underline{\omega}$	$\underline{\omega}$	$\underline{\omega}^2$	$\underline{0}$	$\underline{1}$
$\underline{\omega}^2$	$\underline{\omega}^2$	$\underline{\omega}$	$\underline{1}$	$\underline{0}$

$\times$	$\underline{0}$	$\underline{1}$	$\underline{\omega}$	$\underline{\omega}^2$
$\underline{0}$	$\underline{0}$	$\underline{0}$	$\underline{0}$	$\underline{0}$
$\underline{1}$	$\underline{0}$	$\underline{1}$	$\underline{\omega}$	$\underline{\omega}^2$
$\underline{\omega}$	$\underline{0}$	$\underline{\omega}$	$\underline{\omega}^2$	$\underline{1}$
$\underline{\omega}^2$	$\underline{0}$	$\underline{\omega}^2$	$\underline{1}$	$\underline{\omega}$

Since $\mathbb{Z}_4 \backslash \{\underline{0}\} = \{\underline{1}, \underline{\omega}, \underline{\omega}^2\}$, each physical state will be represented by three vectors in $V_4 = \mathbb{Z}_4^2$ which differ by the multiplicative 'phases' $\underline{\omega}$ or $\underline{\omega}^2$.

Therefore, of the $4^2 - 1 = 15$ non-zero vectors in V_4, every three of them are equivalent, and the $15/3 = 5$ inequivalent ones can be taken to be:

$$\begin{aligned} |a\rangle &= \begin{bmatrix} \underline{1} \\ \underline{0} \end{bmatrix}, \quad |b\rangle = \begin{bmatrix} \underline{0} \\ \underline{1} \end{bmatrix}, \quad |c\rangle = \begin{bmatrix} \underline{\omega} \\ \underline{1} \end{bmatrix}, \\ |d\rangle &= \begin{bmatrix} \underline{\omega}^2 \\ \underline{1} \end{bmatrix}, \quad |e\rangle = \begin{bmatrix} \underline{1} \\ \underline{1} \end{bmatrix}, \end{aligned} \tag{3.61}$$

Let us choose a pair of vectors as a basis and express the other three as linear combinations of those two, *e.g.*

$$\begin{aligned} |c\rangle &= \underline{\omega}\,|a\rangle + |b\rangle\ , \\ |d\rangle &= \underline{\omega}^2\,|a\rangle + |b\rangle\ , \\ |e\rangle &= \quad |a\rangle + |b\rangle\ . \end{aligned} \tag{3.62}$$

Now consider a basis transformation that would interchange $|a\rangle$ and $|b\rangle$. This would leave $|e\rangle$ unchanged, but $|c\rangle$ and $|d\rangle$ would transform into each other:

$$\begin{aligned} |c\rangle &\to |a\rangle + \underline{\omega}\,|b\rangle \cong \underline{\omega}^2\,|a\rangle + |b\rangle = |d\rangle\ , \\ |d\rangle &\to |a\rangle + \underline{\omega}^2\,|b\rangle \cong \underline{\omega}\,|a\rangle + |b\rangle = |c\rangle\ . \end{aligned} \tag{3.63}$$

Thus, single transpositions of the vector labels are impossible. Transpositions must always come in pairs, and these would generate the alternating group $A_5 \cong PGL(2,4)$, which is the group of all even permutations of the five labels *abcde*. This is the group of 'rotations' for $DQM(2,4)$.

The inequivalent dual-vectors of V_4^* can be taken to be

$$\begin{aligned} \langle \bar{a}| &= \begin{bmatrix} \underline{0} & \underline{1} \end{bmatrix}, \\ \langle \bar{b}| &= \begin{bmatrix} \underline{1} & \underline{0} \end{bmatrix}, \\ \langle \bar{c}| &= \begin{bmatrix} \underline{1} & \underline{\omega} \end{bmatrix}, \\ \langle \bar{d}| &= \begin{bmatrix} \underline{1} & \underline{\omega}^2 \end{bmatrix}, \\ \langle \bar{e}| &= \begin{bmatrix} \underline{1} & \underline{1} \end{bmatrix}. \end{aligned} \tag{3.64}$$

The actions of these dual-vectors on the vectors are:

	$\|a\rangle$	$\|b\rangle$	$\|c\rangle$	$\|d\rangle$	$\|e\rangle$
$\langle\bar{a}\|$	$\underline{0}$	$\underline{1}$	$\underline{1}$	$\underline{1}$	$\underline{1}$
$\langle\bar{b}\|$	$\underline{1}$	$\underline{0}$	$\underline{\omega}$	$\underline{\omega}^2$	$\underline{1}$
$\langle\bar{c}\|$	$\underline{1}$	$\underline{\omega}$	$\underline{0}$	$\underline{1}$	$\underline{\omega}^2$
$\langle\bar{d}\|$	$\underline{1}$	$\underline{\omega}^2$	$\underline{1}$	$\underline{0}$	$\underline{\omega}$
$\langle\bar{e}\|$	$\underline{1}$	$\underline{1}$	$\underline{\omega}^2$	$\underline{\omega}$	$\underline{0}$

Thus,

$$\begin{aligned} \langle\bar{r}|s\rangle &= \underline{0} \quad \text{if } r = s, \\ &\neq \underline{0} \quad \text{if } r \neq s, \end{aligned} \tag{3.65}$$

and the relation $|\langle\bar{r}|s\rangle| = 1 - \delta_{rs}$ is obtained as before. Again, maintaining this anti-orthogonality relation would require relabeling the dual vectors in the same way as the vectors under basis transformations.

From the set of five dual-vectors, we can define $5 \times 4 = 20$ observables with outcomes ± 1, or 10 if we count the 'spins' pointing in opposite directions as the same observable. These 'spins' can be associated with actual directions in 3D, and their $PGL(2,4) \cong A_5$ transformations can be associated with rotations in $SO(3)$ as shown in Fig. 3.4 via the following procedure:

First, label the faces of an icosahedron with five letters *abcde*, each letter appearing four time, as shown in Fig. 3.4a. This pattern will place each letter at the vertices of a tetrahedron. The icosahedral group Y [81] which rotates the icosahedron onto itself consists of 60 elements. Each of these elements will lead to an even permutation of the five letters on the faces of the icosahedron. Thus, there exist a one-to-one correspondence between elements of the icosahedral group and the 60 permutations of A_5.

The 'direction' of the 'spin' observable A_{ab} can be associated with the direction of the arrow shown in Fig. 3.4b. All 20 'spin' directions can be mapped this way, and Fig. 3.4c shows the resulting array of spin-directions. These 20 'spins' transform into each other under $A_5 \cong Y$ rotations.

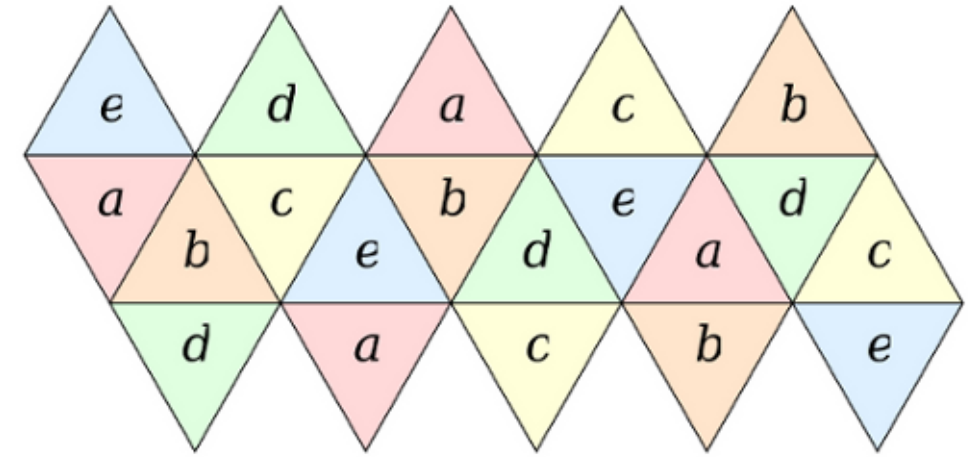

(a)

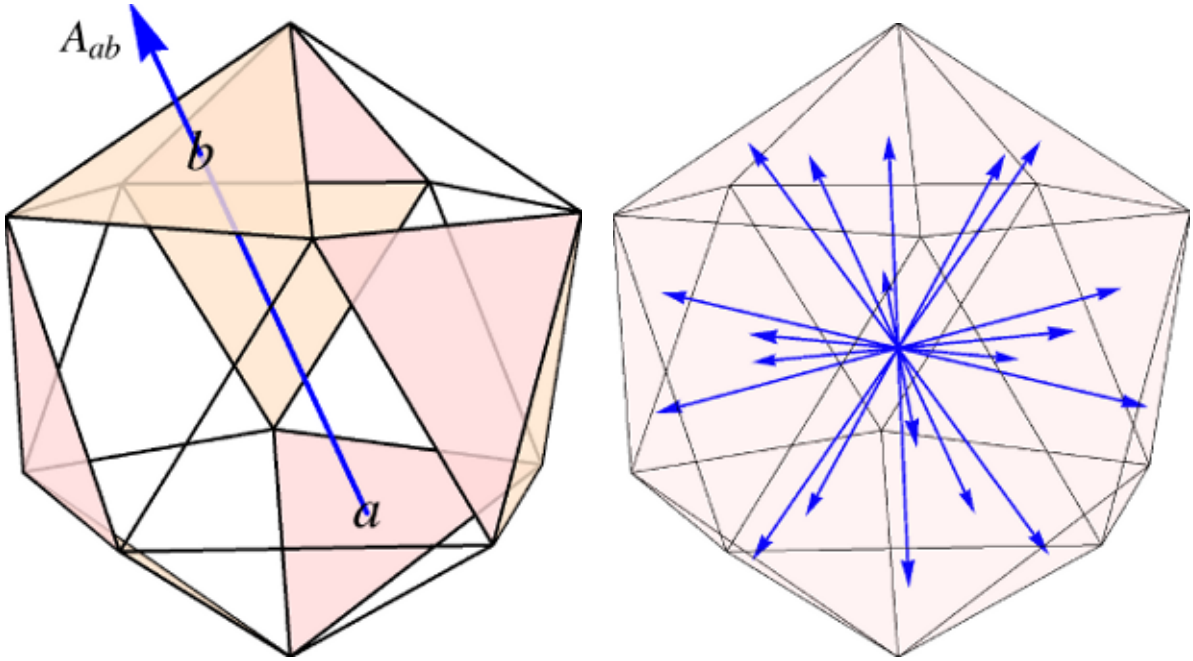

(b) (c)

Figure 3.4: To map 'rotations' in $PGL(2,4) \cong A_5$ to rotations in $SO(3)$: (a) label the faces of an icosahedron with five symbols as shown above left. Then, to every even permutation of the five labels *abcde* will correspond a rotation belonging to the icosahedral group. (b) The 'spin' observable A_{ab} in $DQM(2,4)$ can be mapped onto a direction in 3D space as shown. (c) The urchin diagram showing all 20 'spin' directions of $DQM(2,4)$.

Conjugate Classes of S_6		S_6	$PGL(2,5)$	Conjugate Classes of S_5		A_5
	−	120	20		−	
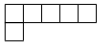	+	144	24		+	√
	−	90	30		−	
	+	90	0			
	+	40	20		+	√
	−	120	0			
	−	15	10		−	
	+	45	15		+	√
	+	40	0			
	−	15	0			
	+	1	1		+	√
total		720	120			

Table 3.3: $PGL(2,5)$ is a subgroup of S_6, which is isomorphic to S_5. This table shows how many elements in each conjugate class of S_6 are in $PGL(2,5)$, and the conjugate class in S_5 that they correspond to. The signs adjacent to the Young tableaux indicate the signature of the permutations in each class. Only the even permutations in $PGL(2,5)$, which form an invariant subgroup of order 60 isomorphic to A_5, can be mapped to elements in $SO(3)$.

3.2.11 $\mathbb{Z}_5$ case

$DQM(2,5)$ is constructed on the field consisting of five elements, $GF(5) = \mathbb{Z}_5 = \mathbb{Z}/5\mathbb{Z} = \{\underline{0}, \underline{1}, \underline{2}, \underline{3}, \underline{4}\}$. The addition and multiplication tables of this field are:

$+$	$\underline{0}$	$\underline{1}$	$\underline{2}$	$\underline{3}$	$\underline{4}$
$\underline{0}$	$\underline{0}$	$\underline{1}$	$\underline{2}$	$\underline{3}$	$\underline{4}$
$\underline{1}$	$\underline{1}$	$\underline{2}$	$\underline{3}$	$\underline{4}$	$\underline{0}$
$\underline{2}$	$\underline{2}$	$\underline{3}$	$\underline{4}$	$\underline{0}$	$\underline{1}$
$\underline{3}$	$\underline{3}$	$\underline{4}$	$\underline{0}$	$\underline{1}$	$\underline{2}$
$\underline{4}$	$\underline{4}$	$\underline{0}$	$\underline{1}$	$\underline{2}$	$\underline{3}$

$\times$	$\underline{0}$	$\underline{1}$	$\underline{2}$	$\underline{3}$	$\underline{4}$
$\underline{0}$	$\underline{0}$	$\underline{0}$	$\underline{0}$	$\underline{0}$	$\underline{0}$
$\underline{1}$	$\underline{0}$	$\underline{1}$	$\underline{2}$	$\underline{3}$	$\underline{4}$
$\underline{2}$	$\underline{0}$	$\underline{2}$	$\underline{4}$	$\underline{1}$	$\underline{3}$
$\underline{3}$	$\underline{0}$	$\underline{3}$	$\underline{1}$	$\underline{4}$	$\underline{2}$
$\underline{4}$	$\underline{0}$	$\underline{4}$	$\underline{3}$	$\underline{2}$	$\underline{1}$

We will denote $\underline{4} = -\underline{1}$ and $\underline{3} = -\underline{2}$. Since $\mathbb{Z}_5 \backslash \{\underline{0}\} = \{\pm\underline{1}, \pm\underline{2}\}$, each physical state will be represented by four vectors in $V_5 = \mathbb{Z}_5^2$ which differ by the multiplicative 'phases' $-\underline{1}$ or $\pm\underline{2}$.

Thus, of the $5^2 - 1 = 24$ non-zero vectors in V_5, every four of them are equivalent, and the $24/4 = 6$ inequivalent ones can be taken to be:

$$\begin{aligned} |a\rangle &= \begin{bmatrix} \underline{1} \\ \underline{0} \end{bmatrix}, \quad |b\rangle = \begin{bmatrix} \underline{0} \\ \underline{1} \end{bmatrix}, \quad |c\rangle = \begin{bmatrix} \underline{2} \\ \underline{1} \end{bmatrix}, \\ |d\rangle &= \begin{bmatrix} -\underline{1} \\ \underline{1} \end{bmatrix}, \quad |e\rangle = \begin{bmatrix} -\underline{2} \\ \underline{1} \end{bmatrix}, \quad |f\rangle = \begin{bmatrix} \underline{1} \\ \underline{1} \end{bmatrix}. \end{aligned} \tag{3.66}$$

The group of basis transformations of this space is a subgroup of S_6, the group of permutations of the six vector labels. It consists of both odd and even permutations, and the distribution of its elements among the 11 conjugate classes of S_6 are shown in Table 3.3. There are $120 = 5!$ elements in total in 7 conjugate classes. These numbers match those of S_5 exactly, and in fact, there is an isomorphism between the two, *i.e.* $PGL(2,5) \cong S_5$. Of the 120 elements of $PGL(2,5)$, a subgroup of 60 elements consisting of the even permutations, and isomorphic to A_5, can be mapped onto $SO(3)$ rotations in the icosahedral group Y as we will see below.

The inequivalent dual-vectors of V_5^* can be taken to be

$$\begin{aligned} \langle\bar{a}| &= \begin{bmatrix} \underline{0} & -\underline{1} \end{bmatrix}, \\ \langle\bar{b}| &= \begin{bmatrix} \underline{1} & \underline{0} \end{bmatrix}, \\ \langle\bar{c}| &= \begin{bmatrix} \underline{1} & -\underline{2} \end{bmatrix}, \\ \langle\bar{d}| &= \begin{bmatrix} \underline{1} & \underline{1} \end{bmatrix}, \\ \langle\bar{e}| &= \begin{bmatrix} \underline{1} & \underline{2} \end{bmatrix}, \end{aligned}$$

$$\langle \bar{f}| \;=\; \left[\, \underline{1} \;\; -\underline{1} \,\right]. \tag{3.67}$$

The actions of these dual-vectors on the vectors are:

	$\|a\rangle$	$\|b\rangle$	$\|c\rangle$	$\|d\rangle$	$\|e\rangle$	$\|f\rangle$
$\langle \bar{a}\|$	$\underline{0}$	$-\underline{1}$	$\underline{1}$	$-\underline{1}$	$-\underline{1}$	$-\underline{1}$
$\langle \bar{b}\|$	$\underline{1}$	$\underline{0}$	$\underline{2}$	$-\underline{1}$	$-\underline{2}$	$\underline{1}$
$\langle \bar{c}\|$	$\underline{1}$	$-\underline{2}$	$\underline{0}$	$\underline{2}$	$\underline{1}$	$-\underline{1}$
$\langle \bar{d}\|$	$\underline{1}$	$\underline{1}$	$-\underline{2}$	$\underline{0}$	$-\underline{1}$	$\underline{2}$
$\langle \bar{e}\|$	$\underline{1}$	$\underline{2}$	$-\underline{1}$	$\underline{1}$	$\underline{0}$	$-\underline{2}$
$\langle \bar{f}\|$	$\underline{1}$	$-\underline{1}$	$\underline{1}$	$-\underline{2}$	$\underline{2}$	$\underline{0}$

Thus,

$$\begin{aligned} \langle \bar{r}|s\rangle \;&=\; \underline{0} \quad \text{if } r = s, \\ &\neq\; \underline{0} \quad \text{if } r \neq s, \end{aligned} \tag{3.68}$$

and the relation $|\langle \bar{r}|s\rangle| = 1 - \delta_{rs}$ is obtained as before. Maintaining this anti-orthogonality relation would require relabeling the dual vectors in the same way as the vectors under basis transformations.

From the set of six dual-vectors, we can define $6 \times 5 = 30$ observables with outcomes ± 1, or 15 if we count the 'spins' pointing in opposite directions as the same observable. These 'spins' can be associated with actual directions in 3D, and their transformations under the subgroup of $PGL(2,5)$ mentioned above can be associated with rotations in $SO(3)$, as shown in Fig. 3.5, via the following procedure:

First, label the 12 faces of a dodecahedron with 6 letters $abcdef$, with each letter appearing twice on faces that oppose each other, as shown in Fig. 3.5. Note that the dodecahedron is dual to the icosahedron, under the interchange of vertices and faces, so its symmetry group under rotations is the icosahedral group Y, which was shown to be isomorphic to A_5 in the $q = 4$ case we discussed above. Each of the rotations of the icosahedral group will lead to an even permutation of the six letters on the faces of the dodecahedron. These will generate the subgroup of $PGL(2,5)$ consisting of even permutations only. The 'direction' of the 'spin' observable A_{ab} can be associated with the direction of the arrow shown in Fig. 3.5b. All 30 'spin' directions can be mapped this way, and Fig. 3.5c shows the resulting urchin of spin-directions. These 30 'spins' transform into each other under $A_5 \cong Y$ rotations.

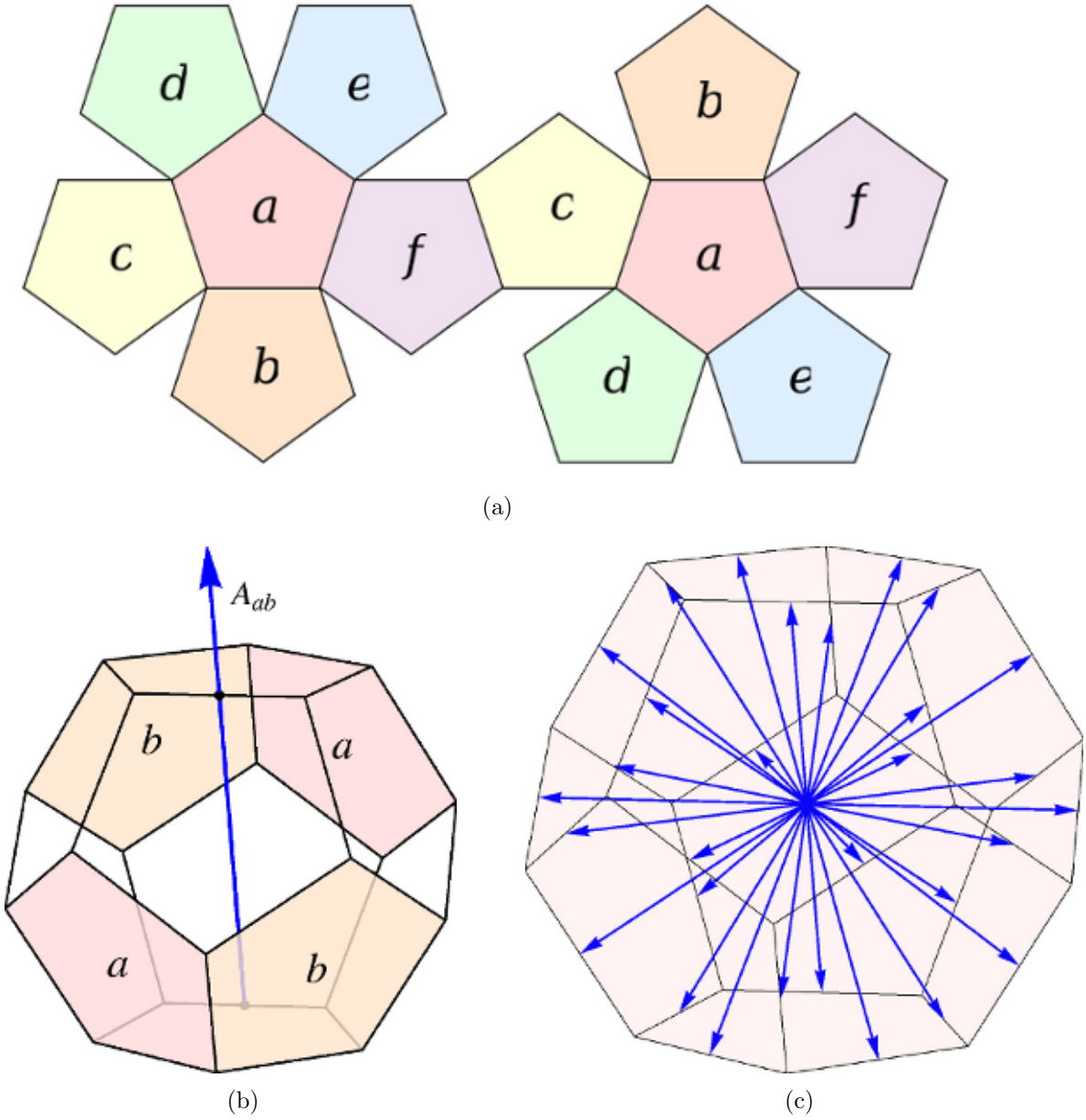

Figure 3.5: Not all 'rotations' in $PGL(2,5) \cong S_5$ can be mapped to rotations in $SO(3)$. The even permutations, isomorphic to A_5, can be mapped as follows: (a) label the faces of a dodecahedron with six symbols as shown above left. Then, to every even permutation of the six labels $abcdef$ will correspond a rotation belonging to the icosahedral group. (b) The 'spin' observable A_{ab} in $DQM(2,5)$ can be mapped onto the direction in 3D space as shown. (c) The urchin diagram showing all 30 'spin' directions of $DQM(2,5)$.

Unfortunately, there are 60 more elements of $PGL(2,5)$ unaccounted for, and these do not seem to be representable as rotations or reflections of the dodecahedron. Thus, in a sense, the 'rotations' in the state space of $DQM(2,5)$ are much richer than a finite group of $SO(3)$ rotations.

3.2.12 Comments

As we have seen, for the $q = 2$, 3, 4, and 5 cases, the group $PGL(2,q)$ itself, or its invariant subgroup, is isomorphic to some polyhedral group, allowing for the identification of those $PGL(2,q)$ group elements with $SO(3)$ rotations. Therefore, our 'spins' can be considered objects that transform like canonical spin under 'rotations' for these cases.

Whether a similar pattern emerges for $DQM(2,7)$ and beyond remains to be explored. In general, the $PGL(2,q)$ group is a subgroup of S_{q+1} of order $q(q^2-1)$. Constructing a correspondence via the methods that were just discussed would require the labeling of the faces of some polyhedron with $q+1$ symbols. Given that only 5 Platonic solids and 13 Archimedean solids are at our disposal, it is not at all clear that such a correspondence exists for generic q.

In the detailed examination of $DQM(2,2)$, $DQM(2,3)$, $DQM(2,4)$ and $DQM(2,5)$, we have encountered a fascinating geometric structure, namely finite projective geometry, that is very similar to the projective geometry of canonical quantum theory [83]. These examples possibly represent the simplest theoretical playground for understanding some outstanding issues in the foundations of quantum theory, quantum information and quantum computation [82] (see also [73]). It is hoped that features of DQM could shed light on questions raised in the geometric formulation of canonical quantum theory and in natural generalizations of the geometric quantum theory [84], which are argued to be relevant to quantum gravity [85].

3.3 Expectation Value Path

We will now follow the second approach to making a modified quantum theory using Galois fields by preserving the canonical formula for an expectation value Eq. (3.10) as far as we are able.

3.3.1 Biorthogonal Systems over Galois Fields

In order to adopt the definition of expectation values via Eq. (3.10) onto a vector space over the Galois field $GF(p^n)$, we must again define analogs of the various components of the formula. In this approach, we find it convenient to define a notion similar to Hermitian conjugation of vectors and linear operators, though, this notion does not require the use of an inner product. We'll start by demonstrating how this can be accomplished via *biorthogonal systems*, of the type described in Ref. [86].

In the following, we restrict our attention to the Galois fields $GF(p^n)$ with $p = 3 \bmod 4$ and $n = 1$ or 2. As we will see below, this restriction allows our formalism to maintain a close parallel to quantum mechanics defined on vector spaces over $\mathbb{R}$ ($n = 1$ case) or $\mathbb{C}$ ($n = 2$ case). As in the previous approach, elements of the finite Galois field $GF(p^n)$ are denoted by underlined symbols and numbers to distinguish them from elements of $\mathbb{R}$ or $\mathbb{C}$. The N-dimensional vector space over $GF(p^n)$ is denoted $V(N, p^n)$.

A biorthogonal system over $V(N, p^n)$ is a set consisting of a basis $\{|1\rangle, |2\rangle, \cdots, |N\rangle\}$ of the vector space $V(N, p^n)$, and a basis $\{\langle 1|, \langle 2|, \cdots, \langle N|\}$ of the dual vector space $V(N, p^n)^*$ such that

$$\langle r|s\rangle = \underline{\delta}_{rs}, \qquad r, s = 1, 2, \cdots, N, \tag{3.69}$$

where

$$\underline{\delta}_{rs} = \begin{cases} \underline{0} & \text{if } r \neq s, \\ \underline{1} & \text{if } r = s. \end{cases} \tag{3.70}$$

As we will be using a type of orthogonality, our present results will be notably different from the use of anti-orthogonality in the previous model.

To explicitly construct biorthogonal systems, it will be useful to first assemble a bit of technology, beginning with a dot product.

Dot Product

Denoting the k-th element of the vector $|a\rangle \in V(N, p^n)$ as $\underline{a}_k \in GF(p^n)$, we can define the 'dot product' in $V(N, p^n)$ as

$$|a\rangle \cdot |b\rangle \;=\; \sum_{k=1}^{N} \underline{a}_k^{\,p}\, \underline{b}_k \;\in\; GF(p^n)\;. \tag{3.71}$$

Note that raising an element to the p-th power is semilinear in $GF(p^n)$ since

$$(\underline{a} + \underline{b})^p \;=\; (\underline{a}^p + \underline{b}^p) \tag{3.72}$$

in a field of characteristic p. When $n = 1$, it is an identity transformation due to Fermat's little theorem

$$a^{p-1} \;=\; 1 \bmod p\;, \quad \forall a \in \mathbb{Z}\;. \tag{3.73}$$

For the case $n = 2$, $p = 3 \bmod 4$, it is an analogue of complex conjugation in $\mathbb{C}$. To see this, first note that the equation

$$\underline{x}^2 + \underline{1} \;=\; \underline{0} \tag{3.74}$$

is irreducible in $GF(p) = \mathbb{Z}_p$ if $p = 3 \bmod 4$. The polynomial $\underline{x}^2 + \underline{1} = \underline{0}$ is reducible for $p = 2$ or $p = 1 \bmod 4$ since in those cases $\underline{p-1}$ will be a solution.

Denote the solutions to this equation as $\pm\underline{i}$. Adjoining $\underline{i}$ to $GF(p) = \mathbb{Z}_p$ gives us $GF(p^2) = \mathbb{Z}_p[\,\underline{i}\,]$. Elements of this field can be expressed as $\underline{a} + \underline{i}\,\underline{b}$, where $\underline{a}, \underline{b} \in \mathbb{Z}_p$. Then

$$(\underline{a} + \underline{i}\,\underline{b})^p \;=\; \underline{a}^p + \underline{i}^p \underline{b}^p \;=\; \underline{a} - \underline{i}\,\underline{b}\;. \tag{3.75}$$

Furthermore,

$$\begin{aligned} (\underline{a} + \underline{i}\,\underline{b})^p (\underline{c} + \underline{i}\,\underline{d}) \;&=\; (\underline{ac} + \underline{bd}) + \underline{i}(\underline{ad} - \underline{bc})\;, \\ (\underline{c} + \underline{i}\,\underline{d})^p (\underline{a} + \underline{i}\,\underline{b}) \;&=\; (\underline{ac} + \underline{bd}) - \underline{i}(\underline{ad} - \underline{bc})\;, \end{aligned} \tag{3.76}$$

in particular,

$$(\underline{a} + \underline{i}\,\underline{b})^p (\underline{a} + \underline{i}\,\underline{b}) \;=\; \underline{a}^2 + \underline{b}^2 \;\in\; \mathbb{Z}_p\;. \tag{3.77}$$

Therefore, $|a\rangle \cdot |b\rangle$ and $|b\rangle \cdot |a\rangle$ are 'complex conjugates' of each other, while $|a\rangle \cdot |a\rangle$ is 'real.' Thus, when $p = 3 \bmod 4$, the fields $GF(p) = \mathbb{Z}_p$ and $GF(p^2) = \mathbb{Z}_p[\,\underline{i}\,]$ take on similar roles as $\mathbb{R}$ and $\mathbb{C}$.

In the following, when we say $GF(p^n)$, we will mean either $GF(p)$ or $GF(p^2)$ with $p = 3 \bmod 4$ unless stated otherwise. Also, borrowing from standard terminology, we will say that two vectors in $V(N, p^n)$ are 'orthogonal' to each other when they have a zero dot product, and that a vector is 'self-orthogonal' when it is orthogonal to itself.

Conjugation of Vectors

Next, choose a basis $\{|1\rangle, |2\rangle, \cdots, |N\rangle\}$ for $V(N, p^n)$ such that:

$$|r\rangle \cdot |s\rangle \begin{cases} \neq \underline{0} & \text{if } r = s \,, \\ = \underline{0} & \text{if } r \neq s \,, \end{cases} \tag{3.78}$$

that is, all the basis vectors are orthogonal to each other, but none are self-orthogonal. Let us call such a basis an 'ortho-nondegenerate' basis. The simplest example of an ortho-nondegenerate basis would be the standard basis, in which the r-th element of the s-th vector is given by $\underline{\delta}_{rs}$, proving that such a basis always exists. On the other hand, not all bases necessarily satisfy this condition since $V(N, p^n)$ typically has multiple self-orthogonal vectors other than the zero vector.

Define the 'conjugate' dual vector for each vector $|r\rangle$ in the selected ortho-nondegenerate basis as

$$\langle r| \;\equiv\; \frac{|r\rangle \cdot}{|r\rangle \cdot |r\rangle} \tag{3.79}$$

where it is crucial that $|r\rangle \cdot |r\rangle \neq \underline{0}$ for $\langle r|$ to exist. Then, the set of dual vectors $\{\langle 1|, \langle 2|, \cdots, \langle N|\}$ provides a basis for the dual vector space $V(N, p^n)^*$ such that $\langle r|s\rangle = \underline{\delta}_{rs}$. Thus, we obtain the set

$$\big\{\{\langle 1|, \langle 2|, \cdots, \langle N|\}, \{|1\rangle, |2\rangle, \cdots, |N\rangle\}\big\} \tag{3.80}$$

which constitutes a biorthogonal system.

3.3.2 Observables

Given a biorthogonal system, we can define the analog of Hermitian operators via

$$\hat{A} \;=\; \sum_{k=1}^{N} \underline{\alpha}_k \; |k\rangle \langle k| \;, \qquad \underline{\alpha}_k \in \; GF(p) \;. \tag{3.81}$$

Due to the biorthogonality of the system, $|k\rangle$ is the eigenvector of $\hat{A}$ with eigenvalue $\underline{\alpha}_k$. Note that the eigenvalues $\underline{\alpha}_k$ are chosen to be elements of $GF(p)$, not $GF(p^2)$, i.e. they are 'real', mirroring the similar property of Hermitian operators.

In the defining biorthogonal system, the matrix representation of $\hat{A}$ is diagonal. In a different biorthogonal system, say $\big\{\{\langle 1'|, \langle 2'|, \cdots, \langle N'|\}, \{|1'\rangle, |2'\rangle, \cdots, |N'\rangle\}\big\}$, its

matrix representation is

$$\begin{aligned} \langle r'|\,\hat{A}\,|s'\rangle &= \sum_{k=1}^{N} \underline{\alpha}_k \,\langle r'|k\rangle\,\langle k|s'\rangle \\ &= \sum_{k=1}^{N} \underline{\alpha}_k \,\frac{(|r'\rangle\cdot|k\rangle)\,(|k\rangle\cdot|s'\rangle)}{(|r'\rangle\cdot|r'\rangle)\,(|k\rangle\cdot|k\rangle)}\,, \end{aligned} \tag{3.82}$$

which in general is not a Hermitian matrix. However, the diagonal elements $\langle r'|\,\hat{A}\,|r'\rangle$ are nevertheless 'real' since $|r'\rangle\cdot|k\rangle$ and $|k\rangle\cdot|r'\rangle$ are 'complex conjugates' of each other, while $|r'\rangle\cdot|r'\rangle$ and $|k\rangle\cdot|k\rangle$ are 'real.' We identify these Hermitian-like operators with physical observables.

3.3.3 Physical States

Since we wish to use Eq. (3.10) to define the expectation value for the observable $\hat{A}$, every physical state $|\psi\rangle$ must have a conjugate dual $\langle\psi|$, which we define via Eq. (3.79). Thus, we demand that all physical states belong to some biorthogonal system. Essentially, all vectors that are not self-orthogonal belong to some biorthogonal system, so this requirement is equivalent to dropping all vectors that are self-orthogonal from the set of physical states.

Note that if we multiply $|\psi\rangle$ with a scalar, that is, a non-zero element of $GF(p^n)$, then its conjugate $\langle\psi|$ will be multiplied by the inverse of that scalar. This will leave $\hat{A}$ and $\langle\psi|\,\hat{A}\,|\psi\rangle$ invariant. Thus, we can identify all vectors that differ with each other by a multiplicative scalar as representing the same physical state, that is, all non-zero elements of $GF(p^n)$ can be considered to be 'phases.' For $V(N,p^n)$, this means that the set of physical states is the non-self-orthogonal subset of the projective space

$$PG(N-1,p^n) \;=\; \Big[V(N,p^n)\backslash\{\underline{\mathbf{0}}\}\Big]\Big/\Big[GF(p^n)\backslash\{\underline{0}\}\Big]\,. \tag{3.83}$$

3.3.4 Expectation Values

With the above definitions of observables and physical states, we can now calculate the quantity $\langle\psi|\,\hat{A}\,|\psi\rangle \in GF(p) = \mathbb{Z}_p$ for observable $\hat{A}$ and state $|\psi\rangle$. We would like to interpret this quantity as the expectation value of the observable $\hat{A}$. However, if $\hat{A}$

is to represent a physical quantity such as spin, one must map the resulting number in $GF(p)$ to a number in $\mathbb{R}$.

We demand that this map from $GF(p)$ to $\mathbb{R}$ be product preserving, just as in the discrete quantum mechanics models, for the same reasons. It is easy to see that the absolute value function given in Eq. (3.15) is a product preserving map for any p. For the $p = 3 \bmod 4$ case, however, in addition to the absolute value function, there is another product preserving map which can be constructed as follows.

First, denote the generator of the multiplicative group $GF(p)\backslash\{\underline{0}\}$ by $\underline{g}$ and express the non-zero elements of $GF(p)$ as $\{\underline{g}, \underline{g}^2, \underline{g}^3, \cdots, \underline{g}^{p-1} = \underline{1}\}$. Define:

$$\varphi(\underline{x}) \;=\; \begin{cases} 0 & \text{if } \underline{x} = \underline{0}\,, \\ +1 & \text{if } \underline{x} = \underline{g}^{\text{even}}\,, \\ -1 & \text{if } \underline{x} = \underline{g}^{\text{odd}}\,. \end{cases} \tag{3.84}$$

It is straightforward to show that $\varphi(\underline{ab}) = \varphi(\underline{a})\,\varphi(\underline{b})$, making φ a group homomorphism from $GF(p)$ to $\{-1, 0, +1\}$.

Note that $p = 3 \bmod 4$ implies $(p-1) =$ even and $(p-1)/2 =$ odd. Therefore,

$$\begin{aligned} \varphi(+\underline{1}) \;&=\; \varphi\left(\underline{g}^{p-1}\right) \;=\; +1\,, \\ \varphi(-\underline{1}) \;&=\; \varphi\left(\underline{g}^{(p-1)/2}\right) \;=\; -1\,, \end{aligned} \tag{3.85}$$

where $-\underline{1}$ denotes the additive inverse of $\underline{1}$ in $GF(p)$. That is, this function respectively maps $-\underline{1}$, $\underline{0}$, and $\underline{1}$ in $GF(p)$ to -1, 0, and 1 in $\mathbb{R}$.

We will use this map to give meaning to Eq. (3.10) as an expectation value in our current model:

$$E(A|\psi) \;=\; \varphi\left(\langle\psi|\,\hat{A}\,|\psi\rangle\right)\,. \tag{3.86}$$

The φ function defined in Eq. (3.84) is the only function that allows us to calculate real expectation values, as we will see via the following argument.

First, we must determine what the physical requirements on φ are. Primarily, it must be a map from $GF(p)$ to $\mathbb{R}$, as we assume that the results of measurements are real numbers. For the expectation value of the identity operator to be 1, we must have that $\varphi(\underline{1}) = 1$. Likewise, for the expectation value of the zero operator to be 0, we must have that $\varphi(\underline{0}) = 0$.

When we consider two particle states,as will be done shortly, if we require that the expectation values of product states should factorize, then φ must respect multiplication. This is done if the image of $GF(p)\backslash\{\underline{0}\}$ is homomorphic to $GF(p)\backslash\{\underline{0}\}$. Since

$GF(p)\backslash\{\underline{0}\}$ is cyclic, any group homomorphic to it must also by cyclic. The only cyclic, multiplicative subgroups of $\mathbb{R}$ are $\{+1\}$, $\{0\}$, and $\{+1,-1\}$.

As the image must contain $+1$, $\{0\}$ is excluded. If we choose $\{+1,-1\}$ as the image of $GF(p)\backslash\{\underline{0}\}$ under φ, we are allowed to interpret eigenvalues of observables as the expectation values of the corresponding eigenstates. Thus, the image of $GF(p)\backslash\{\underline{0}\}$ should be $\{+1,-1\}$ and φ should be surjective between $GF(p)\backslash\{\underline{0}\}$ and $\{+1,-1\}$, to ensure the presence of -1 as an expectation value.

For φ to be a such a surjection, it must be true that $\varphi(\underline{g}) = -1$ whenever $\underline{g}$ is a multiplicative generator of $GF(p)\backslash\{\underline{0}\}$. It then follows that all even powers of $\underline{g}$ should map to $+1$.

Thus, the kernel of φ must contain all $(p-1)/2$ even powers of $\underline{g}$. Note that it does not matter which generator is chosen since any given generator is an odd power of each of the other generators.

The kernel of a group homomorphism, the set of elements that map to the identity, is a subgroup. In order for φ to be surjective from $GF(p)\backslash\{\underline{0}\}$ to $\{+1,-1\}$, its kernel must be a proper subgroup of $GF(p)\backslash\{\underline{0}\}$. As we have shown that the kernel must contain half of the elements of $GF(p)\backslash\{\underline{0}\}$, it can only contain those elements, as the order of the kernel must divide the order of $GF(p)\backslash\{\underline{0}\}$.

Therefore, φ as defined in Eq. (3.84) is the only map that fits the relevant criteria.

An important consequence of Eq. (3.84) adn Eq. (3.86) is that the uncertainty in the measurement of $\hat{A}$ will be given by

$$\begin{aligned}(\Delta A)^2 &= E(A^2|\psi) - \left[E(A|\psi)\right]^2 \\ &= \varphi\left(\langle\psi|\,\hat{A}^2\,|\psi\rangle\right) - \left[\varphi\left(\langle\psi|\,\hat{A}\,|\psi\rangle\right)\right]^2 \ . \end{aligned} \tag{3.87}$$

When $|\psi\rangle$ is an eigenvector of $\hat{A}$ with eigenvalue $\underline{\alpha}$, we find

$$(\Delta A)^2 \ = \ \varphi\left(\underline{\alpha}^2\right) - \left[\varphi\left(\underline{\alpha}\right)\right]^2 \ = \ 0 \ , \tag{3.88}$$

due to the fact that φ is a product preserving map.

3.3.5 2D Vector Space over $GF(3)$

Let's now look at a specific example to see what the explicit consequences are of our choices.

We'll first consider the 2D vector space $V(2,3)$ over $GF(3) = \mathbb{Z}/3\mathbb{Z} = \{\underline{0}, \underline{1}, -\underline{1}\}$, where we denote the additive inverse of $\underline{1}$ as $-\underline{1}$ instead of $\underline{2}$. There are $3^2 - 1 = 8$ non-zero vectors in this space which are the 4 vectors

$$|a\rangle = \begin{bmatrix} \underline{1} \\ \underline{0} \end{bmatrix}, \quad |b\rangle = \begin{bmatrix} \underline{0} \\ \underline{1} \end{bmatrix}, \quad |c\rangle = \begin{bmatrix} \underline{1} \\ \underline{1} \end{bmatrix}, \quad |d\rangle = \begin{bmatrix} \underline{1} \\ -\underline{1} \end{bmatrix}, \tag{3.89}$$

and their multiples by the 'phase' $-\underline{1}$. Checking 'orthogonality', we find:

$$\begin{array}{rcl} |a\rangle\cdot|a\rangle &=& |b\rangle\cdot|b\rangle \;=\; \underline{1}\,, \\ |c\rangle\cdot|c\rangle &=& |d\rangle\cdot|d\rangle \;=\; -\underline{1}\,, \\ |a\rangle\cdot|b\rangle &=& |c\rangle\cdot|d\rangle \;=\; \underline{0}\,. \end{array} \tag{3.90}$$

Thus, none of the vectors are self-orthogonal, and their conjugates are

$$\begin{array}{rcl} \langle a| &=& \begin{bmatrix} \underline{1} & \underline{0} \end{bmatrix}, \quad \langle c| \;=\; \begin{bmatrix} -\underline{1} & -\underline{1} \end{bmatrix}, \\ \langle b| &=& \begin{bmatrix} \underline{0} & \underline{1} \end{bmatrix}, \quad \langle d| \;=\; \begin{bmatrix} -\underline{1} & \underline{1} \end{bmatrix}. \end{array} \tag{3.91}$$

There are two biorthogonal systems in $V(2,3)^* \times V(2,3)$, namely

$$\big\{\{\langle a|\,, \langle b|\}, \{|a\rangle\,, |b\rangle\}\big\} \;\text{ and }\; \big\{\{\langle c|\,, \langle d|\}, \{|c\rangle\,, |d\rangle\}\big\}\,, \tag{3.92}$$

up to different orderings of the vectors and dual-vectors, and signs. All four inequivalent vectors belong to one of these biorthogonal systems so they all represent physical states.

We can now construct spin-like observables with eigenvalues $\pm\underline{1}$. Since $V(2,3)$ has only two biorthogonal systems, the two possible observables are

$$\begin{array}{rcl} \underline{1}\;|a\rangle\langle a| \;\; -\underline{1}\;|b\rangle\langle b| &=& \begin{bmatrix} \underline{1} & \underline{0} \\ \underline{0} & -\underline{1} \end{bmatrix} \;\equiv\; \hat{\sigma}_3\,, \\ \underline{1}\;|c\rangle\langle c| \;\; -\underline{1}\;|d\rangle\langle d| &=& \begin{bmatrix} \underline{0} & \underline{1} \\ \underline{1} & \underline{0} \end{bmatrix} \;\equiv\; \hat{\sigma}_1\,, \end{array} \tag{3.93}$$

up to signs. By construction, $|a\rangle$ and $|b\rangle$ are respectively eigenvectors of $\hat{\sigma}_3$ with eigenvalues $\pm\underline{1}$. Thus, the expected outcome of a measurement of $\hat{\sigma}_3$ on $|a\rangle$ will always be $+1$, while that on $|b\rangle$ will always be -1. Similarly, $|c\rangle$ and $|d\rangle$ are respectively eigenvectors of $\hat{\sigma}_1$ with eigenvalues $\pm\underline{1}$, so the expected outcome of a measurement of $\hat{\sigma}_1$ on $|c\rangle$ will always be $+1$, while that on $|d\rangle$ will always be -1.

On the other hand, the expectation values of $\hat{\sigma}_1$ and $\hat{\sigma}_1^2$ for the state $|a\rangle$ are

$$E(\sigma_1|a) \;=\; \varphi\left(\langle a|\,\hat{\sigma}_1\,|a\rangle\right) \;=\; \varphi\left(\underline{0}\right) \;=\; 0\,,$$

$$E(\sigma_1^2|a) \;=\; \varphi\left(\langle a|\,\hat{\sigma}_1^2\,|a\rangle\right) \;=\; \varphi\left(\underline{1}\right) \;=\; 1\;, \tag{3.94}$$

so

$$\left[\Delta\sigma_1(a)\right]^2 \;=\; E(\sigma_1^2|a) - \left[E(\sigma_1|a)\right]^2 \;=\; 1\;. \tag{3.95}$$

From these expectation values, we can infer the probabilities of obtaining the outcomes ± 1 when $\hat{\sigma}_1$ is measured on $|a\rangle$. Denoting these probabilities as $P(\pm 1|a)$, we must have

$$\begin{aligned} 1 &= P(+1|a) + P(-1|a)\;, \\ 0 &= P(+1|a) - P(-1|a)\;, \end{aligned} \tag{3.96}$$

which yields

$$P(+1|a) \;=\; P(-1|a) \;=\; \frac{1}{2}\;. \tag{3.97}$$

Therefore, the measurement of $\hat{\sigma}_1$ on $|a\rangle$ will yield the two outcomes $+1$ and -1 with equal probability, consistent with our earlier results in the discrete quantum mechanical model. Similar results are found for the measurement of $\hat{\sigma}_1$ on $|b\rangle$, and those of $\hat{\sigma}_3$ on $|c\rangle$ or $|d\rangle$. The expectation values and uncertainties for both observables and all states are listed in Table 3.4.

Note that the current formalism predicts expectation values but does not specify the probabilities directly. The probabilities must be inferred from the expectations values as shown above. Indeed, though we can write

$$\begin{aligned} \langle a|\,\hat{\sigma}_1\,|a\rangle &= \langle a|\left(\underline{1}\,|c\rangle\,\langle c| - \underline{1}\,|d\rangle\,\langle d|\right)|a\rangle \\ &= \underline{1}\,\langle a|c\rangle\langle c|a\rangle - \underline{1}\,\langle a|d\rangle\langle d|a\rangle\;, \end{aligned} \tag{3.98}$$

we cannot associate $\langle a|c\rangle\langle c|a\rangle = \langle a|d\rangle\langle d|a\rangle = -\underline{1}$ with the probabilities of the outcomes ± 1.

Furthermore, we will see later how, in some cases, the probabilities cannot be uniquely determined from the expectation values. It will be argued later that a theory which predicts expectation values but leaves the probabilities indeterminate can still make physical sense.

	σ_1	$\Delta\sigma_1$	σ_3	$\Delta\sigma_3$
$\|a\rangle$	0	1	1	0
$\|b\rangle$	0	1	-1	0
$\|c\rangle$	1	0	0	1
$\|d\rangle$	-1	0	0	1

Table 3.4: Expectation values and uncertainties of spin-like observables in biorthogonal quantum mechanics on $V(2,3)$.

Before moving on, let's look at the effect of basis transformation on the state space. The group of all possible basis transformations consist of the sixteen matrices given by

$$\begin{aligned} e &\leftrightarrow \pm\begin{bmatrix} \underline{1} & \underline{0} \\ \underline{0} & \underline{1} \end{bmatrix}, & (ab) &\leftrightarrow \pm\begin{bmatrix} \underline{0} & \underline{1} \\ \underline{1} & \underline{0} \end{bmatrix}, \\ (cd) &\leftrightarrow \pm\begin{bmatrix} \underline{1} & \underline{0} \\ \underline{0} & -\underline{1} \end{bmatrix}, & (ab)(cd) &\leftrightarrow \pm\begin{bmatrix} \underline{0} & -\underline{1} \\ \underline{1} & \underline{0} \end{bmatrix}, \\ (ac)(bd) &\leftrightarrow \pm\begin{bmatrix} \underline{1} & \underline{1} \\ \underline{1} & -\underline{1} \end{bmatrix}, & (ad)(bc) &\leftrightarrow \pm\begin{bmatrix} -\underline{1} & \underline{1} \\ \underline{1} & \underline{1} \end{bmatrix}, \\ (acbd) &\leftrightarrow \pm\begin{bmatrix} \underline{1} & -\underline{1} \\ \underline{1} & \underline{1} \end{bmatrix}, & (adbc) &\leftrightarrow \pm\begin{bmatrix} \underline{1} & \underline{1} \\ -\underline{1} & \underline{1} \end{bmatrix}. \end{aligned} \tag{3.99}$$

However, since we identify vectors that only differ by multiplicative phases as representing the same physical state, we identify the matrices that only differ by a multiplicative phase as representing the same transformation on the projective space $PG(1,3)$, each of which corresponds to a permutation of the vector labels a, b, c, and d as indicated above. These eight transformations constitute the projective orthogonal group $PO(2,3) \cong D_4$, namely, the group of 2×2 matrices $\underline{O}$ with elements in $GF(3)$ which satisfy the condition

$$\underline{O}^{\mathrm{T}}\underline{O} \;=\; \pm\underline{\mathbf{1}}_{2\times 2}\;, \tag{3.100}$$

with matrices which differ by a sign identified. This group is a subgroup of the projective general linear group $PGL(2,3) \cong S_4$.

The isomorphism between $PO(2,3)$ and D_4 is implemented by labeling the four corners of a square as shown in Fig. 3.6. Every rotation of the quadrangle in D_4 leads to a permutation of the four vertex labels, which is the corresponding element of $PO(2,3)$. The two spin observables $\hat{\sigma}_1$ and $\hat{\sigma}_3$ transform under $PO(2,3)$ permutations as

$$e \quad : \quad \hat{\sigma}_1 \to \hat{\sigma}_1\;,\; \hat{\sigma}_3 \to \hat{\sigma}_3\;,$$

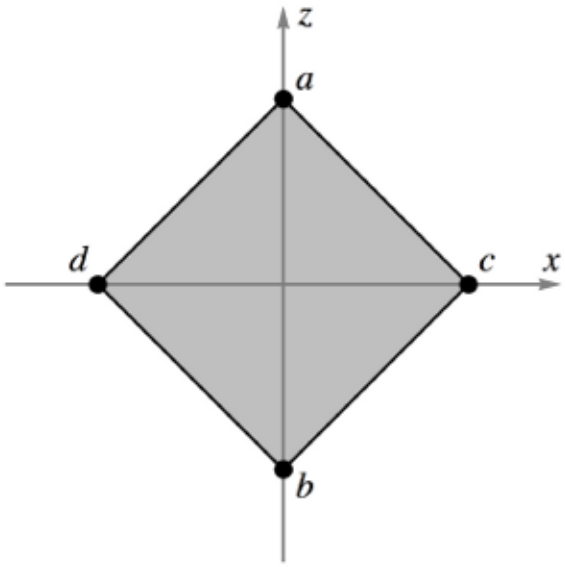

Figure 3.6: The correspondence between the dihedral group D_4 and the projective orthogonal group $PO(2,3)$. Every D_4 rotation of the quadrangle corresponds to a permutation of the four vertex labels *abcd* belonging to $PO(2,3)$.

$$\begin{aligned}
(ab) &: \hat{\sigma}_1 \to \hat{\sigma}_1 \ , \ \hat{\sigma}_3 \to -\hat{\sigma}_3 \ , \\
(cd) &: \hat{\sigma}_1 \to -\hat{\sigma}_1 \ , \ \hat{\sigma}_3 \to \hat{\sigma}_3 \ , \\
(ab)(cd) &: \hat{\sigma}_1 \to -\hat{\sigma}_1 \ , \ \hat{\sigma}_3 \to -\hat{\sigma}_3 \ , \\
(ac)(bd) &: \hat{\sigma}_1 \to \hat{\sigma}_3 \ , \ \hat{\sigma}_3 \to \hat{\sigma}_1 \ , \\
(ad)(bc) &: \hat{\sigma}_1 \to -\hat{\sigma}_3 \ , \ \hat{\sigma}_3 \to -\hat{\sigma}_1 \ , \\
(acbd) &: \hat{\sigma}_1 \to -\hat{\sigma}_3 \ , \ \hat{\sigma}_3 \to \hat{\sigma}_1 \ , \\
(adbc) &: \hat{\sigma}_1 \to \hat{\sigma}_3 \ , \ \hat{\sigma}_3 \to -\hat{\sigma}_1 \ ,
\end{aligned} \tag{3.101}$$

just as they should under rotations of the quadrangle.

3.3.6 2D Vector Space over $GF(9)$

Next, consider the 2D vector space $V(2,9)$ over $GF(9) = \mathbb{Z}_3[\underline{i}\,]$. This field consists of $3^2 = 9$ elements given explicitly by $\{\underline{0}, \underline{1}, -\underline{1}, \underline{i}, -\underline{i}, \underline{1}+\underline{i}, \underline{1}-\underline{i}, -\underline{1}+\underline{i}, -\underline{1}-\underline{i}\}$.

There are $9^2 - 1 = 80$ non-zero vectors in $V(2,9)$. These are the scalar multiples of

	σ_1	$\Delta\sigma_1$	σ_2	$\Delta\sigma_2$	σ_3	$\Delta\sigma_3$
$\|a\rangle$	0	1	0	1	1	0
$\|b\rangle$	0	1	0	1	-1	0
$\|c\rangle$	1	0	0	1	0	1
$\|d\rangle$	-1	0	0	1	0	1
$\|e\rangle$	0	1	1	0	0	1
$\|f\rangle$	0	1	-1	0	0	1

Table 3.5: Expectation values and uncertainties of spin-like observables in biorthogonal quantum mechanics on $V(2,9)$.

$80/8 = 10$ vectors consisting of the four listed in Eq. (3.89) and the following six:

$$\begin{aligned} |e\rangle &= \begin{bmatrix} \underline{1} \\ \underline{i} \end{bmatrix}, \quad |g\rangle = \begin{bmatrix} \underline{1} \\ \underline{1}+\underline{i} \end{bmatrix}, \quad |i\rangle = \begin{bmatrix} \underline{1} \\ -\underline{1}+\underline{i} \end{bmatrix}, \\ |f\rangle &= \begin{bmatrix} \underline{1} \\ -\underline{i} \end{bmatrix}, \quad |h\rangle = \begin{bmatrix} \underline{1} \\ \underline{1}-\underline{i} \end{bmatrix}, \quad |j\rangle = \begin{bmatrix} \underline{1} \\ -\underline{1}-\underline{i} \end{bmatrix}. \end{aligned} \tag{3.102}$$

The dot products of these six vectors with themselves are

$$\begin{aligned} |e\rangle\cdot|e\rangle &= |f\rangle\cdot|f\rangle = -\underline{1}\,, \\ |g\rangle\cdot|g\rangle &= |h\rangle\cdot|h\rangle = |i\rangle\cdot|i\rangle = |j\rangle\cdot|j\rangle = \underline{0}\,. \end{aligned} \tag{3.103}$$

As we can see $|g\rangle$, $|h\rangle$, $|i\rangle$, and $|j\rangle$ are all self-orthogonal. The conjugates of $|e\rangle$ and $|f\rangle$ are

$$\langle e| = \begin{bmatrix} -\underline{1} & \underline{i} \end{bmatrix}, \qquad \langle f| = \begin{bmatrix} -\underline{1} & -\underline{i} \end{bmatrix}. \tag{3.104}$$

Thus, in addition to the two biorthogonal systems listed in Eq. (3.92), $V(2,9)^* \times V(2,9)$ has a third given by

$$\left\{\{\langle e|, \langle f|\}, \{|e\rangle, |f\rangle\}\right\}, \tag{3.105}$$

and $|e\rangle$ and $|f\rangle$ are added to the list of physical states.

The above biorthogonal system contributes a third operator to the list of spin-like observables in Eq. (3.93):

$$\underline{1}\ |e\rangle\langle e| \ \ -\underline{1}\ |f\rangle\langle f| \ = \begin{bmatrix} \underline{0} & -\underline{i} \\ \underline{i} & \underline{0} \end{bmatrix} \equiv \hat{\sigma}_2\,. \tag{3.106}$$

By construction, $|e\rangle$ and $|f\rangle$ are respectively eigenvectors of $\hat{\sigma}_2$ with eigenvalues $\pm\underline{1}$. The expectation values and uncertainties of all three observables for all six states are listed in Table 3.5.

the group of allowed basis transformation are represented by the following matrices:

$$
\begin{aligned}
e &\leftrightarrow \eta \begin{bmatrix} \underline{1} & \underline{0} \\ \underline{0} & \underline{1} \end{bmatrix}, \quad (ab)(ef) \leftrightarrow \eta \begin{bmatrix} \underline{0} & \underline{1} \\ \underline{1} & \underline{0} \end{bmatrix}, \\
(cd)(ef) &\leftrightarrow \eta \begin{bmatrix} \underline{1} & \underline{0} \\ \underline{0} & -\underline{1} \end{bmatrix}, \quad (ab)(cd) \leftrightarrow \eta \begin{bmatrix} \underline{0} & -\underline{1} \\ \underline{1} & \underline{0} \end{bmatrix}, \\
(acbd) &\leftrightarrow \eta \begin{bmatrix} \underline{1} & -\underline{1} \\ \underline{1} & \underline{1} \end{bmatrix}, \quad (ac)(bd)(ef) \leftrightarrow \eta \begin{bmatrix} \underline{1} & \underline{1} \\ \underline{1} & -\underline{1} \end{bmatrix}, \\
(adbc) &\leftrightarrow \eta \begin{bmatrix} \underline{1} & \underline{1} \\ -\underline{1} & \underline{1} \end{bmatrix}, \quad (ad)(bc)(ef) \leftrightarrow \eta \begin{bmatrix} -\underline{1} & \underline{1} \\ \underline{1} & \underline{1} \end{bmatrix}, \\
(aebf) &\leftrightarrow \eta \begin{bmatrix} \underline{1} & \underline{i} \\ \underline{i} & \underline{1} \end{bmatrix}, \quad (ae)(bf)(cd) \leftrightarrow \eta \begin{bmatrix} \underline{1} & -\underline{i} \\ \underline{i} & -\underline{1} \end{bmatrix}, \\
(afbe) &\leftrightarrow \eta \begin{bmatrix} \underline{1} & -\underline{i} \\ -\underline{i} & \underline{1} \end{bmatrix}, \quad (af)(be)(cd) \leftrightarrow \eta \begin{bmatrix} \underline{1} & \underline{i} \\ -\underline{i} & -\underline{1} \end{bmatrix}, \\
(cedf) &\leftrightarrow \eta \begin{bmatrix} \underline{1} & \underline{0} \\ \underline{0} & \underline{i} \end{bmatrix}, \quad (ab)(ce)(df) \leftrightarrow \eta \begin{bmatrix} \underline{0} & -\underline{i} \\ \underline{1} & \underline{0} \end{bmatrix}, \\
(cfde) &\leftrightarrow \eta \begin{bmatrix} \underline{1} & \underline{0} \\ \underline{0} & -\underline{i} \end{bmatrix}, \quad (ab)(cf)(de) \leftrightarrow \eta \begin{bmatrix} \underline{0} & \underline{i} \\ \underline{1} & \underline{0} \end{bmatrix}, \\
(ace)(bdf) &\leftrightarrow \eta \begin{bmatrix} \underline{1} & -\underline{i} \\ \underline{1} & \underline{i} \end{bmatrix}, \quad (adf)(bce) \leftrightarrow \eta \begin{bmatrix} \underline{1} & \underline{i} \\ -\underline{1} & \underline{i} \end{bmatrix}, \\
(acf)(bde) &\leftrightarrow \eta \begin{bmatrix} \underline{1} & \underline{i} \\ \underline{1} & -\underline{i} \end{bmatrix}, \quad (ade)(bcf) \leftrightarrow \eta \begin{bmatrix} -\underline{1} & \underline{i} \\ \underline{1} & \underline{i} \end{bmatrix}, \\
(aec)(bfd) &\leftrightarrow \eta \begin{bmatrix} \underline{1} & \underline{1} \\ \underline{i} & -\underline{i} \end{bmatrix}, \quad (afd)(bec) \leftrightarrow \eta \begin{bmatrix} -\underline{1} & \underline{1} \\ \underline{i} & \underline{i} \end{bmatrix}, \\
(aed)(bfc) &\leftrightarrow \eta \begin{bmatrix} \underline{1} & -\underline{1} \\ \underline{i} & \underline{i} \end{bmatrix}, \quad (afc)(bed) \leftrightarrow \eta \begin{bmatrix} \underline{1} & \underline{1} \\ -\underline{i} & \underline{i} \end{bmatrix},
\end{aligned}
\tag{3.107}
$$

Identifying matrices that differ by a multiplicative phase, we obtain a group of basis transformation with 24 elements, each of which corresponds to a permutation of the vector labels $abcdef$ as indicated above. This group is the projective unitary group $PU(2,9)$ consisting of 2×2 matrices $\underline{U}$ with elements in $GF(9)$ which satisfy the condition

$$\underline{U}^\dagger \underline{U} \;=\; \pm \underline{\mathbf{1}}_{2\times 2}\,, \tag{3.108}$$

with matrices that differ by a multiplicative phase identified. This group is a subgroup of $PGL(2,9)$ which is isomorphic to the octahedral group O, which is also isomorphic to S_4.

The isomorphism between $PU(2,9)$ and the octahedral group O is implemented by labeling the six vertices of the octahedron as shown in Fig. 3.7. Every rotation of

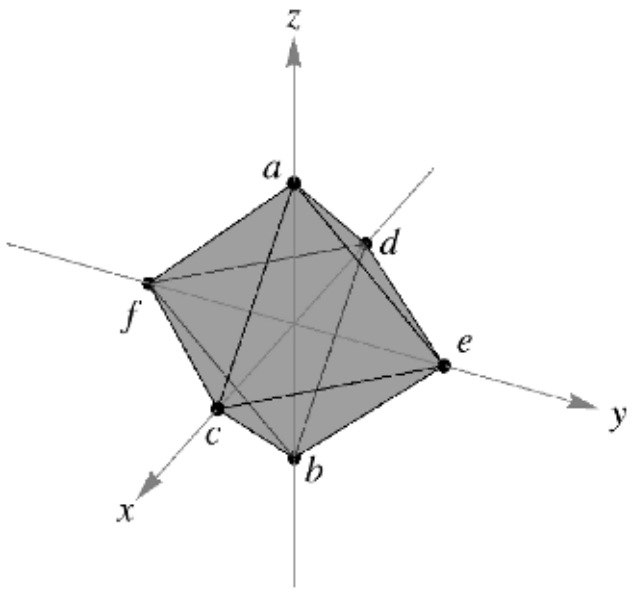

Figure 3.7: The correspondence between the octahedral group O and the projective unitary group $PU(2,9)$. Every O rotation of the octahedron corresponds to a permutation of the six vertex labels $abcdef$ belonging to $PU(2,9)$.

the octahedron in O will lead to a permutation of the vertex labels corresponding to an element of $PU(2,9)$. For instance, the 180° rotation around the x-axis lead to the permutation $(ab)(ef)$. The spin observables transform under $PU(2,9)$ as

$$
\begin{aligned}
e &: \hat{\sigma}_1 \to \hat{\sigma}_1\ ,\ \hat{\sigma}_2 \to \hat{\sigma}_2\ ,\ \hat{\sigma}_3 \to \hat{\sigma}_3\ ,\\
(ab)(ef) &: \hat{\sigma}_1 \to \hat{\sigma}_1\ ,\ \hat{\sigma}_2 \to -\hat{\sigma}_2\ ,\ \hat{\sigma}_3 \to -\hat{\sigma}_3\ ,\\
(ab)(cd) &: \hat{\sigma}_1 \to -\hat{\sigma}_1\ ,\ \hat{\sigma}_2 \to \hat{\sigma}_2\ ,\ \hat{\sigma}_3 \to -\hat{\sigma}_3\ ,\\
(cd)(ef) &: \hat{\sigma}_1 \to -\hat{\sigma}_1\ ,\ \hat{\sigma}_2 \to -\hat{\sigma}_2\ ,\ \hat{\sigma}_3 \to \hat{\sigma}_3\ ,\\
(aebf) &: \hat{\sigma}_1 \to \hat{\sigma}_1\ ,\ \hat{\sigma}_2 \to -\hat{\sigma}_3\ ,\ \hat{\sigma}_3 \to \hat{\sigma}_2\ ,\\
(afbe) &: \hat{\sigma}_1 \to \hat{\sigma}_1\ ,\ \hat{\sigma}_2 \to \hat{\sigma}_3\ ,\ \hat{\sigma}_3 \to -\hat{\sigma}_2\ ,\\
(acbd) &: \hat{\sigma}_1 \to -\hat{\sigma}_3\ ,\ \hat{\sigma}_2 \to \hat{\sigma}_2\ ,\ \hat{\sigma}_3 \to \hat{\sigma}_1\ ,\\
(adbc) &: \hat{\sigma}_1 \to \hat{\sigma}_3\ ,\ \hat{\sigma}_2 \to \hat{\sigma}_2\ ,\ \hat{\sigma}_3 \to -\hat{\sigma}_1\ ,\\
(cedf) &: \hat{\sigma}_1 \to \hat{\sigma}_2\ ,\ \hat{\sigma}_2 \to -\hat{\sigma}_1\ ,\ \hat{\sigma}_3 \to \hat{\sigma}_3\ ,\\
(cfde) &: \hat{\sigma}_1 \to -\hat{\sigma}_2\ ,\ \hat{\sigma}_2 \to \hat{\sigma}_1\ ,\ \hat{\sigma}_3 \to \hat{\sigma}_3\ ,\\
(ae)(bf)(cd) &: \hat{\sigma}_1 \to -\hat{\sigma}_1\ ,\ \hat{\sigma}_2 \to \hat{\sigma}_3\ ,\ \hat{\sigma}_3 \to \hat{\sigma}_2\ ,\\
(af)(be)(cd) &: \hat{\sigma}_1 \to -\hat{\sigma}_1\ ,\ \hat{\sigma}_2 \to -\hat{\sigma}_3\ ,\ \hat{\sigma}_3 \to -\hat{\sigma}_2\ ,\\
(ac)(bd)(ef) &: \hat{\sigma}_1 \to \hat{\sigma}_3\ ,\ \hat{\sigma}_2 \to -\hat{\sigma}_2\ ,\ \hat{\sigma}_3 \to \hat{\sigma}_1\ ,\\
(ad)(bc)(ef) &: \hat{\sigma}_1 \to -\hat{\sigma}_3\ ,\ \hat{\sigma}_2 \to -\hat{\sigma}_2\ ,\ \hat{\sigma}_3 \to -\hat{\sigma}_1\ ,\\
(ab)(ce)(df) &: \hat{\sigma}_1 \to \hat{\sigma}_2\ ,\ \hat{\sigma}_2 \to \hat{\sigma}_1\ ,\ \hat{\sigma}_3 \to -\hat{\sigma}_3\ ,
\end{aligned}
$$

$$\begin{array}{rcl}
(ab)(cf)(de) & : & \hat{\sigma}_1 \to -\hat{\sigma}_2\ ,\ \hat{\sigma}_2 \to -\hat{\sigma}_1\ ,\ \hat{\sigma}_3 \to -\hat{\sigma}_3\ , \\
(ace)(bdf) & : & \hat{\sigma}_1 \to \hat{\sigma}_2\ ,\ \hat{\sigma}_2 \to \hat{\sigma}_3\ ,\ \hat{\sigma}_3 \to \hat{\sigma}_1\ , \\
(adf)(bce) & : & \hat{\sigma}_1 \to \hat{\sigma}_2\ ,\ \hat{\sigma}_2 \to -\hat{\sigma}_3\ ,\ \hat{\sigma}_3 \to -\hat{\sigma}_1\ , \\
(acf)(bde) & : & \hat{\sigma}_1 \to -\hat{\sigma}_2\ ,\ \hat{\sigma}_2 \to -\hat{\sigma}_3\ ,\ \hat{\sigma}_3 \to \hat{\sigma}_1\ , \\
(ade)(bcf) & : & \hat{\sigma}_1 \to -\hat{\sigma}_2\ ,\ \hat{\sigma}_2 \to \hat{\sigma}_3\ ,\ \hat{\sigma}_3 \to -\hat{\sigma}_1\ , \\
(aec)(bfd) & : & \hat{\sigma}_1 \to \hat{\sigma}_3\ ,\ \hat{\sigma}_2 \to \hat{\sigma}_1\ ,\ \hat{\sigma}_3 \to \hat{\sigma}_2\ , \\
(afc)(bed) & : & \hat{\sigma}_1 \to \hat{\sigma}_3\ ,\ \hat{\sigma}_2 \to -\hat{\sigma}_1\ ,\ \hat{\sigma}_3 \to -\hat{\sigma}_2\ , \\
(aed)(bfc) & : & \hat{\sigma}_1 \to -\hat{\sigma}_3\ ,\ \hat{\sigma}_2 \to -\hat{\sigma}_1\ ,\ \hat{\sigma}_3 \to \hat{\sigma}_2\ , \\
(afd)(bed) & : & \hat{\sigma}_1 \to -\hat{\sigma}_3\ ,\ \hat{\sigma}_2 \to \hat{\sigma}_1\ ,\ \hat{\sigma}_3 \to -\hat{\sigma}_2\ ,
\end{array} \tag{3.109}$$

just as they should under the corresponding rotations of the octahedron in 3D space.

3.3.7 Spin Correlations

In the examples considered above, spin-like observables were represented by Pauli matrices, with elements in $GP(3^n)$, acting on the 2D vector spaces $V(2,3^n)$, $n = 1$ or 2. If we associate this model with the spin of one particle, two particle spin-states will be represented by vectors in $V(2,3^n) \otimes V(2,3^n) = V(4,3^n)$, $n = 1$ or 2, while the product spins will be represented by Kronecker products of the Pauli matrices. In this section, we will look at the correlations of these spins.

$n = 1$ case

The space $V(4,3)$ has $3^4 - 1 = 80$ non-zero vectors, every two of which differ by only a multiplicative phase, namely $-\underline{1}$, leaving $80/2 = 40$ inequivalent vectors. Of these, $4^2 = 16$ are products of physical states in $V(2,3)$, all of which are also physical in $V(4,3)$ since

$$(\langle\psi| \otimes \langle\phi|)(|\psi\rangle \otimes |\phi\rangle) \ = \ \langle\psi|\psi\rangle\langle\phi|\phi\rangle \ = \ \underline{1}\ , \tag{3.110}$$

if $\langle\psi|\psi\rangle = \langle\phi|\phi\rangle = \underline{1}$. Of the remaining $40 - 16 = 24$ vectors, 16 are self-orthogonal, e.g.

$$\begin{bmatrix} \underline{1} \\ \underline{1} \\ \underline{1} \\ \underline{0} \end{bmatrix} \cdot \begin{bmatrix} \underline{1} \\ \underline{1} \\ \underline{1} \\ \underline{0} \end{bmatrix} \ = \ \underline{1} + \underline{1} + \underline{1} + \underline{0} \ = \ \underline{0}\ , \tag{3.111}$$

leaving $24 - 16 = 8$ physical entangled states.

To label these states, we first note that the eight elements of $PO(2,3)$ fall into five conjugacy classes given by

$$\begin{array}{l} \{e\}\,, \\ \{(ab)(cd)\}\,, \\ \{(ab),(cd)\}\,, \\ \{(ac)(bd),(ad)(bc)\}\,, \text{ and} \\ \{(acbd),(adbc)\}\,. \end{array} \tag{3.112}$$

The eight physical entangled states in $V(4,3)$ also fall into five classes that transform among themselves under global $PO(2,3)$. They can be classified and labeled according to their transformation properties under the full global $PGL(2,3)$.

$$\begin{aligned} |S\rangle &= \left[\begin{array}{cccc} \underline{0} & \underline{1} & -\underline{1} & \underline{0} \end{array}\right]^{\mathrm{T}}, \\ |(ab)\rangle &= \left[\begin{array}{cccc} \underline{1} & \underline{0} & \underline{0} & -\underline{1} \end{array}\right]^{\mathrm{T}}, \\ |(cd)\rangle &= \left[\begin{array}{cccc} \underline{0} & \underline{1} & \underline{1} & \underline{0} \end{array}\right]^{\mathrm{T}}, \\ |(ab)(cd)\rangle &= \left[\begin{array}{cccc} \underline{1} & \underline{0} & \underline{0} & \underline{1} \end{array}\right]^{\mathrm{T}}, \\ |(ad)(bc)\rangle &= \left[\begin{array}{cccc} \underline{1} & \underline{1} & \underline{1} & -\underline{1} \end{array}\right]^{\mathrm{T}}, \\ |(ac)(bd)\rangle &= \left[\begin{array}{cccc} -\underline{1} & \underline{1} & \underline{1} & \underline{1} \end{array}\right]^{\mathrm{T}}, \\ |(acbd)\rangle &= \left[\begin{array}{cccc} \underline{1} & -\underline{1} & \underline{1} & \underline{1} \end{array}\right]^{\mathrm{T}}, \\ |(adbc)\rangle &= \left[\begin{array}{cccc} \underline{1} & \underline{1} & -\underline{1} & \underline{1} \end{array}\right]^{\mathrm{T}}. \end{aligned} \tag{3.113}$$

Here, $|S\rangle$ is the singlet state which is invariant under all transformations in $PGL(2,3)$. The state $|(ab)(cd)\rangle$ is also a singlet under $PO(2,3)$ transformations, but transforms into $|(ac)(bd)\rangle$ and $|(ad)(cd)\rangle$ under the full $PGL(2,3)$. The other states transform in pairs under $PO(2,3)$, falling into the same classes as the $PO(2,3)$ transformations themselves as listed in Eq. (3.112).

Under local $PO(2,3)$ transformations, that is, $PO(2,3)$ transformations acting on only one of the $V(2,3)$ vector spaces in $V(4,3) = V(2,3) \times V(2,3)$, all eight states fall into the same class and can be transformed into the singlet state $|S\rangle$. Explicitly, we have:

$$\begin{aligned} |S\rangle &= (cd)_1\,|(cd)\rangle \;=\; (cd)_2\,|(cd)\rangle \\ &= (ab)_1\,|(ab)\rangle \;=\; (ab)_2\,|(ab)\rangle \\ &= (ab)_1(cd)_1\,|(ab)(cd)\rangle \;=\; (ab)_2(cd)_2\,|(ab)(cd)\rangle \\ &= (ac)_1(bd)_1\,|(ac)(bd)\rangle \;=\; (ac)_2(bd)_2\,|(ac)(bd)\rangle \\ &= (ad)_1(bc)_1\,|(ad)(bc)\rangle \;=\; (ad)_2(bc)_2\,|(ad)(bd)\rangle \end{aligned}$$

$$\begin{aligned} &= (acbd)_1\,|(acbd)\rangle \;=\; (acbd)_2\,|(adbc)\rangle \\ &= (adbc)_1\,|(adbc)\rangle \;=\; (adbc)_2\,|(acbd)\rangle \;, \end{aligned} \tag{3.114}$$

where the subscript indicates which $V(2,3)$ space the transformations are acting on.

Product spins are represented by $\hat{\sigma}_i \otimes \hat{\sigma}_j$, $i,j = 1$ or 3. For product states, the expectation value of product spins factorizes due to the product preserving property of φ:

$$\begin{aligned} E(\sigma_i\sigma_j|\psi\phi) &= \varphi\Big[\big(\langle\psi| \otimes \langle\phi|\big)\big(\hat{\sigma}_i \otimes \hat{\sigma}_j\big)\big(|\psi\rangle \otimes |\phi\rangle\big)\Big] \\ &= \varphi\big(\langle\psi|\,\hat{\sigma}_i\,|\psi\rangle\,\langle\phi|\,\hat{\sigma}_j\,|\phi\rangle\big) \\ &= \varphi\big(\langle\psi|\,\hat{\sigma}_i\,|\psi\rangle\big)\,\varphi\big(\langle\phi|\,\hat{\sigma}_j\,|\phi\rangle\big) \\ &= E(\sigma_i|\psi)\,E(\sigma_j|\phi)\;. \end{aligned} \tag{3.115}$$

This factorization is necessary if we are to have isolated one particle states. Again, the product preserving map φ plays a fundamental role. The explicit representations of the product spin operators are

$$\begin{aligned} \hat{\sigma}_1 \otimes \hat{\sigma}_1 &= \begin{bmatrix} \underline{0} & \underline{0} & \underline{0} & \underline{1} \\ \underline{0} & \underline{0} & \underline{1} & \underline{0} \\ \underline{0} & \underline{1} & \underline{0} & \underline{0} \\ \underline{1} & \underline{0} & \underline{0} & \underline{0} \end{bmatrix}, \\ \hat{\sigma}_1 \otimes \hat{\sigma}_3 &= \begin{bmatrix} \underline{0} & \underline{0} & \underline{1} & \underline{0} \\ \underline{0} & \underline{0} & \underline{0} & -\underline{1} \\ \underline{1} & \underline{0} & \underline{0} & \underline{0} \\ \underline{0} & -\underline{1} & \underline{0} & \underline{0} \end{bmatrix}, \\ \hat{\sigma}_3 \otimes \hat{\sigma}_1 &= \begin{bmatrix} \underline{0} & \underline{1} & \underline{0} & \underline{0} \\ \underline{1} & \underline{0} & \underline{0} & \underline{0} \\ \underline{0} & \underline{0} & \underline{0} & -\underline{1} \\ \underline{0} & \underline{0} & -\underline{1} & \underline{0} \end{bmatrix}, \\ \hat{\sigma}_3 \otimes \hat{\sigma}_3 &= \begin{bmatrix} \underline{1} & \underline{0} & \underline{0} & \underline{0} \\ \underline{0} & -\underline{1} & \underline{0} & \underline{0} \\ \underline{0} & \underline{0} & -\underline{1} & \underline{0} \\ \underline{0} & \underline{0} & \underline{0} & \underline{1} \end{bmatrix}. \end{aligned} \tag{3.116}$$

Using these expressions, we can calculate the spin correlations of this system and determine the Clauser-Horne-Shimony-Holt (CHSH) bound. To reiterate, the CHSH bound is the upper bound of the absolute value of the following combination of correlators:

$$C(A,a\,;B,b\,|\Psi)$$

$$\equiv \quad E(AB|\Psi) + E(Ab|\Psi) + E(aB|\Psi) - E(ab|\Psi) \; , \tag{3.117}$$

where A and a are two observables of particle 1, and B and b are two observables of particle 2. All four observables are assumed to take on only the values ± 1 upon measurement. For classical hidden variable theory, the bound on $|C(A, a\,; B, b\,|\Psi)|$ is 2, while for canonical quantum mechanics, it is the Cirel'son bound: $2\sqrt{2}$ [40].

In the current case, each of the four observables A, a, B, and b is either σ_1 or σ_3. The cases in which the operators are the negatives of either σ_1 or σ_3 need not be considered since

$$\begin{aligned} & C(A, a\,; B, b\,|\Psi) \\ & \quad = \quad C(A, -a\,; b, B\,|\Psi) \;\; = \;\; -C(-A, a\,; b, B\,|\Psi) \\ & \quad = \quad C(a, A\,; B, -b\,|\Psi) \;\; = \;\; -C(a, A\,; -B, b\,|\Psi) \; . \end{aligned} \tag{3.118}$$

To compress our notation, let us define

$$C_{ijk\ell}(\Psi) \;\; = \;\; C(\sigma_i, \sigma_j; \sigma_k, \sigma_\ell|\Psi) \; . \tag{3.119}$$

There are only four possible combinations of indices to consider: C_{1313}, C_{1331}, C_{3113}, and C_{3131}. Only the CHSH correlators for entangled states are of interest, since those for the product states cannot exceed the classical bound. Furthermore, all eight entangled states can be transformed into the singlet state $|S\rangle$ by an appropriate local $PO(2,3)$ transformation, so one only needs to consider correlations for this one state. It is straightforward to show that

$$\begin{aligned} \langle S|\, \hat{\sigma}_1 \otimes \hat{\sigma}_1\, |S\rangle \;\; & = \;\; \langle S|\, \hat{\sigma}_3 \otimes \hat{\sigma}_3\, |S\rangle \;\; = \;\; -\underline{1} \; , \\ \langle S|\, \hat{\sigma}_1 \otimes \hat{\sigma}_3\, |S\rangle \;\; & = \;\; \langle S|\, \hat{\sigma}_3 \otimes \hat{\sigma}_1\, |S\rangle \;\; = \;\; \underline{0} \; . \end{aligned} \tag{3.120}$$

From this, we find

$$\begin{aligned} C_{1313}(S) \;\; & = \;\; C_{3131}(S) \;\; = \;\; 0 \; , \\ C_{1331}(S) \;\; & = \;\; C_{3113}(S) \;\; = \;\; -2 \; . \end{aligned} \tag{3.121}$$

Thus, the CHSH bound for this model is the classical value of 2.

A major result of the discrete quantum mechanical model from the last section is that the CHSH bound of 2 does not necessarily imply that the predictions of a given model can be mimicked by a classical hidden variable theory. In the current case, however, they can be.

Let us denote the classical values of σ_1 and σ_3 of particle 1 as X_1 and Z_1, and those of the particle 2 as X_2 and Z_2, respectively. The first line of Eq. (3.120) implies that

the pairs (X_1, X_2) and (Z_1, Z_2) are completely anti-correlated. Therefore, the only classical configurations possible are $(X_1, Z_1; X_2, Z_2) = (+,+;-,-)$, $(+,-;-,+)$, $(-,+;+,-)$, and $(-,-;+,+)$. To reproduce the second line of Eq. (3.120), we only need to demand that the probabilities of these configurations satisfy:

$$\begin{aligned} \frac{1}{2} &= P(+,+;-,-) + P(-,-;+,+) \\ &= P(+,-;-,+) + P(-,+;+,-) \,. \end{aligned} \tag{3.122}$$

Thus, an entire class of hidden variable mimics exists.

$n = 2$ case

The space $V(4,9)$ has $9^4 - 1 = 6560$ non-zero vectors, every eight of which differ by only a multiplicative phase, i.e. an element of $GF(9)\backslash\{0\}$, leaving $6560/8 = 820$ inequivalent states. Of the $10^2 = 100$ product states, the $6^2 = 36$ products of physical states in $V(2,9)$ are also physical in $V(4,9)$. The remaining 64 product states are self-orthogonal and unphysical. Of the $820 - 100 = 720$ entangled states, 216 are self-orthogonal, leaving $720 - 216 = 504$ physical entangled states.

These 504 physical entangled states fall into classes that transform among themselves under global $PU(2,9)$ transformations. Since we cannot list all 504 states here, we will only mention that they fall into 17 classes of 24 elements each, 4 classes of 12 elements each, 4 classes of 8 elements each, 2 classes of 6 elements each, 1 class of 3 elements, and the singlet state $|S\rangle = [\,\underline{0}, \underline{1}, -\underline{1}, \underline{0}\,]^{\mathrm{T}}$.

This can be verified by a direct search, or through use of Burnside's lemma and the orbit-stabilizer theorem, which can be found in any decent abstract algebra textbook (such as [57]).

For a group, G, acting on a set, X, a subset that is preserved by the action of the entire group is called an orbit. The set of orbits forms a partition of the set X. To calculate the number of orbits, here denoted $|X/G|$, one can use Burnside's lemma:

$$|X/G| \;=\; \frac{1}{|G|} \sum_{g \in G} |X^g| \,, \tag{3.123}$$

where X^g is the set of elements in X that are invariant under the action of g.

For global $PU(2,9)$ transformations, Burnside's lemma indicates that there should be 29 orbits in the set of entangled states. To calculate the length of these orbits,

one could use the orbit-stabilizer theorem, which states that the order of the orbit containing an element is equal to the order of the group divided by the order of the stabilizer subgroup of that element. The stabilizer subgroup of an element is the subgroup under which that element is invariant.

This computation indicates that there are 408 states that belong to orbits of order 24, 48 states that belong to orbits of order 12, 32 states that belong to orbits of order 8, 12 states that belong to orbits of order 6, 3 states that belong to orbits of order 3, and 1 state that belongs to an orbit of order 1.

Under local $PU(2,9)$ transformations, the same 504 entangled states fall into three classes with 24, 288, and 192 elements each. Again, this result can be arrived at through a manual search or through the group theoretic means mentioned above.

These classes can be represented by the following three states:

$$|S\rangle = \begin{bmatrix} \underline{0} \\ \underline{1} \\ -\underline{1} \\ \underline{0} \end{bmatrix}, \quad |T\rangle = \begin{bmatrix} \underline{1} \\ \underline{0} \\ \underline{1}+\underline{i} \\ \underline{1} \end{bmatrix}, \quad |U\rangle = \begin{bmatrix} \underline{1} \\ \underline{0} \\ \underline{1} \\ \underline{1}+\underline{i} \end{bmatrix}, \tag{3.124}$$

with the duals

$$\begin{array}{rcl} \langle S| & = & \begin{bmatrix} \underline{0} & -\underline{1} & \underline{1} & \underline{0} \end{bmatrix}, \\ \langle T| & = & \begin{bmatrix} \underline{1} & \underline{0} & \underline{1}-\underline{i} & \underline{1} \end{bmatrix}, \\ \langle U| & = & \begin{bmatrix} \underline{1} & \underline{0} & \underline{1} & \underline{1}-\underline{i} \end{bmatrix}. \end{array} \tag{3.125}$$

Let's now turn our attention to calculating the CHSH correlators so that we can determine the maximum value.

As all of the entangled states transform into either $|S\rangle$, $|T\rangle$, or $|U\rangle$, we only need to calculate the correlators for these states to obtain the CHSH bound. Also, since there are three spin observables ($\hat{\sigma}_1$, $\hat{\sigma}_2$, and $\hat{\sigma}_3$) this time, the number of possible CHSH correlators is $6^2 = 36$.

Let us first look at the correlators involving only $\hat{\sigma}_1$ and $\hat{\sigma}_3$. The correlations for the state $|S\rangle$ are the same as those listed in Eq. (3.120) and (3.121).

Those for the state $|T\rangle$ are

$$\begin{array}{rcl} \langle T|\,\hat{\sigma}_1 \otimes \hat{\sigma}_1\,|T\rangle & = & \langle T|\,\hat{\sigma}_1 \otimes \hat{\sigma}_3\,|T\rangle \;=\; -\underline{1}\,, \\ \langle T|\,\hat{\sigma}_3 \otimes \hat{\sigma}_1\,|T\rangle & = & \underline{1}\,, \end{array}$$

state	0	1	2	3	4
$\|S\rangle$	6	24	6	0	0
$\|T\rangle$	6	18	6	6	0
$\|U\rangle$	12	12	4	4	4

Table 3.6: The number of CHSH correlators with the respective absolute values for the three states $|S\rangle$, $|T\rangle$, and $|U\rangle$.

$$\langle T|\,\hat{\sigma}_3 \otimes \hat{\sigma}_3\,|T\rangle \;=\; \underline{0}\,, \tag{3.126}$$

from which we obtain

$$\begin{aligned} C_{1313}(T) &= -1\,, \\ C_{3113}(T) &= C_{3131}(T) \;=\; 1\,, \\ C_{1331}(T) &= -3\,. \end{aligned} \tag{3.127}$$

Similarly, for the state $|U\rangle$ we have

$$\begin{aligned} \langle U|\,\hat{\sigma}_1 \otimes \hat{\sigma}_1\,|U\rangle &= \langle U|\,\hat{\sigma}_1 \otimes \hat{\sigma}_3\,|U\rangle \\ &= \langle U|\,\hat{\sigma}_3 \otimes \hat{\sigma}_3\,|U\rangle \;=\; -\underline{1}\,, \\ \langle U|\,\hat{\sigma}_3 \otimes \hat{\sigma}_1\,|U\rangle &= \underline{1}\,, \end{aligned} \tag{3.128}$$

and

$$\begin{aligned} C_{1313}(U) &= C_{3113}(U) \;=\; C_{3131}(U) \;=\; 0\,, \\ C_{1331}(U) &= -4\,. \end{aligned} \tag{3.129}$$

As can be seen, the absolute value of the correlator C_{1331} for the states $|T\rangle$ and $|U\rangle$ exceed not only the classical bound of 2 but also the Cirel'son bound of $2\sqrt{2}$.

In a similar fashion, all 36 spin combinations for the three states can be calculated and the have obtained the tally shown in Table 3.6. Thus, we find that the CHSH bound for this model is 4.

Unlike the $n = 1$ case, which had a CHSH bound of 2, the above correlations cannot be reproduced by any classical hidden variable theory. For instance, the first line of Eq. (3.126) demands that the pairs (X_1, X_2) and (X_1, Z_2) are completely anti-correlated, while the second line demands that the pair (Z_1, X_2) is completely correlated. But then $X_1 = \pm 1$ would imply $X_2 = \mp 1$ and $Z_2 = \mp 1$, the first of which implies $Z_1 = \mp 1$. Therefore, the pair (Z_1, Z_2) must also be completely correlated which contradicts the third line of Eq. (3.126). Similarly, Eq. (3.128) demands

that the pairs (X_1, X_2), (X_1, Z_2), and (Z_1, Z_2) are completely anti-correlated, while (Z_1, X_2) is completely correlated. But then $X_1 = \pm 1$ would imply $X_2 = \mp 1$ and $Z_2 = \mp 1$, the former of which implies $Z_1 = \mp 1$ while the latter $Z_1 = \pm 1$, leading to a contradiction. Of course, this is not surprising since the CHSH bound for classical hidden variable theories is 2. The unexpected result is that the CHSH bound of our model also exceeds the quantum Cirel'son bound of $2\sqrt{2}$.

3.3.8 Expectation Values without Definite Probabilities

In canonical quantum mechanics, the states that correspond to $|S\rangle$, $|T\rangle$, and $|U\rangle$ are

$$\left|\tilde{S}\right\rangle = \frac{1}{\sqrt{2}}\begin{bmatrix} 0 \\ 1 \\ -1 \\ 0 \end{bmatrix}, \quad \left|\tilde{T}\right\rangle = \frac{1}{2}\begin{bmatrix} 1 \\ 0 \\ 1+i \\ 1 \end{bmatrix}, \quad \left|\tilde{U}\right\rangle = \frac{1}{2}\begin{bmatrix} 1 \\ 0 \\ 1 \\ 1+i \end{bmatrix}, \tag{3.130}$$

Calculating the correlations of canonical spin $\tilde{\sigma}_i$ for the state $\left|\tilde{S}\right\rangle$ in canonical quantum mechanics, we find

$$\begin{aligned} \left\langle \tilde{S}\right| \tilde{\sigma}_1 \otimes \tilde{\sigma}_1 \left|\tilde{S}\right\rangle &= \left\langle \tilde{S}\right| \tilde{\sigma}_3 \otimes \tilde{\sigma}_3 \left|\tilde{S}\right\rangle = -1\,, \\ \left\langle \tilde{S}\right| \tilde{\sigma}_1 \otimes \tilde{\sigma}_3 \left|\tilde{S}\right\rangle &= \left\langle \tilde{S}\right| \tilde{\sigma}_3 \otimes \tilde{\sigma}_1 \left|\tilde{S}\right\rangle = 0\,, \end{aligned} \tag{3.131}$$

which agree with those for $|S\rangle$ in Eq. (3.120) via the product preserving map φ. For $\left|\tilde{T}\right\rangle$ and $\left|\tilde{U}\right\rangle$, however, we find:

$$\begin{aligned} \left\langle \tilde{T}\right| \tilde{\sigma}_1 \otimes \tilde{\sigma}_1 \left|\tilde{T}\right\rangle &= \left\langle \tilde{T}\right| \tilde{\sigma}_1 \otimes \tilde{\sigma}_3 \left|\tilde{T}\right\rangle = \frac{1}{2}\,, \\ \left\langle \tilde{T}\right| \tilde{\sigma}_3 \otimes \tilde{\sigma}_1 \left|\tilde{T}\right\rangle &= -\frac{1}{2}\,, \\ \left\langle \tilde{T}\right| \tilde{\sigma}_3 \otimes \tilde{\sigma}_3 \left|\tilde{T}\right\rangle &= 0\,, \\ \left\langle \tilde{U}\right| \tilde{\sigma}_1 \otimes \tilde{\sigma}_1 \left|\tilde{U}\right\rangle &= \left\langle \tilde{U}\right| \tilde{\sigma}_1 \otimes \tilde{\sigma}_3 \left|\tilde{U}\right\rangle \\ &= \left\langle \tilde{U}\right| \tilde{\sigma}_3 \otimes \tilde{\sigma}_3 \left|\tilde{U}\right\rangle = \frac{1}{2}\,, \\ \left\langle \tilde{U}\right| \tilde{\sigma}_3 \otimes \tilde{\sigma}_1 \left|\tilde{U}\right\rangle &= -\frac{1}{2}\,, \end{aligned} \tag{3.132}$$

	++	+−	−+	−−	E.V.
$\left\|\tilde{S}\right\rangle$	0	$\frac{1}{2}$	$\frac{1}{2}$	0	-1
$\left\|\tilde{T}\right\rangle$	$\frac{1}{4}$	0	$\frac{1}{2}$	$\frac{1}{4}$	0
$\left\|\tilde{U}\right\rangle$	$\frac{1}{4}$	0	$\frac{1}{4}$	$\frac{1}{2}$	$+\frac{1}{2}$

Table 3.7: The probabilities of the four possible outcomes ++, +−, −+, and −− in canonical quantum mechanic when $\tilde{\sigma}_3 \otimes \tilde{\sigma}_3$ is measured on the canonical states $\left|\tilde{S}\right\rangle$, $\left|\tilde{T}\right\rangle$, and $\left|\tilde{U}\right\rangle$.

Thus, the correspondence here is

$$-\underline{1} \;\leftrightarrow\; \frac{1}{2}\,, \qquad \underline{1} \;\leftrightarrow\; -\frac{1}{2}\,, \tag{3.133}$$

which is to be expected since $\underline{1} \div \underline{2} = \underline{2} = -\underline{1}$ in $GF(3)$. So the large correlation is due to the fact that $GF(3)$ has only three elements $\{-\underline{1}, \underline{0}, \underline{1}\}$ which are mapped to $\{-1, 0, 1\} \in \mathbb{R}$ by the product preserving map φ. The fact that the only spin-correlations possible are 0 or ± 1 will of course persist for larger values of $p = 3 \mod 4$ as long as we use φ.

What are the corresponding probabilities? Let us take the spins in the Z-direction, $\sigma_3 \otimes \sigma_3$, as an example. The probabilities of the outcomes $(\sigma_3\sigma_3) = (++)$, $(+-)$, $(-+)$, and $(--)$ in canonical quantum mechanics are listed in Table 3.7. As can be seen, they reproduce the correlations listed above as they should.

In biorthogonal quantum mechanics, however, the probabilities of individual outcomes are ill defined. Taking the point of view that the probabilities must be inferred from the expectation values, we have the constraints

$$\begin{aligned} &P(++|T) + P(+-|T) + P(-+|T) + P(--|T) = 1\,, \\ &P(++|T) - P(+-|T) - P(-+|T) + P(--|T) = 0\,, \end{aligned} \tag{3.134}$$

for $|T\rangle$, and

$$\begin{aligned} &P(++|U) + P(+-|U) + P(-+|U) + P(--|U) = 1\,, \\ &P(++|U) - P(+-|U) - P(-+|U) + P(--|U) = -1\,, \end{aligned} \tag{3.135}$$

for $|U\rangle$. These constraints imply

$$\begin{aligned} \frac{1}{2} &= P(++|T) + P(--|T) \\ &= P(+-|T) + P(-+|T) \ , \\ 0 &= P(++|U) + P(--|U) \ , \\ 1 &= P(+-|U) + P(-+|U) \ , \end{aligned} \tag{3.136}$$

but beyond this, the probabilities cannot be specified. Therefore, though our formalism predicts definite expectation values, it leaves probabilities indeterminate. Physically, we interpret this to mean that if the same measurement is repeated many times, the average of the outcomes will converge to the predicted expectation value, while the frequencies of each outcome will continue to fluctuate.

In canonical quantum mechanics, it is possible to construct the probability distribution for the measurement outcomes of some observable through use of the system of equations formed by the expectation values of the powers of the observable in question. This is not possible for spin observables in the model under consideration due to the cyclic nature of the underlying field. Explicitly, the system of equations:

$$\begin{aligned} E(A|\psi) &= \sum_i P_i \alpha_i \\ E(A^2|\psi) &= \sum_i P_i (\alpha_i)^2 \\ \dots &= \dots \\ E(A^n|\psi) &= \sum_i P_i (\alpha_i)^n \end{aligned}$$

will be singular if n is greater than the least common multiple of the multiplicative orders of the eigenvalues α_i of A since the cyclic nature of the field is necessarily shared by the eigenvalues when the product preserving map also preserves the eigenvalues. In our examples, using $GF(3)$ as the 'real' field, the eigenvalues of spin observables, $\{+1, -1\}$, have multiplicative orders no greater than 2. Thus, when we form a four level system by entangling two particles, we find that the system of equations needed to solve for the probabilities of these four measurement outcomes is singular and cannot be used to assign consistent probabilities.

3.3.9 Comments

As was mentioned in the first chapter, it has been conjectured that a 'doubly' quantized theory may contain super-quantum correlations with a CHSH bound which exceeds the Cirel'son value of $2\sqrt{2}$. Although we have found such supercorrelations, it is unclear whether or not the discreteness led to by the choice of Galois fields is of a type that may be considered a second quantization. One of the future goals is to study these models for arbitrary large Galois fields.

It might be conjectured that a state in such a theory might be thought of as a 'superposition' of various 'singly' quantized states, each of which predicts definite probabilities. A 'measurement' in a 'doubly' quantized theory could then be expected to collapse the 'doubly' quantized state to a 'singly' quantized one, selecting a particular probability distribution from all possible ones. Every 'measurement' would then lead to a different probability distribution, so no definite probability will be predicted. In this model, we have observed indeterminate probabilities, but it is unclear whether they are of the sort just described.

Another point of interest is in whether or not similar theories can be constructed for other spaces that lack inner products, like Banach spaces. This will certainly be a topic of future research.

Bibliography

[1] L. N. Chang, Z. Lewis, D. Minic and T. Takeuchi, Adv. High Energy Phys. **2011**, 493514 (2011) [arXiv:1106.0068 [hep-th]].

[2] L. N. Chang, Z. Lewis, D. Minic, T. Takeuchi and C. -H. Tze, Adv. High Energy Phys. **2011**, 593423 (2011) [arXiv:1104.3359 [quant-ph]].

[3] J. A. Wheeler, Annals Phys. **2**, 604 (1957).

[4] C. A. Mead, Phys. Rev. **135**, B849 (1964),

[5] T. Padmanabhan, Annals Phys. **165**, 38 (1985); Class. Quant. Grav. **4**, L107 (1987); Phys. Rev. Lett. **78**, 1854 (1997) [arXiv:hep-th/9608182].

[6] M. Maggiore, Phys. Lett. B **304**, 65 (1993) [arXiv:hep-th/9301067],

[7] L. J. Garay, Int. J. Mod. Phys. A **10**, 145 (1995) [arXiv:gr-qc/9403008].

[8] M. B. Green, J. H. Schwarz and E. Witten, *Superstring Theory, Vol. I and Vol. II*, Cambridge University Press (1988),
J. Polchinski, *String Theory, Vol. I and Vol. II*, Cambridge University Press (1998),
K. Becker, M. Becker and J. H. Schwarz, *String Theory and M-Theory: A Modern Introduction*, Cambridge University Press (2007).

[9] H. Kragh, Revue d'Histoire des Sciences, Tome **48**, n°4, 401 (1995). The original work by Heisenberg on the lattice world appeared in 1930 in his letter to Bohr. This is reconstructed in B. Carazza and H. Kragh, Am. Jour. Phys. **63**, 595 (1995).

[10] W. Heisenberg and W. Pauli, Z. Phys. **56**, 1 (1929).

[11] M. Born, Nature **132**, 282 (1933).

[12] H. S. Snyder, Phys. Rev. **71**, 38 (1947); Phys. Rev. **72**, 68 (1947).

[13] C. N. Yang, Phys. Rev. **72**, 874 (1947).

[14] C. A. Mead, Phys. Rev. **143**, 990 (1966).

[15] S. Weinberg, Phys. Rev. Lett. **62**, 485 (1989); Annals Phys. **194**, 336 (1989).

[16] C. M. Bender, D. C. Brody and H. F. Jones, eConf **C0306234**, 617 (2003) [Phys. Rev. Lett. **89**, 270401 (2002)] [Erratum-ibid. **92**, 119902 (2004)] [arXiv:quant-ph/0208076].

[17] M. Maggiore, Phys. Rev. D **49**, 5182 (1994) [arXiv:hep-th/9305163]; Phys. Lett. B **319**, 83 (1993) [arXiv:hep-th/9309034].

[18] A. Kempf, G. Mangano, R. B. Mann, Phys. Rev. **D52**, 1108-1118 (1995) [hep-th/9412167].

[19] D. Amati, M. Ciafaloni and G. Veneziano, Phys. Lett. B **216**, 41 (1989),

[20] D. J. Gross and P. F. Mende, Phys. Lett. B **197**, 129 (1987); Nucl. Phys. B **303**, 407 (1988),

[21] W. Heisenberg, *The Physical Principles of the Quantum Theory*, University of Chicago Press 1930, Dover edition 1949.

[22] L. Susskind and E. Witten, arXiv:hep-th/9805114,
A. W. Peet and J. Polchinski, Phys. Rev. D **59**, 065011 (1999).

[23] A. Kempf, J. Math. Phys. **35**, 4483 (1994) [hep-th/9311147].

[24] S. Benczik, L. N. Chang, D. Minic, N. Okamura, S. Rayyan and T. Takeuchi, Phys. Rev. D **66**, 026003 (2002) [arXiv:hep-th/0204049];

[25] F. Brau, J. Phys. A **A32**, 7691-7696 (1999). [quant-ph/9905033].

[26] F. Brau, F. Buisseret, Phys. Rev. **D74**, 036002 (2006). [hep-th/0605183].

[27] S. Weinberg, Rev. Mod. Phys. **61**, 1 (1989),
S. M. Carroll, Living Rev. Rel. **4**, 1 (2001) [arXiv:astro-ph/0004075],
E. Witten, arXiv:hep-ph/0002297,
N. Straumann, arXiv:gr-qc/0208027,
S. Nobbenhuis, Found. Phys. **36**, 613 (2006) [arXiv:gr-qc/0411093].

[28] T. Banks, Phys. Today **57N3**, 46 (2004).

[29] J. Polchinski, arXiv:hep-th/0603249.

[30] E. J. Copeland, M. Sami and S. Tsujikawa, Int. J. Mod. Phys. D **15**, 1753 (2006) [arXiv:hep-th/0603057],
E. Komatsu *et al.* [WMAP Collaboration], Astrophys. J. Suppl. **192**, 18 (2011) [arXiv:1001.4538 [astro-ph.CO]].

[31] L. N. Chang, D. Minic, N. Okamura and T. Takeuchi, Phys. Rev. D **65**, 125028 (2002) [hep-th/0201017].

[32] T. Banks, Int. J. Mod. Phys. A **16**, 910 (2001).

[33] M. Gell-Mann, P. Ramond and R. Slansky, in *Supergravity*, ed. by D. Freedman et al., North Holland (1979),
T. Yanagida, Prog. Theor. Phys. 64, 1103 (1980),
R. Mohapatra, G. Senjanovic, Phys. Rev. Lett. 44, 912 (1980),
S. Weinberg, Phys. Rev. D **22**, 1694 (1980).

[34] D. Helbing, I. J. Farkas and T. Viscek, Phys. Rev. Lett. **84** 1240 (2000);
D. Helbing, Rev. Mod. Phys. **73** 1067 (2001);
B. Schmittmann, K. Hwang and R. K. P. Zia, Europhys. Lett. **19** 19 (1992);
R. K. P. Zia, E. L. Praestgaard and O. G. Mouritsen, Am. J. Phys. **70** 384 (2002).

[35] D. Minic and H. C. Tze, Phys. Rev. D **68**, 061501 (2003); Phys. Lett. B **581**, 111 (2004), and arXiv:hep-th/0401028,
V. Jejjala, M. Kavic, D. Minic, Int. J. Mod. Phys. **A22**, 3317 (2007),
V. Jejjala, M. Kavic, D. Minic and C. H. Tze, arXiv:0804.3598 [hep-th]; Int. J. Mod. Phys. **D18**, 2257, (2009) and references therein.

[36] L. N. Chang, D. Minic and T. Takeuchi, Mod. Phys. Lett. A **25**, 2947 (2010) [arXiv:1004.4220 [hep-th]].

[37] Y. J. Ng and H. Van Dam, Mod. Phys. Lett. **A 9** 335 (1994); **A 10** 2801 (1995), F. Karolyhazy, Nuovo Cim. **A 42** 390 (1966); Y. J. Ng, Entropy **10**, 441 (2008). Non-relativistic space-time foam has more general "turbulent" scaling, V. Jejjala, D. Minic, Y. J. Ng and C. H. Tze, Class. Quant. Grav. **25**, 225012 (2008).

[38] A. Einstein, Investigations on the Theory of the Brownian Movement, www.bnpublishing.net (2011)

[39] S. J. Freedman and J. F. Clauser, Phys. Rev. Lett. **28**, 938 (1972);
J. F. Clauser and M. A. Horne, Phys. Rev. **D 10**, 526 (1974);
A. Aspect et al., Phys. Rev. Lett. **47**, 460 (1981);
A. Aspect et al., Phys. Rev. Lett. **49**, 91 (1982);
A. Aspect et al., Phys. Rev. Lett. **49**, 1804 (1982).

[40] B. S. Cirel'son, Lett. Math. Phys. **4** 93 (1980); In particular, consult, L. J. Landau, Phys. Lett. **A 120** (1987) 52.

[41] S. Popescu and D. Rorchlich, Foundations of Physics, **24** 379 (1994).

[42] J. S. Bell, Physics **1**, 195 (1964);
J. S. Bell, *Speakable and Unspeakable in Quantum Mechanics*, Cambridge University Press (1987).

[43] J. F. Clauser, M. A. Horne, A. Shimony and R. A. Holt, Phys. Rev. Lett. **23**, 880 (1969).

[44] S. J. Summers and R. Werner, Comm. Math. Phys. **110** (1987) 247; Journ. Math. Phys. **28** (1987), 2440; *ibid* 2448.

[45] See, D. Dieks, arXiv:quant-ph/0206172 .

[46] Y. Aharonov and D. Rochlich, *Quantum Paradoxes: Quantum Theory for the Perplexed*, Wiley-VCH (2005).
For a recent review, D. Rohrlich, arXiv:1011.5322v1 [quant-ph], and references therein.

[47] W. van Dam, Chapter 9 in *Nonlocality and Communication Complexity*, D.Phil. thesis, University of Oxford, Department of Physics, 2000. See also W. Van Dam, arXiv: quant-ph/0501159.

[48] G. Brassard, H. Burhman, N. Linden, A. A. Méthot, A. Tapp and F. Unger, Phys. Rev. Lett. **96**, 250401 (2006).

[49] G. Brassard, Nature Phys. **1**, 2 (2005),
S. Popescu, Nature Phys. **2**, 507 (2006),
J. Barrett, Phys. Rev. A **75**, 032304 (2007),
N. Brunner and P. Skrzypczyk, Phys. Rev. Lett. **102**, 160403 (2009).

[50] G. Ver Steeg and S. Wehner, arXiv:0811.3771[quant-ph].

[51] L. D. Faddeev, Asia-Pacific Physics News, **3**, 21, 1988. Also in *Frontiers in Physics, High Technology and Mathematics* (ed. Cerdeira and Lundqvist) p. 238-246, World Scientific (1989).

[52] J. Polchinski, *String Theory, Vol. I and Vol. II*, Cambridge University Press (1998);
K. Becker, M. Becker and J. H. Schwarz, *String Theory and M-Theory: A Modern Introduction*, Cambridge University Press (2007).
Also, M. B. Green, J. H. Schwarz, E. Witten, *Superstring Theory, Vol. I*, Cambridge University Press (1988), where it was suggested that string field theory can be viewed as a generalization of quantum theory.

[53] B. S. DeWitt (1967). Phys. Rev. **160**: 1113 (1967); Phys.Rev. **162** 1195,1239, (1967).

[54] *Feynman's Thesis: A New Approach to Quantum Theory,* edited by L. M. Brown, World Scientific, 2005.

[55] M. A. Vasiliev, arXiv:hep-th/9910096;
X. Bekaert, S. Cnockaert, C. Iazeolla and M. A. Vasiliev, arXiv:hep-th/0503128 and references therein.

[56] Y. Nambu, "Field Theory of Galois Fields," in *Quantum Field Theory and Quantum Statistics*, Vol. 1, pp. 625-636, eds. I. A. Batalin et al. (IOP Publishing, 1987). Also in World Scientific Series in 20th Century Physics - Vol. 13, *Broken Symmetry, selected papers of Y. Nambu*, eds. T. Eguchi and K. Nishijima (World Scientific, 1995).

[57] D. Dummit, R. Foote, *Abstract Algebra*, 3rd ed., Wiley, 2003

[58] S. Kochen and E.P. Specker, "The problem of hidden variables in quantum mechanics", Journal of Mathematics and Mechanics 17, 5987 (1967)

[59] L. Hardy, Phys. Rev. Lett. **71**, 1665 (1993).

[60] D. M. Greenberger, M. A. Horne, A. Zeilinger, arXiv:0712.0921v1 [quant-ph],
D. M. Greenberger, M. A. Horne, A. Shimony, and A. Zeilinger, Am. J. Phys. 58, 1131 (1990)

[61] R. Shankar, *Principles of Quantum Mechanics*, Springer 1980

[62] F. Schwabl, *Quantum Mechanics*, Springer 1992

[63] A. Kempf, J. Phys. A **30**, 2093 (1997) [arXiv:hep-th/9604045].

[64] L. N. Chang, D. Minic, N. Okamura, T. Takeuchi, Phys. Rev. **D65**, 125027 (2002). [hep-th/0111181].

[65] Z. Lewis and T. Takeuchi, Phys. Rev. D **84**, 105029 (2011) [arXiv:1109.2680 [hep-th]].

[66] S. Benczik, L. N. Chang, D. Minic and T. Takeuchi, Phys. Rev. A **72**, 012104 (2005) [hep-th/0502222].

[67] I. S. Gradshteyn and I. M. Ryzhik, "Table of Integrals, Series and Products," 7th edition (Acedemic Press, 2007); M. Abramowitz and I. A. Stegun, "Handbook of Mathematical Functions, with Formulas, Graphs, and

[68] D. Hilbert, L. Nordheim, J. von Neumann, "Über die Grundlagen der Quantenmechanik", Mathematische Annalen 98: p.1 - p.30, 1928

[69] A. N. Kolmogorov, S. V. Fomin, *Introductory Real Analysis*, Prentice-Hall, 1970

[70] Goldstein, Safkp, Poole, *Classical Mechanics*, 3rd ed., Addison-Wesley, 2001

[71] L. Landau, E. M. Lifshitz, *Mechanics, Third Edition: Volume 1*, Butterworth-Heinemann, 1976

[72] R. P. Feynman, A. R. Hibbs, *Quantum Mechanics and Path Integrals*, McGraw-Hill Companies; 1965

[73] D. R. Finkelstein, *Quantum relativity: A Synthesis of the ideas of Einstein and Heisenberg,* Springer (1996), pages 76-78; D. Finkelstein and S. R. Finkelstein, Int. J. Theor. Phys. **22**, 753 (1983).

[74] B. Schumacher and M. D. Westmoreland, arXiv:1010.2929 [quant-ph].

[75] L. N. Chang, Z. Lewis, D. Minic and T. Takeuchi, arXiv:1205.4800 [quant-ph].

[76] L. N. Chang, Z. Lewis, D. Minic and T. Takeuchi, arXiv:1206.0064 [quant-ph].

[77] L. N. Chang, Z. Lewis, D. Minic and T. Takeuchi, arXiv:1208.5189 [math-ph].

[78] J. W. P. Hirschfeld, *Projective Geometries over Finite Fields,* 2nd ed., Oxford University Press, 1998.

[79] V. I. Arnold, *Dynamics, Statistics and Projective Geometry of Galois Fields*, Cambridge University Press, 2011.

[80] S. Ball and Z. Weiner, *An Introduction to Finite Geometry,* `http://www-ma4.upc.es/~simeon/IFG.pdf`

[81] M. Hamermesh, *Group Theory and its Application to Physical Problems,* Dover, 1962.

[82] See, for instance: R. P. James, G. Ortiz, and A. Sabry, arXiv:1101.3764 [quant-ph].

[83] For a comprehensive review, consult A. Ashtekar and T. A. Schilling, gr-qc/9706069.

[84] For a review see: V. Jejjala, M. Kavic and D. Minic, Int. J. Mod. Phys. A **22**, 3317 (2007).

[85] D. Minic and H. C. Tze, Phys. Rev. D **68**, 061501 (2003); Phys. Lett. B **581**, 111 (2004); hep-th/0401028.

[86] See for example, J. Dieudonné, "On biorthogonal systems," Michigan Math. J. **2**, 7 (1953).

Appendix A

A Useful Integral Formula for Gegenbauer Polynomials

The following integral formula is necessary in calculating the expectation value of $\hat{p}^2$. For two non-negative integers m and n such that $m \leq n$, and $\lambda > \frac{1}{2}$, we have

$$\begin{aligned} &\int_{-1}^{1} c^{2\lambda-3}\, C_m^\lambda(s)\, C_n^\lambda(s)\, ds \\ &= \begin{cases} \dfrac{4\pi\,\Gamma\big(m+2\lambda\big)}{(2\lambda-1)\big[\,2^\lambda\Gamma\big(\lambda\big)\,\big]^2 m!} & \text{if } n-m = \text{even}, \\ \\ 0 & \text{if } n-m = \text{odd}, \end{cases} \end{aligned} \tag{A.1}$$

where $c = \sqrt{1-s^2}$. We were unable to find this result in any of the standard tables of integrals [67] though *Mathematica* seems to be aware of it. Here we present a proof.

We start from recursion relations which can be found in Ref. [67]. In section 8.933 of Gradshteyn and Ryzhik, we have:

$$\begin{aligned} (n+2\lambda)\, C_n^\lambda(x) &= 2\lambda\Big[\, C_n^{\lambda+1}(x) - x\, C_{n-1}^{\lambda+1}(x)\,\Big]\,, \\ n\, C_n^\lambda(x) &= 2\lambda\Big[\, x\, C_{n-1}^{\lambda+1}(x) - C_{n-2}^{\lambda+1}(x)\,\Big]\,. \end{aligned} \tag{A.2}$$

Eliminating $C_{n-1}^{\lambda+1}(x)$ and then shifting λ by one unit, we obtain

$$C_n^\lambda(x) - C_{n-2}^\lambda(x) \;=\; \left(\frac{n+\lambda-1}{\lambda-1}\right) C_n^{\lambda-1}(x)\;, \tag{A.3}$$

which is Equation 22.7.23 of Abramowitz and Stegun. Iterating this relation, we deduce that

$$\begin{aligned} C_{2k}^\lambda(x) &= C_0^\lambda(x) + \sum_{i=1}^{k} \left(\frac{2i+\lambda-1}{\lambda-1}\right) C_{2i}^{\lambda-1}(x)\;, \\ C_{2k+1}^\lambda(x) &= C_1^\lambda(x) + \sum_{i=1}^{k} \left(\frac{2i+\lambda}{\lambda-1}\right) C_{2i+1}^{\lambda-1}(x)\;. \end{aligned} \tag{A.4}$$

Since

$$\begin{aligned} C_0^\lambda(x) &= 1 \;=\; C_0^{\lambda-1}(x)\;, \\ C_1^\lambda(x) &= 2\lambda\, x \;=\; \left(\frac{\lambda}{\lambda-1}\right) C_1^{\lambda-1}(x)\;, \end{aligned} \tag{A.5}$$

we can write

$$\begin{aligned} C_{2k}^\lambda(x) &= \sum_{i=0}^{k} \left(\frac{2i+\lambda-1}{\lambda-1}\right) C_{2i}^{\lambda-1}(x)\;, \\ C_{2k+1}^\lambda(x) &= \sum_{i=0}^{k} \left(\frac{2i+\lambda}{\lambda-1}\right) C_{2i+1}^{\lambda-1}(x)\;. \end{aligned} \tag{A.6}$$

Thus, the even C_n^λ's can be expressed as a sum of the even $C_n^{\lambda-1}$'s, and the odd C_n^λ's as a sum of the odd $C_n^{\lambda-1}$'s. Invoking the orthogonality relation, Eq. (2.49), which is valid when $\lambda > -\frac{1}{2}$, it is clear that

$$\int_{-1}^{1} c^{2\lambda-3}\, C_{2k}^\lambda(s)\, C_{2\ell+1}^\lambda(s)\, ds \;=\; 0 \tag{A.7}$$

for $\lambda > \frac{1}{2}$. So for the integral of Eq. (A.1) to be non-zero, m and n must be both even, or both odd. For two non-negative integers k and ℓ such that $k \le \ell$, we find

$$\int_{-1}^{1} c^{2\lambda-3}\, C_{2k}^\lambda(s)\, C_{2\ell}^\lambda(s)\, ds$$

$$
\begin{aligned}
&= \int_{-1}^{1} c^{2\lambda-3}\left[\sum_{i=0}^{k}\left(\frac{2i+\lambda-1}{\lambda-1}\right)C_{2i}^{\lambda-1}(s)\right] \\
&\qquad \times\left[\sum_{j=0}^{\ell}\left(\frac{2j+\lambda-1}{\lambda-1}\right)C_{2j}^{\lambda-1}(s)\right]ds \\
&= \sum_{i=0}^{k}\sum_{j=0}^{\ell}\left(\frac{2i+\lambda-1}{\lambda-1}\right)\left(\frac{2j+\lambda-1}{\lambda-1}\right) \\
&\qquad \times\int_{-1}^{1} c^{2\lambda-3}\,C_{2i}^{\lambda-1}(s)\,C_{2j}^{\lambda-1}(s)\,ds \\
&= \sum_{i=0}^{k}\left(\frac{2i+\lambda-1}{\lambda-1}\right)^{2}\frac{2\pi\,\Gamma(2i+2\lambda-2)}{(2i+\lambda-1)\big[\,2^{\lambda-1}\Gamma(\lambda-1)\,\big]^{2}(2i)!} \\
&= \frac{2\pi}{\big[\,2^{\lambda-1}\Gamma(\lambda)\,\big]^{2}}\sum_{i=0}^{k}\frac{(2i+\lambda-1)\,\Gamma(2i+2\lambda-2)}{(2i)!}\,,
\end{aligned}
$$

$$
\begin{aligned}
&\int_{-1}^{1} c^{2\lambda-3}\,C_{2k+1}^{\lambda}(s)\,C_{2\ell+1}^{\lambda}(s)\,ds \\
&= \int_{-1}^{1} c^{2\lambda-3}\left[\sum_{i=0}^{k}\left(\frac{2i+\lambda}{\lambda-1}\right)C_{2i+1}^{\lambda-1}(s)\right] \\
&\qquad \times\left[\sum_{j=0}^{\ell}\left(\frac{2j+\lambda}{\lambda-1}\right)C_{2j+1}^{\lambda-1}(s)\right]ds \\
&= \sum_{i=0}^{k}\sum_{j=0}^{\ell}\left(\frac{2i+\lambda}{\lambda-1}\right)\left(\frac{2j+\lambda}{\lambda-1}\right) \\
&\qquad \times\int_{-1}^{1} c^{2\lambda-3}\,C_{2i+1}^{\lambda-1}(s)\,C_{2j+1}^{\lambda-1}(s)\,ds \\
&= \sum_{i=0}^{k}\left(\frac{2i+\lambda}{\lambda-1}\right)^{2}\frac{2\pi\,\Gamma(2i+2\lambda-1)}{(2i+\lambda)\big[\,2^{\lambda-1}\Gamma(\lambda-1)\,\big]^{2}(2i+1)!} \\
&= \frac{2\pi}{\big[\,2^{\lambda-1}\Gamma(\lambda)\,\big]^{2}}\sum_{i=0}^{k}\frac{(2i+\lambda)\,\Gamma(2i+2\lambda-1)}{(2i+1)!}\,. \qquad \text{(A.8)}
\end{aligned}
$$

The sums in the above expressions are given by

$$
\sum_{i=0}^{k}\frac{(2i+\lambda-1)\,\Gamma(2i+2\lambda-2)}{(2i)!} \;=\; \frac{\Gamma(2k+2\lambda)}{2(2\lambda-1)(2k)!}\,,
$$

$$\sum_{i=0}^{k} \frac{(2i+\lambda)\,\Gamma(2i+2\lambda-1)}{(2i+1)!} \;=\; \frac{\Gamma(2k+2\lambda+1)}{2(2\lambda-1)(2k+1)!}\;. \tag{A.9}$$

These relations can be proved by induction in k. Putting everything together, we obtain Eq. (A.1).

Using this formula, we find the matrix elements of the operator $\hat{p}^2$ to be:

$$\begin{aligned}\langle m|\,\hat{p}^2\,|n\rangle \;&=\; \langle n|\,\hat{p}^2\,|m\rangle \\ &= \begin{cases} \dfrac{1}{\beta}\left[-\delta_{mn} + \dfrac{2\sqrt{(\lambda+m)(\lambda+n)}}{2\lambda-1}\sqrt{\dfrac{n!\,\Gamma(2\lambda+m)}{m!\,\Gamma(2\lambda+n)}}\right] \\ \qquad\qquad \text{for } n-m = \text{even},\ m \le n, \\ 0 \qquad\qquad\qquad\qquad \text{for } n-m = \text{odd}. \end{cases}\end{aligned} \tag{A.10}$$

In particular, the diagonal elements are given by

$$\langle n|\,\hat{p}^2\,|n\rangle \;=\; \frac{1}{\beta}\left(\frac{2n+1}{2\lambda-1}\right)\;. \tag{A.11}$$

The expectation value of $\hat{x}^2$ is obtained from

$$\frac{k}{2}\langle\hat{x}^2\rangle \;=\; \langle\hat{H}\rangle - \frac{\langle\hat{p}^2\rangle}{2m}\;. \tag{A.12}$$